



UNIVERSITY OF BIRMINGHAM

Power System Reliability Enhancement with Reactive Power Compensation and Operational Risk Assessment with Smart Maintenance for Power Generators

By

Manuel Sebastian Alvarez Alvarado

A thesis submitted to

The University of Birmingham for the degree of

DOCTOR OF PHILOSOPHY

School of Electronic, Electrical
and Systems Engineering

The University of Birmingham

March 2020

UNIVERSITY OF
BIRMINGHAM

University of Birmingham Research Archive
e-theses repository

This unpublished thesis/dissertation is copyright of the author and/or third parties. The intellectual property rights of the author or third parties in respect of this work are as defined by The Copyright Designs and Patents Act 1988 or as modified by any successor legislation.

Any use made of information contained in this thesis/dissertation must be in accordance with that legislation and must be properly acknowledged. Further distribution or reproduction in any format is prohibited without the permission of the copyright holder.

DEDICATORY

I dedicate this work to God for giving me the perseverance to achieve my goals.

To my mother Alexandra Georgina Alvarado Guillen because she is my inspiration; To my father Manuel Enrique Alvarez Valverde for showing me the strength that drives me to reach my dreams; To my sister Melanie Estefanía Alvarez Alvarado for teaching that innocence is a pathway to keep my life with simplicity and harmony; To my brother Erick Andrés Alvarez Alvarado because he encouraged me to overcome any obstacles; To my fiancée Karina Marisabel Marín Morocho for opening her heart, bringing a new meaning to my life.

This research is the product of a long effort and dedication. I thank God for giving me the gift of science and understanding, but above all the strength and inspiration that is reflected in my family, friends, and colleagues.

Without them, this work would never have been a reality.

Thank you so much!!

ACKNOWLEDGEMENTS

Firstly, I thank God for giving me the knowledge gift.

My deepest appreciation to my supervisor Dr. Dilan Jayaweera, for his tremendous direction and guidance. His innovative ideas and advices opened a pathway to reach milestones in the field of power system reliability assessment. I am glad to have been supervised by Dr. Dilan Jayaweera, his patience, dedication and knowledge are the keys of the success of this research.

Special thanks to Secretaría de Educación Superior, Ciencia, Tecnología e Innovación (SENESCYT) and Facultad de Ingeniería en Electricidad y Computación (FIEC) from Escuela Superior Politécnica del Litoral (ESPOL), for their financial support. Without them this dream could not be true.

I would like to thank my colleagues Zafar A. Khan, Abdullah Altamimi, Hasan Gunduz, Daniel Donaldson, Waleed Alabri, Bader Alharbi, and Wilson Vasquez for their support and encouragement throughout my PhD. A special thanks to Luis Soriano and Fernanda Medina, who made my stay in the UK wonderful, for supported me and encouraged me to persevere towards my achievements. Thanks to all friends who have supported me.

I owe a special thanks to Karina Marin, who have been extremely supportive throughout this entire process and made countless sacrifices to help me get to this point. Thank you so much, because your love gave me the strength to achieve my goals. My love is all for you.

Last but not least, I would like thanks to my parents for their unwavering support, for showing that research is the key to human development. I thank everyone who made this work possible such as relatives, friends, and colleagues who trusted and had faith in me.

ABSTRACT

Modern power systems incorporate advanced contingency measures with the aim of enhancing system performance. Among them, the strategic installation of reactive power compensators into a power system is commonly practised to minimize power losses and improve system reliability. Such a practice requires a robust optimization technique that could reduce the computational burden and provide optimal planning and operation of the compensators. This thesis proposes an advanced optimization technique, named as Accelerated Quantum Particle Swarm Optimization (AQPSO) to determine the optimal placement, sizing and dispatch strategy of the reactive power compensators with the aim of improving the system level reliability. The uniqueness of the technique is the incorporation of the concept ‘best observation’, which accelerates the search towards the optimal solution.

The implementation of advanced maintenance strategies is another common contingency measure used to enhance system performance. In this context, this thesis proposes a novel Smart Maintenance (SM) strategy for power generators that maximize the generation adequacy and provide increased economic benefits in a framework of system reliability. The uniqueness of the SM approach is the incorporation of the ‘obsolescence’ state through the stages of the bathtub curve and half-arch shape to model the aging process and then quantify the operational risk of the generators using fuzzy logic theory. Further, SM combines the proposed AQPSO and Sequential Median Latin Hypercube to obtain a comprehensive maintenance schedule.

The investigation presented in this thesis contributes with novel AQPSO-based algorithms to enhance power system reliability with the operation of reactive power compensation; a more realistic and accurate aging reliability model of power generators; a detailed SM mathematical framework and an algorithm for the scheduling of proactive maintenance of generators of small and large-power systems. The proposed models are significant in the journey to the smart operation of a power system with diverse levels of applications.

List of Publications & Awards

Parts of these research outcomes were published in journal articles and conferences. It is relevant to highlight that some publications received awards. Each publication is listed below.

Conference papers

1. * **M. S. Alvarez-Alvarado** and D. Jayaweera, “Smart Maintenance Model for Operational Planning of Static Synchronous Compensators,” in *13th IEEE PES PowerTech Conference*, 2019. (Published)
2. **M. S. Alvarez-Alvarado** and D. Jayaweera, “A Multi-Stage Accelerated Quantum Particle Swarm Optimization for Planning and Operation of Static Var Compensators,” in *2018 IEEE Third Ecuador Technical Chapters Meeting (ETCM)*, 2018, pp. 1–6. (Published)
3. ‡ **M. S. Alvarez-Alvarado** and D. Jayaweera, “A New Approach for Reliability Assessment of a Static V ar Compensator Integrated Smart Grid,” in *2018 IEEE International Conference on Probabilistic Methods Applied to Power Systems (PMAPS)*, 2018, pp. 1–7. (Published)
4. **M. S. Alvarez-Alvarado** and D. Jayaweera, “Aging Reliability Model for Generation Adequacy,” in *2018 IEEE International Conference on Probabilistic Methods Applied to Power Systems (PMAPS)*, 2018, pp. 1–6. (Published)
5. † **M. S. Alvarez-Alvarado** and D. Jayaweera, “Reliability model for a static var compensator,” in *2017 IEEE Second Ecuador Technical Chapters Meeting (ETCM)*, 2017, pp. 1–6. (Published)

Journal papers

6. **M. S. Alvarez-Alvarado** and D. Jayaweera, “Reliability Based Smart Maintenance of Generators in Smart Power Systems,” *IET Gener. Transm. Distrib.*, 2020. (Published)
7. **M. S. Alvarez-Alvarado** and D. Jayaweera, “Operational Risk Assessment with Smart Maintenance of Power Generators,” *Int. J. Electr. Power Energy Syst.*, 2019. (Published)
8. **M. S. Alvarez-Alvarado**, C. D. Rodríguez-Gallegos, and D. Jayaweera, “Optimal planning and operation of static VAR compensators in a distribution system with non-linear loads,” *IET Gener. Transm. Distrib.*, vol. 12, no. 15, pp. 3726–3735, 2018. (Published)
9. **M. S. Alvarez-Alvarado** and D. Jayaweera, “Bathtub curve as a Markovian process to describe the reliability of repairable components,” *IET Gener. Transm. Distrib.*, vol. 12, no. 21, pp. 5683–5689, 2018. (Published)

* Best presentation award 3rd Annual School of Engineering PGR Symposium, Birmingham-UK, May 2019.

‡ Best paper award PMAPS Roy Billinton Student Paper Gold Award, Boise-USA, June 2018.

† Best paper award PES session in the Second Ecuadorian Technical Chapters Meeting, Salinas-Ecuador, 2017.

Table of Content

Chapter 1: Introduction	1
1.1 Background and Motivation.....	1
1.2 Scope of the Research	3
1.3 Aim and Objectives.....	4
1.4 Research Contributions	6
1.6 Thesis Structure.....	8
Chapter 2: Literature Review.....	12
2.1 Reliability Assessment in Modern Power Systems.....	12
2.1.1 HLI: Generation.....	12
2.1.2 HLII: Transmission.....	16
2.1.3 HLIII: Distribution	17
2.2 Bathtub Curve and Aging Models.....	18
2.3 Reactive Compensation for Reliability Enhancement	19
2.4 Maintenance Evolution	22
2.5 Risk and Maintenance of Power Generators	24
2.6 Summary	26
Chapter 3: Reliability Assessment Theories.....	28
3.1 Reliability Concept.....	28
3.2 Alternating Renewal Process	30
3.3 Reliability Features of Electrical Power Generators	33

3.3.1 Hydro Unit Generation	33
3.3.2 Thermal Unit Power Generation.....	34
3.4 Reliability Features of FACTS.....	35
3.5 Reliability Assessment in Power Systems	39
3.5.1 Monte Carlo Simulation	39
3.5.2 Generation Adequacy Analysis	40
3.5.3 Composite System Reliability Analysis	42
3.6 Risk Quantification	42
3.7 Summary	44
Chapter 4: Reliability Model with Aging Features.....	45
4.1 Time Dependent Transitions Rates	45
4.1.1 Bathtub Curve	46
4.1.2 Half-Arch Shape.....	46
4.2 States and Stages	47
4.2.1 States in the Infant Mortality Stage.....	47
4.2.2 States in the Useful Lifetime and Wear Out Stages	47
4.2.3 State in the End Lifetime Stage.....	48
4.3 Reliability Framework.....	49
4.3.1 Probability Vector of States.....	49
4.3.2 Degradation Rate	50
4.3.3 Availability and Unavailability	51

4.4 Quantification of the Degradation.....	52
4.5 Aging Impact in Reliability Evaluation	52
4.5.1 Degradation of the Unit Generation	55
4.5.2 Reliability Model of the Unit generation.....	56
4.5.3 Generation Adequacy with Aging Features.....	58
4.6 Summary	59
Chapter 5: Accelerated Quantum Particle Swarm Optimization	60
5.1 AQPSO Methodology	61
5.2 Mathematical Framework of Quantum Particle Motion	63
5.3. Composite System Reliability Evaluation with Reactive Compensation Using AQPSO.....	67
5.3.1 Case Study	67
5.3.2 Problem Formulation.....	67
5.3.3 Proposed Algorithm.....	69
5.3.4 Results and Discussion	72
5.4 Planning and Operation of Static Var Compensators.....	74
5.4.1 System Layout Description	74
5.4.2 Problem Formulation.....	75
5.4.3 Proposed Algorithm.....	76
5.4.4 Results and Discussion	81
5.5 Summary	85

Chapter 6: Smart Maintenance Scheme for Generators.....	86
6.1 Smart Maintenance Mathematical Framework	87
6.1.1 Kijima Model: Virtual Age, Actual Age and Maintenance.....	87
6.1.2 Markov Chain: Probability Vector of all Possible States	88
6.1.3 Fuzzy Logic to Quantify Maintenance Effort.....	93
6.1.4 Maintenance Effort Impact on Failure Rate	96
6.2 Smart Maintenance Procedure	97
6.3 Generation Adequacy using Smart Maintenance	100
6.3.1 Case Study	100
6.3.2 Problem Formulation.....	101
6.3.3 Proposed Algorithm.....	104
6.3.4 Smart Maintenance Schedule	107
6.3.5 Operation and Number of Maintenances.....	109
6.3.6 Unit Generation Degradation.....	111
6.3.7 Unit Generation Reliability Model.....	112
6.3.8 Smart Maintenance Maximum Net Benefit.....	114
6.3.9 Smart Maintenance Computational Efficiency.....	115
6.4 Summary.....	117
Chapter 7: Closure.....	119
7.1 Conclusions	119
7.2 Future Research.....	123

Appendix.....	125
A.1 Roy Billinton Test System (RBTS).....	125
A.2 IEEE Reliability Test System (RTS).....	127
References.....	130

List of Figures

Figure 1.1 Thesis topic area (blue boxes) within power system reliability field	4
Figure 1.2 Interdependency between chapters	10
Figure 1.3 Pictorial summary of the research	11
Figure 2.1 Literature review scope of the reliability levels	13
Figure 2.2 Generation System Representation.....	14
Figure 2.3 Transmission System Representation	14
Figure 2.4 Distribution System Representation	14
Figure 2.5 The evolution of maintenance	24
Figure 3.1 Reliability Schemes [144]	29
Figure 3.2 Markov chain of a repairable component [144]	31
Figure 3.3 Hydro generator reliability topology	34
Figure 3.4 FACTS categorization	36
Figure 3.5 SVC electrical circuit [172], [173]	37
Figure 3.6 SVC U-I characteristic [174], [175]	37
Figure 3.7 STATCOM electrical circuit [176], [177].....	37
Figure 3.8 STATCOM U-I characteristic [178], [179].....	37
Figure 3.9 SVC/STATCOM reliability model [180]	38
Figure 3.10 Generation-Demand margin model	41
Figure 3.11 Flowchart for a composite system reliability evaluation.....	43
Figure 3.12 Risk of not meeting the predicted maximum demand.....	44
Figure 4.1 State-space diagram based on the Bathtub curve and Half-Arch shape [199].	48
Figure 4.2 Bathtub curve and Half-arch shape for each unit generation [199].....	53
Figure 4.3 Yearly load Profile [198]	54
Figure 4.4 State space diagram for each case [199].....	54

Figure 4.5 Degradation function of each generator [199].....	55
Figure 4.6 Availability and unavailability of each generator [199].....	57
Figure 4.7 Reliability indices [199]	58
Figure 5.1 AQPSO flowchart.....	61
Figure 5.2 Memory attribute of a particle	62
Figure 5.3 Communication attribute of a particle	62
Figure 5.4 Motion of a particle in a quantum delta potential well.....	65
Figure 5.5 Flowchart for optimum reliability assessment through VAr compensation [180] 71	
Figure 5.6 SVC placement and sizing that minimize EENS [180].....	72
Figure 5.7 Optimization Technique Convergence [180]	74
Figure 5.8 Load profiles for AQPSO Second Case Study [205]	75
Figure 5.9 AQPSOsp flowchart for optimum SVC planning [205]	77
Figure 5.10 AQPSOop flowchart for optimum SVC operation [205].....	78
Figure 5.11 SVC optimal placement and size for AQPSO second case study [205].....	82
Figure 5.12 Optimal dispatch strategy for each SVC [205].....	83
Figure 5.13 Voltage profile for AQPSO second case study [205].....	83
Figure 6.1 Smart maintenance concepts	87
Figure 6.2 Virtual age evolution	88
Figure 6.3 Markov chain of the operational states.....	91
Figure 6.4 Design of a thermal unit with auxiliary support	91
Figure 6.5 Membership functions	95
Figure 6.6 Maintenance Exertion Degree: a) 3d plot; b) contour plot.....	96
Figure 6.7 Maintenance impact on failure rate	97
Figure 6.8 Smart Maintenance flowchart.....	98
Figure 6.9 PM cost as a function of the exertion degree.....	101

Figure 6.10 State estimation rule using SMLH.....	102
Figure 6.11 Flowchart for effective maintenance plan through SM.....	106
Figure 6.12 SM plan for hydro unit generation	108
Figure 6.13 SM plan for thermal unit generation.....	108
Figure 6.14 Degradation of each unit generation under different PM strategies.....	112
Figure 6.15 Reliability model for each UG under different PM strategies.....	113
Figure 6.16 Net benefit evolution	115
Figure 6.17 SM Optimization technique convergence.....	117
Figure A.1 RBTS single line diagram [6].....	125
Figure A.2 Normalized yearly load profile [6]	126
Figure A.3 RTS single line diagram [6].....	127

List of Tables

Table 2.1 Power System Adequacy Hierarchical Levels [34]	14
Table 2.2 Predictive Maintenance Strategies	23
Table 3.1 Reliability Features of Hydro Unit Generation [6], [30], [154], [156]–[161].....	33
Table 3.2 Reliability Features of Thermal Unit Generation [6], [160], [161], [164]–[167] ...	35
Table 3.3 SVC and STATCOM Electrical Features	37
Table 3.4 Static Var Compensator Reliability Features [109], [181]–[184].....	37
Table 3.5 Static Synchronous Compensator Reliability Features [180], [184]–[189].....	38
Table 4.1 Generators Reliability Data [199]	53
Table 5.1 Static Var Compensators Available for AQPSO First Case Study [180]	67
Table 5.2 Impact of the SVC on power system reliability [180]	73
Table 5.3 Optimization Technique Robustness for AQPSO first case study [180]	74
Table 5.4 Static Var Compensators Available for AQPSO Second Case Study [205].....	75
Table 5.5 Optimization Technique Robustness for AQPSO second case study [205]	85
Table 6.1 Operational States Labels.....	90
Table 6.2 Thermal Unit Power Output.....	91
Table 6.3 Maintenance Exertion Degree Qualitative Descriptors.....	94
Table 6.4 Availability Qualitative Descriptors	94
Table 6.5 Factor of Operation Qualitative Descriptors	94
Table 6.6 Maintenance Exertion Degree Control Rules	95
Table 6.7 Generators Maintenance Cost	100
Table 6.8 Summary of the Operational States of each UG	110
Table 6.9 Summary of the Maintenances performed to each UG.....	110
Table 6.10 SM Optimization Techniques Robustness	116

Table A.1 RBTS Unit Generation Reliability Data [6].....	126
Table A.2 RBTS Transmission Lines Reliability Data [6]	126
Table A.3 RTS Unit Generation Reliability Data [160].....	128
Table A.4 RTS Unit Generation Reliability Data [160].....	128
Table A.5 RTS Transmission Lines Reliability Data [160].....	129

List of Algorithms

Algorithm 3.1 Monte Carlo Pseudocode	40
Algorithm 5.1 Accelerated Quantum Particle Swarm Optimization Pseudocode	66

Nomenclature

P	Probability [%]
P_0	Probability of being in the state of operation as good as new [%]
P_1	Probability of being in rated operation state [%]
P_2	Probability of being in not operational state [%]
P_3	Probability of being in obsolescence state [%]
P_4	Probability of being in derated operation state [%]
P_I	Probability of being in policy of replacement state [%]
P_{II}	Probability of being in overloaded operation [%]
P_f	Probability of failure [%]
P_r	Probability of repair [%]
\mathbf{P}	Probability vector [%]
$\dot{\mathbf{P}}$	Derivative probability vector [%]
\mathbf{H}	Stochastic matrix of transition states [1/yr]
\mathbf{H}^T	Transpose of the stochastic matrix of transition states [1/yr]
\mathbf{I}	Identity matrix
\mathbf{G}	Transient-Absorption matrix
$\bar{\mathbf{0}}$	Zero Matrix
\mathbf{N}	Fundamental matrix

R	Reliability [%]
M	Maintainability [%]
f_f	Probability function of failure [p.u.]
f_r	Probability function of repair [p.u.]
ω	Frequency domain [hr ⁻²]
t	Time domain [hr]
Δt	Time interval [hr]
τ_f	Time to failure [hr]
τ_r	Time to repair [hr]
τ_u	Time of operation since the last repair [hr]
τ_{ov}	Overloaded operation time [s]
$\Delta\tau$	Maintenance execution time interval [hr]
$\Delta\tau_{ov}$	Overload execution time interval [hr]
T_U	Time of guarantee [s]
T_V	Maximum useful lifetime [s]
T_W	End lifetime [s]
TS	Time Simulation [yr]
λ	Failure rate [1/yr]
λ_I	Policy of replacement failure rate [1/yr]

λ_{aux}	Auxiliary circuit failure rate [1/yr]
λ_{main}	Main circuit failure rate [1/yr]
a	Failure rate displacement parameter [1/yr]
α	Failure rate scale [1/yr]
ω	Failure rate location parameter [yr]
μ	Repair rate [1/yr]
μ_I	Policy of replacement repair rate [1/yr]
μ_{aux}	Auxiliary circuit repair rate [1/yr]
μ_{main}	Main circuit repair rate [1/yr]
b	Repair rate displacement parameter [1/yr]
β	Repair rate scale [1/yr]
γ	Repair rate power parameter [1/yr]
d	Auxiliary variable [1/yr]
ϕ	Degradation rate [1/yr]
δ	Transition rate from infant mortality to useful life [1/yr]
ρ	Transition rate from rated operation to overloaded operation [1/yr]
θ	Transition rate from overloaded operation to rated operation [1/yr]
Λ	Degradation [p.u.]
χ	Eigenvalue of the transpose of the stochastic matrix of transition states [1/yr]

\mathbf{v}	Eigenvector of the transpose of the stochastic matrix of transition states [p.u.]
\mathbf{Y}	Eigenmatrix [p.u.]
\mathbf{C}	Initial condition vector [p.u.]
c	Initial condition constant [p.u.]
Γ	Virtual age [yr]
q	Degree of maintenance [p.u.]
z	Maintenance exertion degree [p.u.]
ϑ	Maintenance type factor [p.u.]
CM	Corrective maintenance counter [p.u.]
PM	Preventive maintenance counter [p.u.]
n	Maintenance counter [p.u.]
i	Row index for matrices [p.u.]
j	Column index for matrices [p.u.]
k	Iteration counter [p.u.]
ϵ	Convergence tolerance value [p.u.]
ℓ	Particle counter [p.u.]
q	Particle personal best [p.u.]
g	Particle global best [p.u.]
D	Particle local attractor [p.u.]

\mathfrak{S}	Probability of finding the quantum particle [%]
u	Random number uniformly distributed [p.u.]
r	Constant acceleration coefficients [p.u.]
x	Position inside a quantum well
Δx	Relative position
δ	Delta function
l	Characteristic length of the quantum delta potential well
ε	Contraction-expansion coefficient
ζ	Power derated factor
EXS	Mathematical expectation of the system
OF	Objective function
obs	Observer [p.u]
OBS	Set of observers [p.u.]
B	Best observation [p.u.]
s	State [p.u.]
S	Set of states State
F	Set of failures events
G	Set of stratification
Θ	Set of operating states [p.u.]

Ω	Set of non-operating states [p.u.]
Ξ	Set of derated states [p.u.]
A	Availability [%]
U	Unavailability [%]
\mathring{A}	Semi-availability [%]
\beth	Risk [%]
<i>EXF</i>	Experiment function
σ	Component counter [p.u.]
<i>exp</i>	Experiment counter [p.u.]
<i>gen</i>	Generator counter [p.u.]
<i>line</i>	Line counter [p.u.]
<i>SVC</i>	SVC counter [p.u.]
<i>load</i>	Load counter [p.u.]
<i>NC</i>	Total number of components [p.u.]
<i>NS</i>	Total number of states [p.u.]
<i>NE</i>	Total number of experiments [p.u.]
<i>It</i>	Total number of iterations [p.u.]
<i>NO</i>	Total number of observers [p.u.]
<i>SS</i>	Total number of particles [p.u.]

N_{Li}	Total number of lines [p.u.]
N_{Lo}	Total number of loads [p.u.]
N_{SVC}	Total number of available SVCs [p.u.]
NG	Total number of available generators
N_{bus}	Total number of buses [p.u.]
N_{PM}	Total number of preventive maintenances executed [p.u.]
N_{CM}	Total number of corrective maintenances executed [p.u.]
LC	Load curtailment [MWh]
P_{gen}	Active power injected by the generator [MW]
$P_{min_{gen}}$	Minimum power injected by the generator [MW]
$P_{max_{gen}}$	Maximum power injected by the generator [MW]
P_{line}	Active power consumed by the line [MW]
$P_{max_{line}}$	Maximum active power that the line can carry [MW]
P_{load}	Active power consumed by the load [MW]
Q_{gen}	Reactive power injected by the generator [MVar]
Q_{SVC}	Reactive power injected by the SVC [MVar]
$Q_{min_{SVC}}$	Minimum reactive power injected by the SVC [MVar]
$Q_{max_{SVC}}$	Maximum reactive power injected by the SVC [MVar]
V_{bus}	Bus voltage [p.u.]

$V_{min_{bus}}$	Minimum bus voltage allowed [p.u.]
$V_{max_{bus}}$	Maximum bus voltage allowed [p.u.]
\wp_{gt}	Total power system generation [MW]
\wp_{dt}	Total power system demand [MW]
ΔL	Power losses reduction [MW]
I_{line}	Current that flows through the conductor (No reactive compensation)
I_{line}'	Current that flows through the conductor (Reactive compensation considered)
R	Conductor resistance [ohm]
E	Energy demanded [Mwh]
e	Energy price [£/MWh]
w	Price per reactive compensator capacity [£/MVar]
$SavingL$	Savings due to power losses reduction [£]
$CostSVC$	SVC Acquisition and installation cost [£]
$CostAcq$	Acquisition cost [£]
$CostOp$	Cost of operation [£]
$CostPM$	Cost of preventive maintenance [£]
$CostCM$	Cost of corrective maintenance [£]
$CostM$	Total cost of maintenance [£]
NB	Net benefit [£]

<i>MTTA</i>	Meantime to absorption [yr]
<i>MTTF</i>	Meantime to failure [hr]
<i>MTTR</i>	Meantime to repair [hr]
<i>LLD</i>	Loss of load duration [hr]
<i>ENS</i>	Energy not supplied [Mwh]
<i>EENS</i>	Expected energy not supplied [Mwh/yr]
<i>LOLE</i>	Loss of load expectation [hr/yr]
<i>LOEE</i>	Loss of energy expectation [MWh/yr]
<i>LOLP</i>	Loss of load probability [p.u.]
<i>XLOL</i>	Expected loss of load [MW]

Chapter 1: Introduction

1.1 Background and Motivation

The power system is an electrical network, of which the purpose is to provide electricity to the customers securely, efficiently, and economically. Even though the efficiency can be addressed from many different aspects, the Federal Energy Regulatory Commission (FERC) and Department of Energy (DOE) recognized that a key driver of the efficiency prevails on the reliability of the concerned system. The term ‘reliability’ in a power system context refers to the capacity to provide continuous service and be able to satisfy electrical demand. The reliability plays an important role in power system since is essential for planning and operation of power systems [1].

Power system consists of a significant number of components (assets) and it is among the most complex systems of engineering. In 2008, the Council of European Energy Regulators (CEER) presented a report indicating that many European power systems (including the United Kingdom) present in average an interruption of service less or equal than two hours per year [2]. While two hours per year may seem small, this reliability index represents around 82 gigawatt-hours per year of energy not supplied for the UK [3], [4], leading to a yearly financial loss of around 10 million of sterling pounds for power utilities [5]. Therefore, there is still much work to do to provide continuous service to satisfy the electrical demand.

Power industry is looking for more realistic reliability models to replace the traditional model, which is presented as an alternating renewal process between two common states: ‘operating’ and ‘failure’ [6]. Even though the traditional model is easy to implement, it presents many deficiencies. In the first instance, the model disregards the aging effect since the end lifetime of the component is not considered. Consequently, the model brings inaccuracies in the reliability assessment. Some efforts to include aging using Weibull

distribution are proposed [7-8], however, deeper scrutiny on these reveals that determination of the degradation of the component is not clear. The second instance is that alternating renewal process does not consider the inclusion of preventive maintenance into the model, instead, it just considers corrective maintenance. The last instance is the underestimation of other operating states of the component such as the policy of replacement, derated operation, overloaded operation, which bring inaccuracies to the reliability evaluation. Therefore, the first motivation of the research presented in this thesis arises from the need to incorporate innovative models that consider real world implementations and drive to accurate reliability evaluation.

There are different contingency measures to improve the reliability of the power grid at the different power system levels. At a generation level, the integration of low carbon generators (renewable generation) into the power system is commonly used in developed countries, such as the UK [9]. This is because the renewable generation increases the capacity of power generation, enhancing the generation adequacy of the system [10]–[13]. At the transmission and distribution level, the analysis is extended to lines and transformers outages that produce voltage and frequency instabilities. Moreover, the problem can be extended since the lines or transformers that are in operation may carry more current and some of them may reach the overloaded state. This could result in load curtailment and increment in electric power losses. As a solution, the strategical incorporation of reactive compensators into the power system is expected to maintain system integrity during post-contingency operation [14]. However, the optimization problem of planning and operation of reactive compensators is a complex process that demands high computer processing memory and time. Hence, the second motivation of this thesis arises from the need of implementing an advanced optimization technique with low computational burden, which

could be used to enhance power system reliability and operation by the employment of reactive compensation.

Power industry employs maintenance actions as another potential contingency measure to ensure continuous operation of the power system [15]. Maintenance is defined as the process of preserving in an adequate condition a component in order to avoid premature failures. Conventional maintenance is being superseded with advanced maintenance strategies due to the high cost. For this reason, in the last decade, researchers in the UK [16]–[18] and other European countries [19]–[21] have been looking for novel maintenance strategies. Among the advanced maintenance strategies, the reliability centred maintenance (RCM) emerged as one of the most popular in the USA [22]–[24]. The main deficiency of RCM is that it focuses on maximizing the availability of the individual component without considering the composite system operation. Some authors have proposed the inclusion of smart-inspections [25], smart-devices [26] and smart-services [27] to develop a new scheme of maintenance. However, a gap in these visions is that the mathematical framework is not clearly described to validate the robustness. Thus, the third motivation of this thesis arises from the necessity of developing a new smart maintenance mathematical framework and an algorithm for the scheduling of proactive maintenance that maximizes the net benefits of generation adequacy.

1.2 Scope of the Research

This research focuses on power system reliability enhancement with reactive power compensation and operational risk assessment with smart maintenance (SM) for power generators. For this purpose, it is required to develop a comprehensive reliability model based on the bathtub curve and half-arch shape that respectively describe the failure and repair rates of power generators. Such a model is useful to carry out a more realistic and accurate generation adequacy assessment. The strategic installation of reactive power

compensators and implementation of SM approach formulate an optimization problem, which is solved using a novel optimization technique called Accelerated Quantum Particle Swarm Optimization (AQPSO). In order to demonstrate the efficacy of the proposed optimization technique, AQPSO, Particle Swarm Optimisation (PSO) and genetic algorithm (GA) are used separately to determine the optimal planning and operation of reactive power compensators. Regarding the SM mathematical framework, it involves specific issues related to reliability and risk concepts such as Kijima model [28], Markov chain [29], and Fuzzy logic [30], which are critically identified and analysed. In addition, the optimum preventive maintenance schedule of power generators is solved using the proposed AQPSO in combination with the Sequential Median Latin Hypercube [31]. Figure 1.1 shows how the topic of this thesis fits in the field of power system reliability assessment.

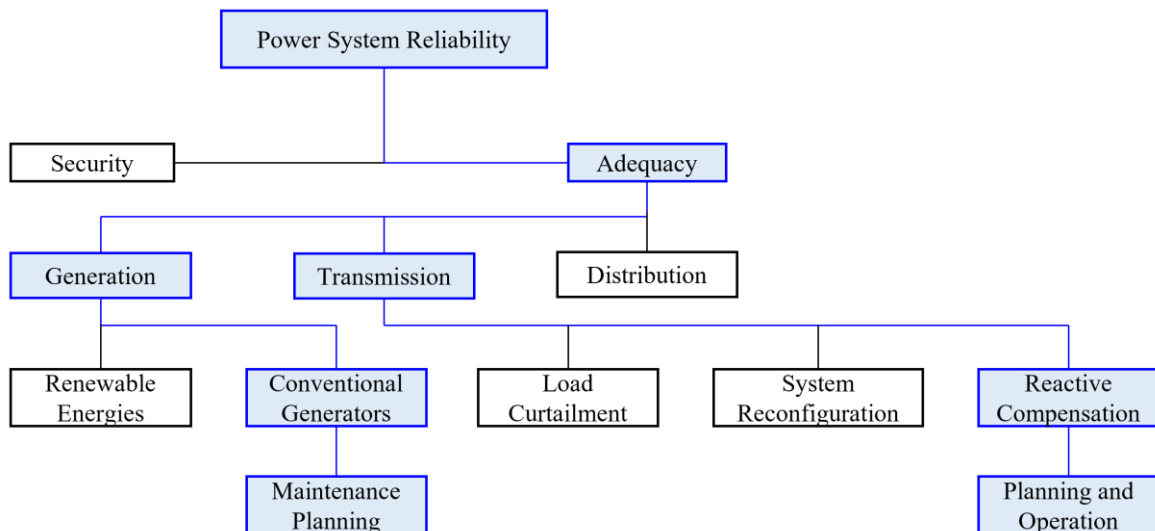


Figure 1.1 Thesis topic area (blue boxes) within power system reliability field

1.3 Aim and Objectives

At power system transmission level, the aim is to investigate the optimum planning and operation of the reactive power compensators to minimize power losses and expected energy not supplied. At power system generation level, the aim is to develop an innovative

smart maintenance model for power generators that considers the aging effect, degradation, maintenance exertion degree, and operational risk that maximize the economic benefits of generation adequacy. In order to achieve these aims, the investigations have been carried out through the following objectives:

- To develop a novel mathematical model that incorporates the aging effect that allows describing the degradation of power generators.
- To quantify the impact of aging on power systems generation adequacy assessment using the proposed approach. The results must be compared with the traditional alternating renewal process that uses exponential and Weibull distribution function.
- To propose the advanced optimization technique called Accelerated Quantum Particle Swarm Optimization. AQPSO efficacy must be demonstrated by showing its advantages over of the traditional optimization techniques, such as PSO and genetic algorithm (GA).
- To apply AQPSO for the minimization of the energy not supplied (EENS) of the power system by installing optimal static var compensators (SVCs).
- To determine the planning and operation of SVCs that maximizes the power losses and economic benefit by using AQPSO.
- To determine the maintenance exertion degree as a function of the availability and the operational factor, bringing a mathematical relationship that leads to the impact quantification of maintenance on generators failure rate.
- To formulate in mathematical terms the novel smart maintenance scheme, leading to the optimum preventive maintenance plan of generators that maximizes the generation adequacy net benefit.

1.4 Research Contributions

The research brings many contributions to the state of the art, which are summarised in the following list.

- **A more realistic and accurate aging reliability model for power generators.**

The thesis provides a comprehensive mathematical model for power generators based on the bathtub curve and half-arch shape to describe their failure and repair rates, respectively. For the first time, the different operational states of the generators are associated to every stage within the bathtub curve and half-arch shape, bringing more accurate and realistic results than the conventional alternating renewal process that employs exponential and Weibull distribution function.

- **A mathematical formulation to quantify the degradation of the component.**

The research incorporates the degradation rate term as the transition rate that leads to the obsolescence state. The degradation of the component is formulated as a function of the degradation rate and end lifetime of the component. Such formulation contributes to more insight into understanding the behaviour of components availability.

- **The development of an advanced optimization technique more robust than traditional PSO and GA.**

The approach presents mathematical formulations to derive the Accelerated Quantum Particle Swarm Optimization (AQPSO). The research considers two reactive compensation optimization problems, which are solved using AQPSO, PSO and GA. The computational efficacy of AQPSO is validated by performing a computational analysis. The time simulation and convergence iteration of each optimization technique are compared to validate

the robustness of AQPSO. Such robustness could derive to consider APQSO as a potential option to solve different engineering optimization problems.

- **The inclusion of novel AQPSO-based algorithms to enhance power system reliability and operation by the employment of reactive compensation.** The research presents two reactive compensation case studies. In the first instance, AQPSO-based algorithm is used to minimize the expected energy not supplied by strategically installing SVCs into the power system. In the second instance, AQPSO-based algorithm is used to maximize the economic benefit due to power losses reduction by the optimal planning and operation of SVCs. The AQPSO-based algorithms open a pathway to determine a solution for other reactive compensation applications.
- **A novel mathematical formulation that describes the relationship between generator's lifetime, virtual age, degradation, and transition rates.** This is the first study that integrates the Kijima model, Markov chain and fuzzy logic theory to establish a relationship between the reliability parameters of the power generators. This relationship could be practically useful for maintenance management and system reliability applications.
- **An advanced smart-maintenance algorithm for optimal generation adequacy in power systems.** The smart-maintenance algorithm takes as input the individual reliability and risk parameters of the generators. The algorithm combines AQPSO with the Sequential Median Latin Hypercube (SMLH) to determine an effective preventive maintenance schedule of generators that maximizes the generation adequacy net benefit. This is an original application of maintenance studies related to system reliability at generation level.

1.6 Thesis Structure

Figure 1.2 presents a pictorial summary of the research. This thesis consists of seven chapters including this introductory one. The remaining six chapters are outlined below.

Chapter 2 presents relevant literature review for this research. This includes the different techniques employed to conduct a power system reliability assessment at three different hierarchical levels; fundamental understanding of the reactive compensation applications for power system reliability enhancement; existing aging reliability model; and status quo of maintenance and risk in modern power system.

Chapter 3 describes the existing assessment reliability theories. The concept of reliability, maintainability and availability are described. The classical alternating renewal reliability model is derived. The chapter also presents the failure and repair rates for power generators and reactive compensators. In addition, the procedures to conduct the generation adequacy, composite system and risk assessments are also discussed.

Chapter 4 presents a novel aging reliability model for generators based on the behaviour of their transition rates. The bathtub curve and half-arch shape are used to model the failure and repair rates, respectively. In this chapter, the states at each stage of the bathtub curve is identified. In addition, the chapter also includes the quantification of the degradation. The validation of the proposed approach is shown by a case study, where its suitability to bring realistic reliability indices in comparison with classical reliability models is demonstrated.

Chapter 5 presents a mathematical framework to derive the AQPSO. The proposed optimization technique is used to investigate the impact of the reactive compensator installation in power system from two different point of view. From power system reliability side, AQPSO is used to determine the optimal size and placement of the reactive compensators to minimize expected energy not supplied. From power system operational

side, AQPSO is used to determine the optimal size, placement and strategy dispatch of the reactive compensators that maximizes the economic benefits due to power losses reduction. In addition, the chapter considers a computational analysis to determine AQPSO robustness in comparison with the conventional PSO and GA.

Chapter 6 starts with the mathematical framework required to define the smart-maintenance (SM) scheme, such as the Kijima Model type I, Markov chain and fuzzy logic. The smart maintenance procedure is described in detail and to show. Generation adequacy assessment is conducted using the smart maintenance, and results are compared to the results obtained using the conventional preventive periodic maintenance and reliability centred maintenance in order to study the performance of smart maintenance. It is relevant to mention that this chapter depends on the outcomes obtained in Chapter 4 and Chapter 5. The SM scheme includes the aging phenomenon, and for that purpose, the reliability model obtained in Chapter 4 is used. In addition, SM scheme is formulated as an optimization problem, which is solved employing the AQPSO presented in Chapter 5.

Chapter 7 contains the main conclusions of the research highlighting the research findings. This chapter also presents suggestions for future development of proposed applications and discusses further research topics.

The interdependency of each chapter is depicted in Figure 1.2 In this figure, the chapters are classified by groups. The first group is denoted as ‘Base Theory’ and is formed by chapter 1, 2 and 3. As presented in Figure 1.2, Chapter 1 is the foundation for the rest of the chapters because contains all the metrics (motivation, aim and objectives, and scope of the research) that motivate the development of the research. Chapter 2 and Chapter 3 contains the state of the art of the research, showing the advantages and deficiencies of existing approaches. The next group is named as ‘Contributions’ and this group is characterized by the containing the novelty of the research. This group is formed by Chapter

4, 5 and 6. Figure 1.2 shows that Chapter 4 and Chapter 5 directly depends on the chapters given in the ‘Base theory’ group. Chapter 6 is the core of the research (SM scheme) and it mainly depends on the outcomes obtained in Chapter 4 and Chapter 5. The SM scheme includes the aging phenomenon, and for that purpose, the reliability model obtained in Chapter 4 is used. In addition, the SM scheme is formulated as an optimization problem, which is solved employing the AQPSO presented in Chapter 5. The last group is the ‘Conclusion’ group and it only contains Chapter 7. This chapter depends mainly on the chapter of the ‘Contributions’ group. Chapter 7 consolidate all previous chapter, showing the findings of Chapter 4 ,5 and 6. For a better understanding of the interdependence between chapters Figure 1.3 shows a pictorial summary of the research.

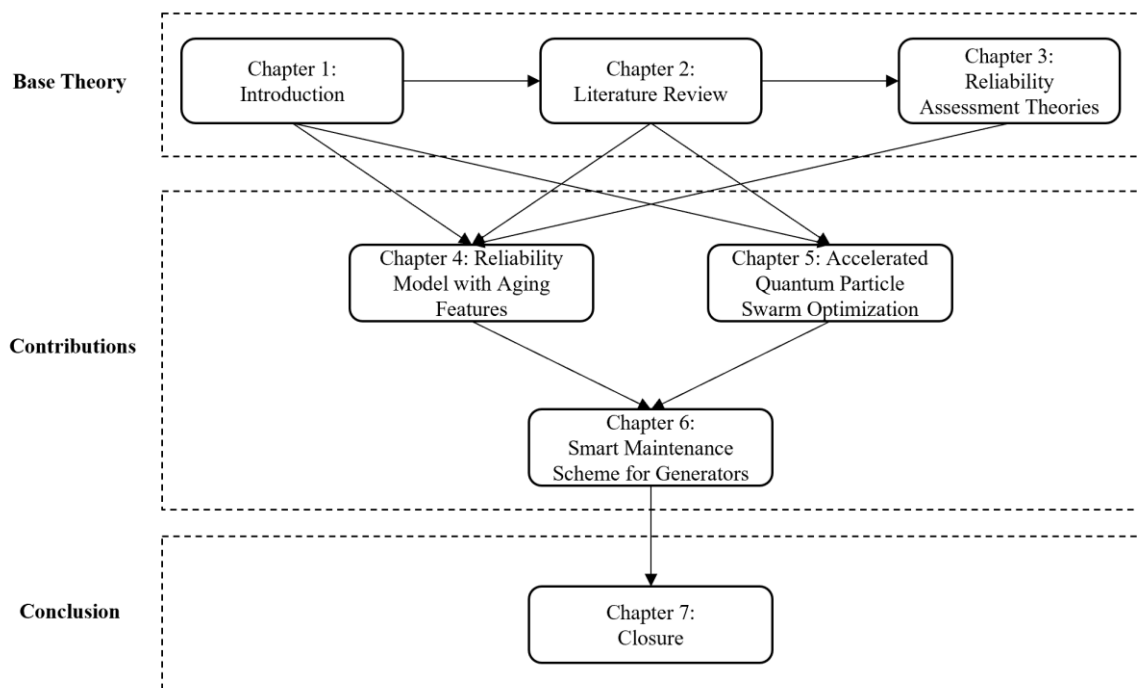


Figure 1.2 Interdependency between chapters

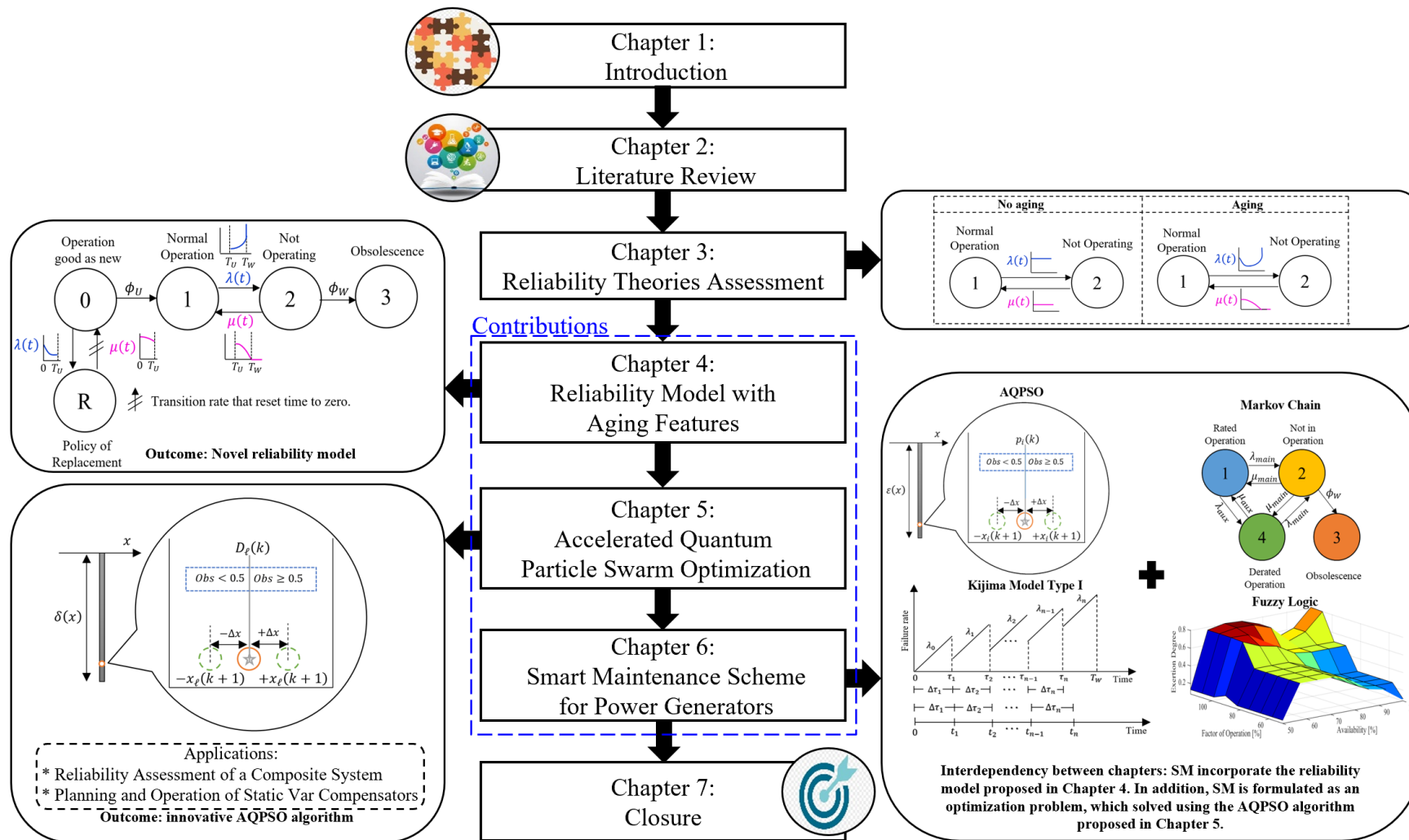


Figure 1.3 Pictorial summary of the research

Chapter 2: Literature Review

This chapter is divided into five sections. Section 2.1 presents a comprehensive state of the art of the reliability assessment conducted at the three-power system hierarchical levels. In Section 2.2, the bathtub curve and aging models are described. Section 2.3 exposes the current trends in the use of reactive compensation to improve the reliability of the power system. Section 2.4 presents the maintenance evolution. In Section 2.5, the concepts of risk and maintenance with relevant literature in the context of power generators are reviewed critically. Finally, the last section brings a summary of the chapter.

2.1 Reliability Assessment in Modern Power Systems

Reliability assessment in modern power systems can be addressed from two broader avenues: adequacy and security [32]. Adequacy refers to the presence of adequate facilities to supply the load demand in a power system under determined operational conditions. The adequacy measures the probability of failure when the system operates under a stationary state [32]. In contrast, security refers to the ability of a power system to deal with sudden disturbances; therefore, security measures the probability of failure when the system operates under dynamic or transient states [32].

Power system adequacy studies are divided into three hierarchical levels as described in Table 2.1 [32]. The literature review scope at each level is presented in Figure 2.1.

2.1.1 HLI: Generation

The first hierarchical level (HLI) is the base level and for this reason could be considered as the most important level. HLI evaluates the risk events in which the generation is not being able to supply the electricity demand [33]. For this purpose, it is required to define power generation reliability models and load profiles techniques. In this context, literature presents the reliability model of conventional generation as an alternating renewal process with the following states: operational, not in service and derated [6], [32], [34]–[37].

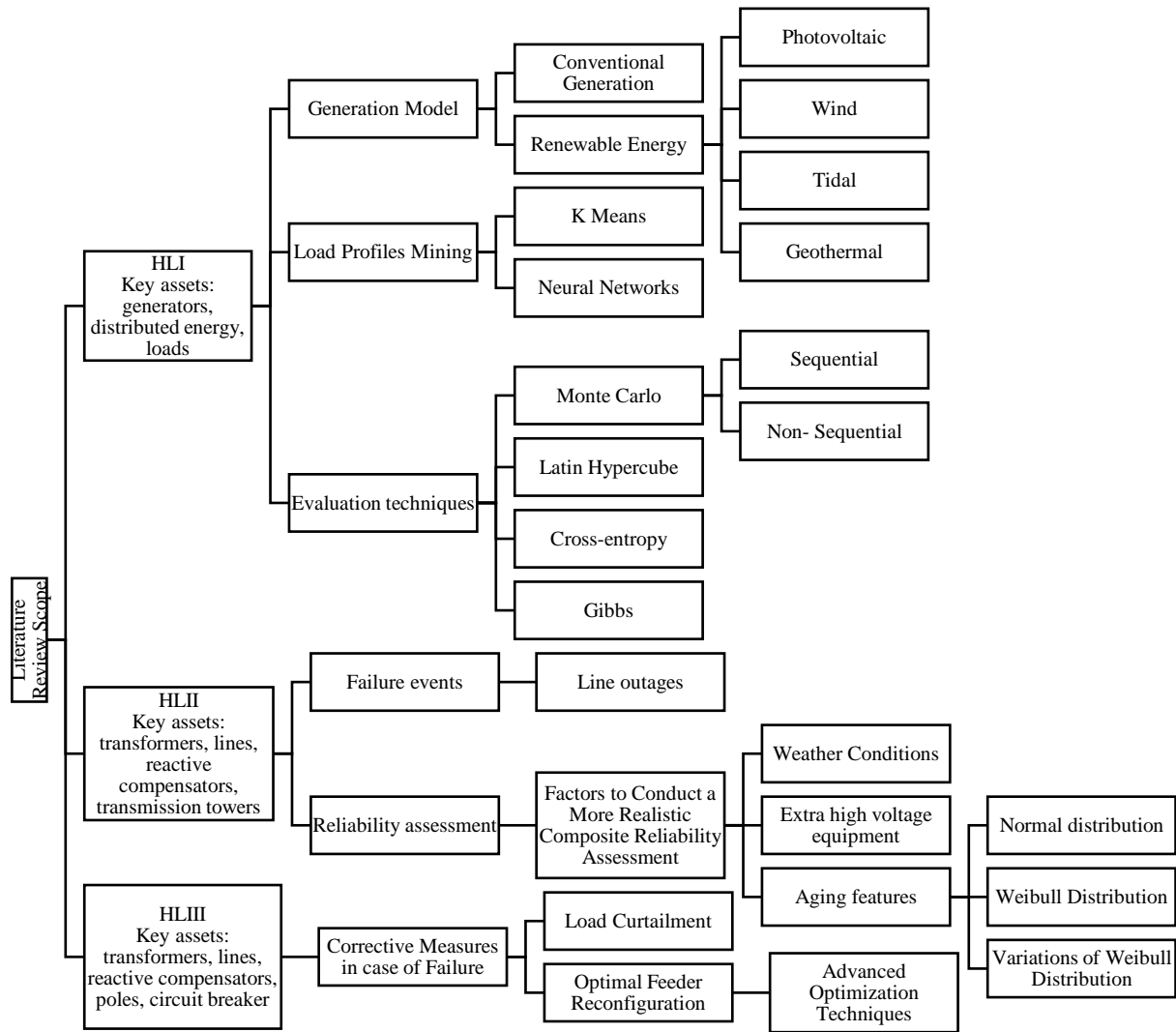
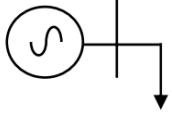
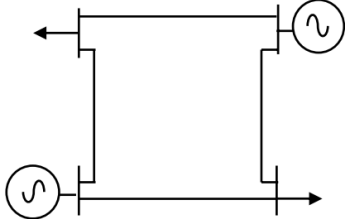
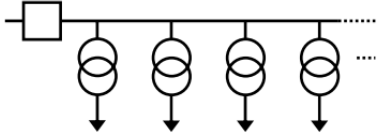


Figure 2.1 Literature review scope of the reliability levels

Table 2.1 Power System Adequacy Hierarchical Levels [29]

Hierarchical Level	Power System Level	Description
I	 <p>Figure 2.2 Generation System Representation</p>	It corresponds to the ability to supply the total energy demand by considering only the power sources installed in the power system. It assumes that transmission and distribution systems are 100% reliable.
II	 <p>Figure 2.3 Transmission System Representation</p>	It corresponds to the ability of the generation-transmission system to supply the demand. It evaluates the impact of failures on generators, lines, buses, and electrical protections involved in the power systems.
III	 <p>Figure 2.4 Distribution System Representation</p>	It encompasses the generation, transmission, and distribution system. It evaluates the adequacy in the main load points located in the primary distribution circuits and considers any component failure installed in the power system.

In the last decade, the use of renewable power in the electricity generation has become popular in most of the developed countries [38]–[40]. This is due to the economic and environmental benefits that it presents to power utilities. For this reason, researchers around the globe are developing new reliability models of renewable power generation. Such models are based on the statistical nature of the renewal source. For wind power generation, the wind speed is characterized by variations of a Weibull probability distribution function [13], [41]. For a photovoltaic generation, the solar irradiance forecast is modelled using variations of the Normal probability distribution function [42], [43]. For tidal and geothermal power generation, there is still much work to do because there is no unanimity in the literature about their reliability models. Nevertheless, stochastic sampling method [44] and

predictive reliability-based indicators [45] are employed to adjust the behaviour of these energy sources.

In regard to the load profile, literature provides different techniques to describe it. Among the existing models, clustering by k-means highlights due to its fast convergence [46]. However, during the last 15 years, the power system load data set have been increasing at a fast rate, reaching a new paradigm called 'big data' [47]. Academics and power industry engineers are looking for novel and robust techniques to deal with these large or complex data sets. To exemplify this fact, reference [48] presents a load demand model using a modified support vector regression, which consists of mapping the training data to a space of greater dimension through a non-linear mapping. The results reveal that the proposed model has a higher degree of prediction accuracy and stability in comparison to traditional loads models. Another innovative technique is exhibited in [49], which offers a novel approach of two stages to classify the energy consumptions profiles. The first stage evaluates the data for the intra-cluster similarity of energy consumption patterns, while the second stage linearizes the complex energy patterns using interpolant and curve-fitting techniques. A more comprehensive study is proposed in [50], in which the authors analyse the load profiles using deep neural networks.

The determination of the operating states of each unit generation is fundamental to proceed with the HLI reliability evaluation. Every state of a unit is determined by applying sampling methods, such as Monte Carlo simulation [51], Cross-Entropy [52], Gibbs [53], and Latin Hypercube [54]. Among the exposed methods, Monte Carlo simulation method appears as the most employed at HLI [55]. The reason is that at this level the computational burden is not so exhaustive in comparison to other levels [56].

Although literature presents different reliability evaluation techniques, the main difference between them lies in the generation and load profile models. A missing element

on these publications is the quantification of the degradation of the component due to aging, which is not clearly identified.

2.1.2 HLII: Transmission

The second hierarchical level focus on risk events that affect the transmission system [33]. In this level, lines outage is a common scenario to analyse since it produces several negative impacts on the power system performance [57]. A line outage may produce variation in the bus voltage magnitude, leading to a voltage instability [58]. Another fact to consider is that some lines may carry more current, causing an increment in power losses [59]. The problem can be extended to cascade failures, driving to a blackout in the worst-case scenario [60]. In the published literature, load curtailment appears as a corrective action to address line outage incidences [32]. This is formulated as an objective function described in the optimal power flow, as evidenced in [6], [61], [62]. The main drawback with load curtailment is that causes an increment in the expected energy not supplied of the system.

To quantify the reliability at the transmission level, a composite system reliability assessment is required [63], [64]. During the assessment, every operational state of each component is analysed to define the final state of the system [65]. In order to conduct a more realistic HLII reliability analysis, some studies can incorporate different phenomena into the reliability model of the components. For instance, [66] considers the uncertainties due to extreme weather conditions and its impact on the occurrence of a cascading failure event, resulting in a flexible restoration model that is useful for practical purposes. In [67], authors examine the influence of installing Extra High Voltage (EHV) AC XLPE Underground Cables (UGCs) on the Netherlands transmission reliability level, bringing a new reliability model for undergrounds cables. In [68], aging failures with Normal and Weibull distribution functions are introduced, with a view of conducting a more accurate reliability evaluation. This last point is the direction in which the state of the art is moving. Researchers around the

globe are looking for innovative models that accurately describe the reliability model of the components.

2.1.3 HLIII: Distribution

The third hierarchical level focus on risk events that affect the distribution system [33]. Similar to HLII, line outages is a common event to study [69]. At this level, load curtailment can be used as a corrective measure, nonetheless, reconfiguration strategy, and distributed energy are becoming popular at present day.

The findings of the use of renewables energies on distribution system reliability are vast. Authors in [70]–[72] determined a reduction of average interruption and average interruption frequency in the distribution system due to the incorporation of photovoltaic (PV) generations. Results in [73]–[75] reveal the installation of wind power generation produces a reduction on the expected energy not supplied, which represents a positive impact of the reliability of the distribution system. References [76]–[78] show improvements on the loss of load probability and expected energy not served reliability indices when energy storage is installed into a distribution system. The economic benefits of hybrid system generation on distribution system reliability are exposed in [79]–[81].

Reliability enhancement using optimal feeder reconfiguration is also well defined in the literature. The key idea is to find the optimal electrical path that reduces power losses of the network and the customer interruption costs simultaneously. The main difference between publications lies in the problem definition and optimization technique employed. A sample includes reference [82], in which a novel self-adaptive modification method based on the clonal selection algorithm is employed to minimize reliability cost. The novelty of the algorithm is its ability to search the problem space globally, which in contrast to traditional metaheuristics techniques, the global search mechanism of the proposed approach inserts an extra population to escape from local optima, resulting in a robust optimization

technique. Authors in [83] propose a new multi-objective improved shuffled frog leaping algorithm to minimize the average interruption frequency index (SAIFI), system average interruption duration index (SAIDI), average energy not supplied (AENS) and the total active power losses. The algorithm is based on a multi-objective improved shuffled frog leaping optimization technique in combination with fuzzy clustering technique. The results reveal its feasibility and the efficiency in comparison with the genetic algorithm, particle swarm optimization and traditional shuffled frog leaping optimization technique. In [84], feeder reconfiguration is carried out using annealed local search to minimize the SAIFI, SAIDI and momentary average interruption frequency index (MAIFI). Even though the emergence of novel reconfiguration strategy enables a reliable better system performance, the potentials from a more robust optimization technique are still waiting to be exploited.

2.2 Bathtub Curve and Aging Models

There are several stochastic models [85]–[89] to evaluate the reliability of a power system component. In all these models, the components are analysed using their probability distribution functions. For the simplicity, most of the publications [85]–[87] employ an exponential distribution function, leading to a time-independent failure rate. This assumption underestimates the aging of the component and brings inaccuracies in a realistic reliability evaluation. Certain efforts have been made to model aging using Weibull distribution functions [88], [89]. However, literature [90]–[93] reports that the bathtub curve is an accurate model to describe the failure rate of repairable components. This curve is divided into three main stages. The first stage is named as infant mortality and during this stage, the failure rate exponentially decreases until reaching its minimum value [94]. Then, the useful life stage takes place in which failure rate stabilizes taking a constant value [94]. The last stage is known as wear out and during this period the failure rate increases at a fast rate [94].

Studies [95]–[97] that consider a constant failure rate in their analysis, only focus their attention on the useful life stage. This supposition disregards aging and leads to unreliable results. In the existing literature appears more exhaustive publications that employ the full bathtub curve for different reliability assessments. Authors in [98] determine a realistic high-voltage direct current transmission system reliability indices by using the bathtub curve to model the failure rate of all components installed in the system. Reference [99] implements an innovative algorithm to assess the reliability of a power system that contains high penetration of photovoltaic (PV) system. The algorithm also includes the bathtub curve to model the failure rate of the PV system. A more detailed study is presented in [100], which introduces six kinds of failure models (including bathtub curve) to evaluate the reliability of proximity sensors of the leading-edge flap in civil aircraft. Although these publications offer a pathway to describe the aging of the component using the bathtub curve, a limitation on them is the use of an alternating renewal process of two operational states to define the reliability model of the components. The use of the bathtub curve without recognizing the different operational states at each stage of the curve could bring unrealistic outcome and hence could under-estimate the true impact of aging.

2.3 Reactive Compensation for Reliability Enhancement

Reactive compensation is defined as the management of reactive power to improve the performance of the power system. Its applications include power factor improvement [101], power losses reduction [102], voltage stability improvement [103] and reduction in electricity bill [104]. The reactive power compensation applications are related to the power quality field. However, it can be extended to other power system fields.

From the reliability point of view, reactive power compensation can be employed as a contingency measure to reduce the load shedding. For this purpose, some publications suggest the employment of capacitor bank [105]–[107]. This is attributed to its acquisition

cost, which is lower in comparison to other compensators. Nevertheless, they present a drawback as these devices lack of dynamic reactive power injection [108]. The operation of the capacitor bank is limited by its static capacity. Although literature presents switched capacitor bank as a solution to this problem [109], their stepwise power injection is still not enough to reach the optimal power system performance [110].

Another suitable option to handle reactive compensation is the Flexible Alternating Current Transmission System (FACTS). These devices are power electronics-based systems, and their main feature is their dynamic control operation [110]. The first FACTS applications in power system reliability appear in [111]–[114]. In [111], thyristor controlled series capacitor (TCSC) is connected between two different lines to increase transmission capacity. As a result, the loss of load expectation (LOLE) and loss of energy expectation (LOEE) are decreased, leading to better reliability performance of the power system. Subsequently, the study is extended by incorporating a more precise TCSC reliability model [112]. Reference [113] investigates the impact of a unified power flow controller (UPPC) on power system reliability. The methodology consists of installing the UPPC to regulate the natural power-sharing of the transmission lines, then, a composite system reliability assessment takes place to quantify power systems reliability. The reliability indices validate the positive influence of the UPPC. In [114], authors propose to combine static synchronous series compensator (SSSC) with a fixed capacitor to introduce a novel hybrid compensating scheme, which is used to regulate the transmission infeed impedance. As a result, transmission system capacity is increased, and the system reliability is strengthened. These publications are important since they inspired other researchers to investigate the influence of other FACTS controllers in power system reliability.

Nowadays, researches are focusing on maximizing system reliability using different FACTSs. The main deficiency in the existing literature is that does not offer an inclusive

study that deals with problem formulation to address optimal planning and operation of FACTS, such that, it maximizes system reliability. That is, [115] analyses system reliability by incorporating static var compensators (SVC) into the power system, without considering optimal planning and operation of FACTS; the same concern goes for [116], [117] with the difference that they use other FACTS controllers. Authors in [118] integrate the optimum placement for SVC, however, their optimum strategy dispatch is not considered. In [119], [120] propose an approach to maximize the reliability benefits using TCSC [119] and SSSC [120], however, the optimal sizing and placement of FACTS are not presented.

Recent investigations present new approaches concerning the optimization techniques for reliability enhancement using reactive compensation. For example, [121] implements a mixed-integer dynamic optimization to determine the allocation of dynamic reactive support; the authors in [121] employ a bacterial foraging oriented method by particle swarm optimization algorithm in order to find the optimal location and size of the available FACTS, such that investment costs are minimized; [122] investigates optimal load curtailment model for congestion management using various FACTS devices like STATCOM, SSSC, UPFC, IPFC, and GUPFC; [123] propose an application of Cuckoo search algorithm to determine optimal location and sizing of SVC to improve power system reliability. Although the presented approaches are effective to reach the global solution to different optimization problems, deeper analysis on them reveals that a challenge is to reduce the computational burden.

Besides the above-presented advantages of reactive power compensators in system reliability, faster optimization techniques with the ability to meet power system reliability challenges need to be explored.

2.4 Maintenance Evolution

Maintenance concept firstly appears during the industrial revolution. By that time, maintenance was considered as a type of ‘necessary rework’ with low relevance for the industry. It was not until the Second World War, where maintenance became important. The first applications appeared in the aviation industry, chemical and petrochemical plants, and nuclear power industry [124]. Maintenance actions allowed continuity of service, driving in huge economic savings to the industry.

British Standards define maintenance as [125]:

“The combination of all technical and administrative actions, including supervision actions, intended to retain an item in, or restore it to, a state in which it can perform a required action.”

Nevertheless, the concept of maintenance has been evolved over time. The first maintenance scheme that appears in the early stages of the maintenance history is the corrective maintenance (CM). CM focuses on the identification, isolation, and rectification of a fault so that the failed component can be restored to an operational condition within the tolerances or limits established for in-service operations. CM is carried out after failure detection and is aimed at restoring an asset to a condition in which it can perform its intended function [126]. The main deficiency with CM is that in some circumstances is preferable to proceed with the renovation of the component rather than maintenance. For example, in case of severe damage in the core of a transformer, the cost of CM is close to the cost of a new transformer acquisition [127], therefore CM is not affordable for this particular case. To overcome CM drawback, in 1998 the IEEE presented the Standard 1902, *IEEE Guide for Maintenance, Operation, and Safety of Industrial and Commercial Power Systems* setting the foundations for preventive maintenance in power industry (PM) [128]. The PM is carried out at predetermined intervals or according to prescribed criteria, aimed at reducing the

failure risk or performance degradation of the equipment. At difference with CM, PM proposes maintenance cycles according to the need of the component. Nevertheless, every component operates under different circumstances, and component maintenance should be scheduled based on the reliability model of the component. This could potentially bring a higher benefit in comparison with the periodic preventive maintenance (PPM) strategy. In response to this need, the maintenance evolved from PM to predictive advances. Predictive maintenance scheme proposes a maintenance schedule optimization problem, of which the typical objective is to minimize the occurrence of failures of a component while maximizing profit [129]. The predictive maintenance strategies are categorized as Reliability-Centred Maintenance (RCM), Risk-Based Inspection (RBI), and Risk-Based Maintenance (RBM), which are described in Table 2.2. Nowadays, maintenance has evolved into a new paradigm within the ‘Asset Management’. This is defined as a comprehensive maintenance plan that combines risk-controlled optimised and life-cycle management of an asset [130]. The strategies under the scheme are based on smart-inspections (SI) [25], smart-devices (SD) [26] and smart-services (SS) [27], resulting in a smart maintenance (SM) model. A schematic representation of the evolution of maintenance is presented in Figure 2.5.

Table 2.2 Predictive Maintenance Strategies

Reliability Centred Maintenance (RCM)	Risk-Based Inspection (RBI)	Risk Based Maintenance (RBM)
The main objective of RCM according to [131] is <i>“to reduce the maintenance cost, by focusing on the most important functions of the system, and avoiding maintenance actions that are not strictly necessary.”</i>	The objective of RBI according to [132] is <i>“to determine what incident could occur in the event of an equipment failure, and how likely is that incident could happen.”</i>	The objective of RBM according to [133] is <i>“to reduce the overall risk of facilities.”</i>

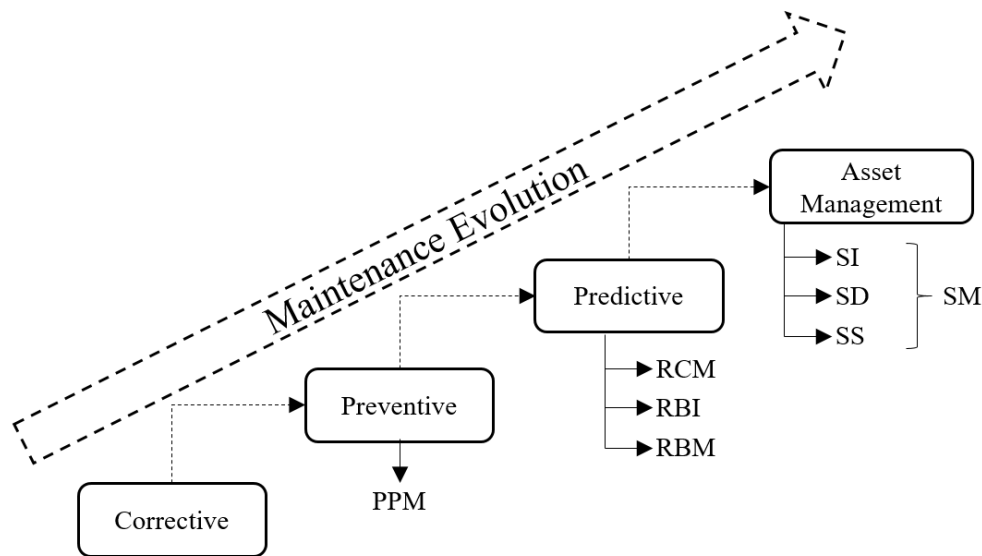


Figure 2.5 The evolution of maintenance

2.5 Risk and Maintenance of Power Generators

In modern power systems, risk presents different facets depending on the hazard situation that may arise. For example, random failures that cannot be controlled by operators [86]; uncertainties in the loads that make load forecast to be inaccurate [134]; energy market that fluctuates the prices depending on the economy of the country [135]; interruptions of service that can be engendered due to natural disasters [136].

Risk evaluation becomes a vital commitment to the power industry. For this reason, the power industry is incorporating new maintenance strategies into their management schedules. For instance, [137] presents a method that uses the supply chain construct for designing power grids that are relatively insensitive to failure in the integrated generation and transmission system; [138] suggests an improved power transformer maintenance plan for reliability centred management, which employs Markov theory to model it; a wide-ranging study in maintenance field is presented in [139], which integrates preventive maintenance strategies in an optimal way to maintain the desired availability and safety integrity level while minimizing the maintenance intervals using Bayesian networks.

Power system planning and operation starts with the power generation. At this level, generator maintenance is vital to preserving the continuity of service in the power system. Normally, a routine generator PM includes turbine functional checks and inspection; turbine bearing lubrication and inspection; gearbox inspection; gearbox oil condition analysis and oil changes; gearbox bearing inspection and lubrication; drive belt inspection and replacement; drive coupling inspection; generator inspection; generator bearing inspection and lubrication; hydraulic system inspection; hydraulic system oil condition analysis and oil changes; check all sensors operate correctly; check controller functions correctly; inspection of intake area, impounding structures, pipeline, sluice(s) [140]. Among the predictive maintenance strategies, RCM is widely used to optimize preventive generators maintenance tasks [141]. The literature presents variations of RCM schedule by incorporating different optimization techniques and objective functions. For instance, [142] presents an approach that uses a genetic algorithm (GA) to determine an effective generator maintenance schedule that maximizes the generation adequacy economic benefit. In [143], a novel generators maintenance strategy is proposed. The objective is to minimize the sum of squares of the reserve generation via system reliability analysis and cost/benefit analysis of generators using a hybrid approach that combines GA and simulated annealing. The findings of this research reveal that the proposed approach is less sensitive to optimization problem parameters variations and offer an effective alternative for generator maintenance planning. A more exhaustive generator maintenance study is conducted in [144] since it presents the maintenance schedule as a multi-objective optimization problem from the reliability and economic perspectives. The variables involved to formulate the problem are the sum of squares of the reserve generation, loss of load expectation and total operating cost. The effective PM schedule that maximizes system reliability is obtained using the Ant Lion Optimizer (ALO) in combination with fuzzy decision mechanism defined by the authors.

The results are encouraging and indicate the viability of the proposed ALO technique. Even though the presented publications expose different approaches for an effective maintenance plan, a challenge in this context is to incorporate other relevant factors to the existing models. Most of the presented studies consider the availability of the component as the predominant factor to schedule preventive maintenance. However, another factor that could be considered is the operational risk parameter. Such parameter is used to describe in percentage terms the hours that the component function under its different operational states since the last maintenance. If the operational risk is avoided, it could bring inaccuracies to the maintenance schedule and may not lead to the optimum benefits. Certain efforts have been made to incorporate the generator's operating hours into RCM strategy [145], [146]. The limitation of these studies is the low information related to the quantification of the effort required during maintenance. Therefore, there is a need to incorporate a more comprehensive maintenance strategy that considers the operational risk to schedule effective preventive maintenance of power generators.

2.6 Summary

This chapter presents a comprehensive literature review of the different methods used to assess the adequacy at the three hierarchical levels. The incorporation of renewable energy and reactive compensators to enhance the reliability of the power system facilities are discussed. The chapter exposes different models to describe the aging effect, and among them, the bathtub curve appears as the most comprehensive model. A challenge in recognizing the operational states at each stage of the bathtub curve is emphasized. The need for faster and robust optimization techniques to maximize the accuracy of the reliability of a power system is identified as a potential research gap. The chapter also presents an epistemology of the evolution of maintenance. The last section of the chapter discussed

different maintenance strategies to mitigate the risk of power generators. The importance of operational risk and need to quantify the effort during maintenance actions are highlighted.

Chapter 3: Reliability Assessment Theories

This chapter presents existing theories to evaluate the reliability of a power system. The chapter is divided into five sections. Section 3.1 describes the Markov chain and the alternating renewal process to describe the traditional reliability model of a repairable components. Section 3.2 presents typical failure and repair rates for hydro and thermal unit generation. Section 3.3 exhibits the failure and repair rate for capacitors bank, static var compensators and synchronous var compensator. Section 3.5 exposes different studies related to risk and reliability evaluation of power systems in their three hierarchical levels. Finally, the last section brings a summary of the chapter.

3.1 Reliability Concept

The ability of a component to offer a continuous operation in a given time interval is defined as reliability [65]. This can be quantified using the operational records of the component. Literature presents two schemes for reliability evaluation: 1. Analytical methods; 2. Probabilistic methods [65]. Based on these, it is possible to estimate future failures that can be avoided by taking preventive actions. Another advantage that these schemes offer lies in the evaluation of historical performance and simulation of past behaviour of the component. The reliability evaluation can be employed to analyse the operational state of a component in the past or future. An illustration is given in Figure 3.1.

Most of the probabilistic methods focus on determining the reliability, maintainability and availability of a system. Mathematically, the reliability is the probability of a component of being in an operating state, which is given by its probability function f_f . If the time to failure is defined by τ_f , then [147]:

$$R(t) = P(t > \tau_f) = \int_{\tau_f}^{\infty} f_f(t) dt \quad (3.1)$$

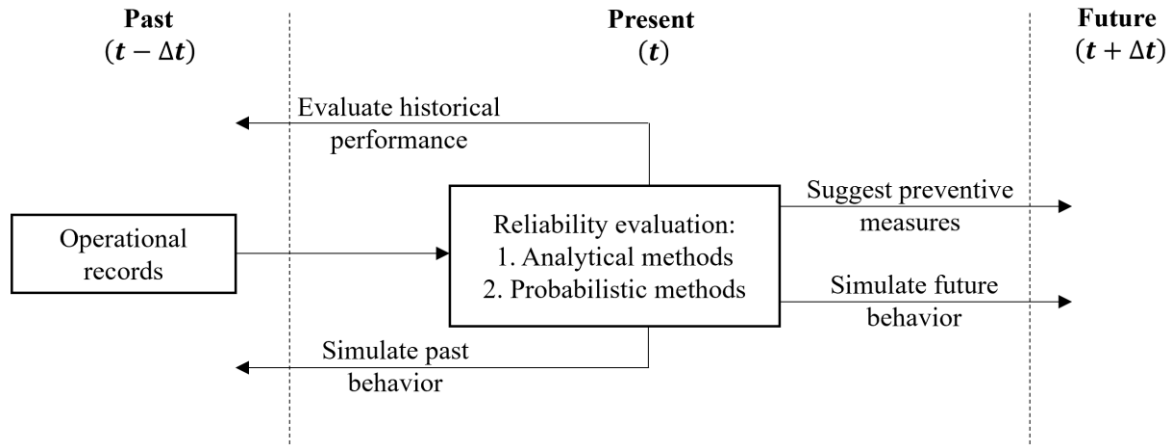


Figure 3.1 Reliability Schemes [148]

On the other hand, the maintainability is the probability of executing an effective repair within a time τ_r , which is defined by the probability density function f_r . Therefore,

$$M(t) = P(0 < t < \tau_r) = \int_{\tau_f}^{\infty} f_r(t) dt \quad (3.2)$$

The availability refers to the probability of being in operation during a specific time interval. Unlike reliability, it incorporates the maintainability information. In order to proceed with availability calculation, two operational considerations are taken into account [149]:

1. The system operates correctly between time intervals $(0, \tau_f]$. This implies that probability of this event happening is given by $R(t)$.
2. The system is operating appropriately since the last repair at time τ_u , such that $\tau_u < \tau_r$. The probability of this condition is given by $\int_0^{\tau_r} R(t - \tau_u) f_r(t) dt$.

Consequently, the availability can be defined as:

$$A(t) = R(t) + \int_0^{\tau_r} R(t - \tau_u) f_r(t) dt \quad (3.3)$$

As can be appreciated, the last term is difficult to deal with, and for this reason stochastic models are used.

3.2 Alternating Renewal Process

As presented in the last section, the availability model involves differential equations, which makes complex to reach the solution. Nevertheless, Markov chain can be employed to facilitate the process. Markov chain is a representation of all possible states in a diagram connected between them by variables called transition rates. For instance, Figure 3.2 presents a space state diagram of a repairable component. Its reliability model is represented as an alternating renewal process between two states: 1. Operating (Available); 2. Not in service (Unavailable) [36]. The transition rate that goes from state “1” to “2” is denoted by λ and it represents the failure rate of the component, while the transition rate that goes from “2” to “1” is denoted by μ and it represents the repair rate of the component. As in most of the published literature [150]–[153], in this section λ and μ comes from an exponential distribution function. Hence, these values are considered as time independent.

In order to find the solution of the model, let Δt defined as the time interval. This is considered very small in such a way that the occurrence probability of more than one fault or repair is also very small, and the occurrence of these events can be neglected. Then, the probabilities of failure and repair are as given in (3.4) and (3.5), respectively.

$$P_f(t) = \lambda \Delta t \quad (3.4)$$

$$P_r(t) = \mu \Delta t \quad (3.5)$$

On the other hand, the probability of being in state “1” at time $t + \Delta t$ is determined by the sum of the probability of not having failed in Δt and the probability of being failed at time t and having been repaired in Δt . Mathematically, this is described as given in (3.6).

$$P_1(t + \Delta t) = P(t) (1 - P_f(t)) + P_2(t) P_r(t) \quad (3.6)$$

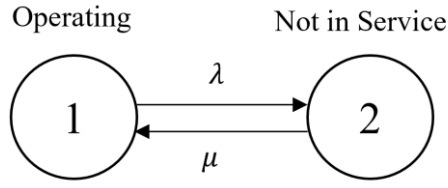


Figure 3.2 Markov chain of a repairable component [148]

Focusing on state “2”, its probability at time $t + \Delta t$ is equal to the probability of being failed in t and not having been repaired in Δt plus the probability of being non-failed in t and having failed in Δt . Therefore,

$$P_2(t + \Delta t) = P_2(t) + (1 - P_r(t)) + P_1(t)P_f(t) \quad (3.7)$$

By replacing (3.4) and (3.5) in (3.6):

$$P_1(t + \Delta t) = P_1(t)(1 - \lambda\Delta t) + P_2(t)\mu\Delta t \quad (3.8)$$

$$\left. \frac{P_1(t + \Delta t) - P_1(t)}{\Delta t} \right|_{\Delta t \rightarrow 0} = -\lambda P_1(t) + \mu P_2(t) \quad (3.9)$$

$$\frac{dP_1(t)}{dt} = -\lambda P_1(t) + \mu P_2(t) \quad (3.10)$$

By replacing (3.4) and (3.5) in (3.7):

$$P_2(t + \Delta t) = P_2(t)(1 - \mu\Delta t) + P_1(t)\lambda\Delta t \quad (3.11)$$

$$\left. \frac{P_2(t + \Delta t) - P_2(t)}{\Delta t} \right|_{\Delta t \rightarrow 0} = -\lambda P_1(t) - \mu P_2(t) \quad (3.12)$$

$$\frac{dP_2(t)}{dt} = \lambda P_1(t) - \mu P_2(t) \quad (3.13)$$

Expressing (3.10) and (3.13) in matrix form:

$$\frac{d}{dt} \begin{bmatrix} P_1(t) \\ P_2(t) \end{bmatrix} = \begin{bmatrix} -\lambda & \mu \\ \lambda & -\mu \end{bmatrix} \quad (3.14)$$

In order to simplify the analysis, $\mathbf{P}(t)$ is defined as the probability vector of all possible states, $\dot{\mathbf{P}}(t)$ is defined as the derivative probability vector of all possible states, and \mathbf{H}^T is defined as the transpose of the stochastic matrix of transition states, then (3.14) can be expressed as follows:

$$\dot{\mathbf{P}}(t) = \mathbf{H}^T \mathbf{P}(t) \quad (3.15)$$

The process continues by employing Laplace transform ($t \rightarrow \varpi$) to (3.15):

$$s\mathbf{P}(\varpi) - \mathbf{P}(\mathbf{0}) = \mathbf{H}^T \mathbf{P}(\varpi) \quad (3.16)$$

$$\mathbf{P}(\varpi) = \frac{\mathbf{P}(\mathbf{0})}{\varpi - \mathbf{H}^T} \quad (3.17)$$

Applying inverse Laplace Transform ($\varpi \rightarrow t$) to (3.17):

$$\mathbf{P}(t) = \mathbf{C}e^{\mathbf{H}^T t} \quad (3.18)$$

where \mathbf{C} is the vector that contains values given by the initial conditions.

The solution for the system still being complicated since the matrix \mathbf{H}^T appears as exponent. To simplify the solution, the Putzer's spectral formula [154] is applied, in which the term $e^{-\mathbf{H}^T t}$ can be expressed as a function of the eigenvalues χ and eigenvectors \mathbf{v} of \mathbf{H}^T . This is shown below:

$$e^{\mathbf{H}^T t} = \sum_{s=1}^{NS} \mathbf{v}_s e^{\chi_s t} \quad (3.19)$$

where NS is the number of states. Therefore, the general solution for the Markov chain is:

$$\mathbf{P}(t) = \sum_{s=1}^{NS} c_s \mathbf{v}_s e^{\chi_s t} \quad (3.20)$$

The alternating renewal process presents a transition matrix $\mathbf{H}^T = \begin{bmatrix} -\lambda & \mu \\ \lambda & -\mu \end{bmatrix}$, then:

$$\chi_1 = 0; \chi_2 = -\lambda - \mu \quad (3.21)$$

$$\mathbf{v}_1 = \begin{bmatrix} \mu/\lambda \\ 1 \end{bmatrix}; \mathbf{v}_2 = \begin{bmatrix} -1 \\ 1 \end{bmatrix} \quad (3.22)$$

In order to get the values for c , it is assumed that at $t = 0$ the component is operating ($P_1|_{t=0} = 1; P_2|_{t=0} = 0$). Therefore, (3.20) can be written as:

$$\begin{bmatrix} 1 \\ 0 \end{bmatrix} = c_1 \begin{bmatrix} \mu/\lambda \\ 1 \end{bmatrix} e^0 + c_2 \begin{bmatrix} -1 \\ 1 \end{bmatrix} e^{(-\lambda-\mu)(0)} \Rightarrow c_1 = \frac{\lambda}{\lambda + \mu}; c_2 = -\frac{\lambda}{\lambda + \mu} \quad (3.23)$$

Finally, the reliability model of the alternating renewal process is given in (3.24).

$$\begin{aligned}
P_1(t) &= \frac{\mu}{\lambda + \mu} + \frac{\lambda}{\lambda + \mu} e^{-(\lambda + \mu)t} \\
P_2(t) &= \frac{\lambda}{\lambda + \mu} - \frac{\lambda}{\lambda + \mu} e^{-(\lambda + \mu)t}
\end{aligned}
\tag{3.24}$$

It is relevant to highlight that the availability and unavailability is represented by P_1 and P_2 , respectively.

3.3 Reliability Features of Electrical Power Generators

Electrical Power generators are essential components in power systems since they supply the demand. In the following sections, the reliability features (failure and repair rates) of hydro and thermal power generators are discussed.

3.3.1 Hydro Unit Generation

From the reliability point of view, a hydro generator is a series system comprised with five main parts: stator, rotor, shaft, wicket gate, and turbine blades. A series system is characterized by its weakest link, that is, the failure rate of the system mainly depends on the most vulnerable component [155]. For a hydro generator, the turbine is the most vulnerable component since it is the only one that is in direct contact with water flow [156]. For this reason, many reliability studies [156]–[158] focus their attention on the turbine. Therefore, failure rate of hydro generator is given by the turbine reliability characteristics.

Table 3.1 Reliability Features of Hydro Unit Generation [6], [34], [157], [159]–[164]

Hydro power generation	Turbine	Failure rate [1/yr]	Repair rate [1/yr]
Small power < 10 MW	Pelton	$1.0 \leq \lambda \leq 3.0$	$180 \leq \mu \leq 220$
	Francis	$2.0 \leq \lambda \leq 3.0$	$170 \leq \mu \leq 200$
	Kaplan	$2.0 \leq \lambda \leq 3.0$	$165 \leq \mu \leq 230$
Medium $10 \text{ MW} \leq \text{power} < 30 \text{ MW}$	Pelton	$1.5 \leq \lambda \leq 4.0$	$150 \leq \mu \leq 189$
	Francis	$2.3 \leq \lambda \leq 3.4$	$130 \leq \mu \leq 190$
	Kaplan	$2.2 \leq \lambda \leq 3.6$	$127 \leq \mu \leq 170$
Large Power $\geq 30 \text{ MW}$	Pelton	$2.9 \leq \lambda \leq 6.0$	$150 \leq \mu \leq 170$
	Francis	$2.0 \leq \lambda \leq 5.0$	$120 \leq \mu \leq 180$
	Kaplan	$2.5 \leq \lambda \leq 5.0$	$120 \leq \mu \leq 180$

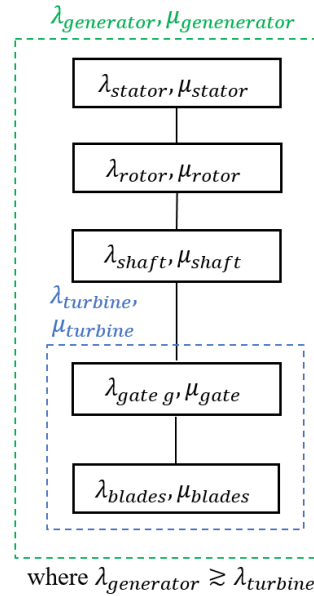


Figure 3.3 Hydro generator reliability topology

Figure 3.3 shows a schematic diagram representing the reliability topology of a hydro generator. Table 3.1 presents the registered [6], [34], [157], [159]–[163] transition rates for small, medium, and large hydro power generation.

3.3.2 Thermal Unit Power Generation

Thermal unit power generations follow a combined thermodynamic cycle to produce energy [165]. The generator incorporates a gas turbine that compresses air and mixes it with fuel that is heated to a very high temperature [166]. The hot air-fuel mixture moves through the gas turbine blades, making them spin (kinetic energy). The generator drive shaft transform the kinetic energy into electrical energy [166]. This process is supported by a heat recovery steam generator that captures exhaust heat from the gas turbine and creates steam. The steam is delivered to the steam turbine [166], producing an extra kinetic energy that is used to generate additional electricity [166].

Thermal unit generation design mainly depends on the source used to produce the heat, which could be: coal, oil or natural gas [165]. The transition rates registered [6], [163], [167]–[170] are shown presented in Table 3.2.

Table 3.2 Reliability Features of Thermal Unit Generation [6], [163], [164], [167]–[170]

Thermal Power Generation	Heat Source	Failure rate [1/yr]	Repair rate [1/yr]
Small power < 10 MW	Coal	$3.0 \leq \lambda \leq 4.0$	$140 \leq \mu \leq 167$
	Oil	$3.0 \leq \lambda \leq 5.0$	$127 \leq \mu \leq 166$
	Natural gas	$2.3 \leq \lambda \leq 4.0$	$113 \leq \mu \leq 140$
Medium $10 \text{ MW} \leq \text{power} < 30 \text{ MW}$	Coal	$4.0 \leq \lambda \leq 5.8$	$150 \leq \mu \leq 189$
	Oil	$4.5 \leq \lambda \leq 7.0$	$132 \leq \mu \leq 150$
	Natural gas	$3.2 \leq \lambda \leq 4.6$	$130 \leq \mu \leq 179$
Large power $\geq 30 \text{ MW}$	Coal	$5.0 \leq \lambda \leq 7.0$	$200 \leq \mu \leq 230$
	Oil	$6.0 \leq \lambda \leq 9.3$	$160 \leq \mu \leq 190$
	Natural gas	$4.0 \leq \lambda \leq 8.0$	$120 \leq \mu \leq 180$

3.4 Reliability Features of FACTS

FACTS devices present different advantages such as reactive compensation, oscillations damping, voltage support, and increasing network stability [171]–[173]. Its main benefit in comparison with capacitor banks, lies in its dynamic operation that allows varying the injected reactive power with the minimum harmonics [174]. The classification of FACTS is based on the topology of its controllers. After deep scrutiny and with a formal arrangement, Figure 3.4 shows FACTS classification. It is relevant to mention that this research focus on two FACTS, they are: Static Var Compensator (SVC) and Static Synchronous Compensator (STATCOM).

SVC and STATCOM are often in modern power systems accredited to its dynamic and fast response at the need for reactive power compensation. Mathematically, the injected current of these compensators is defined as:

$$I_S = jU_{grid}Y_S(\theta) \Rightarrow Q_{\text{dispatched}} \quad (3.25)$$

where U_{grid} is the system voltage, Y_S is the admittance of the reactive compensator, which appears as a function of the firing angle operation θ . Figure 3.5 and Figure 3.7 show a schematic representation of SVC and STATCOM operation, respectively.

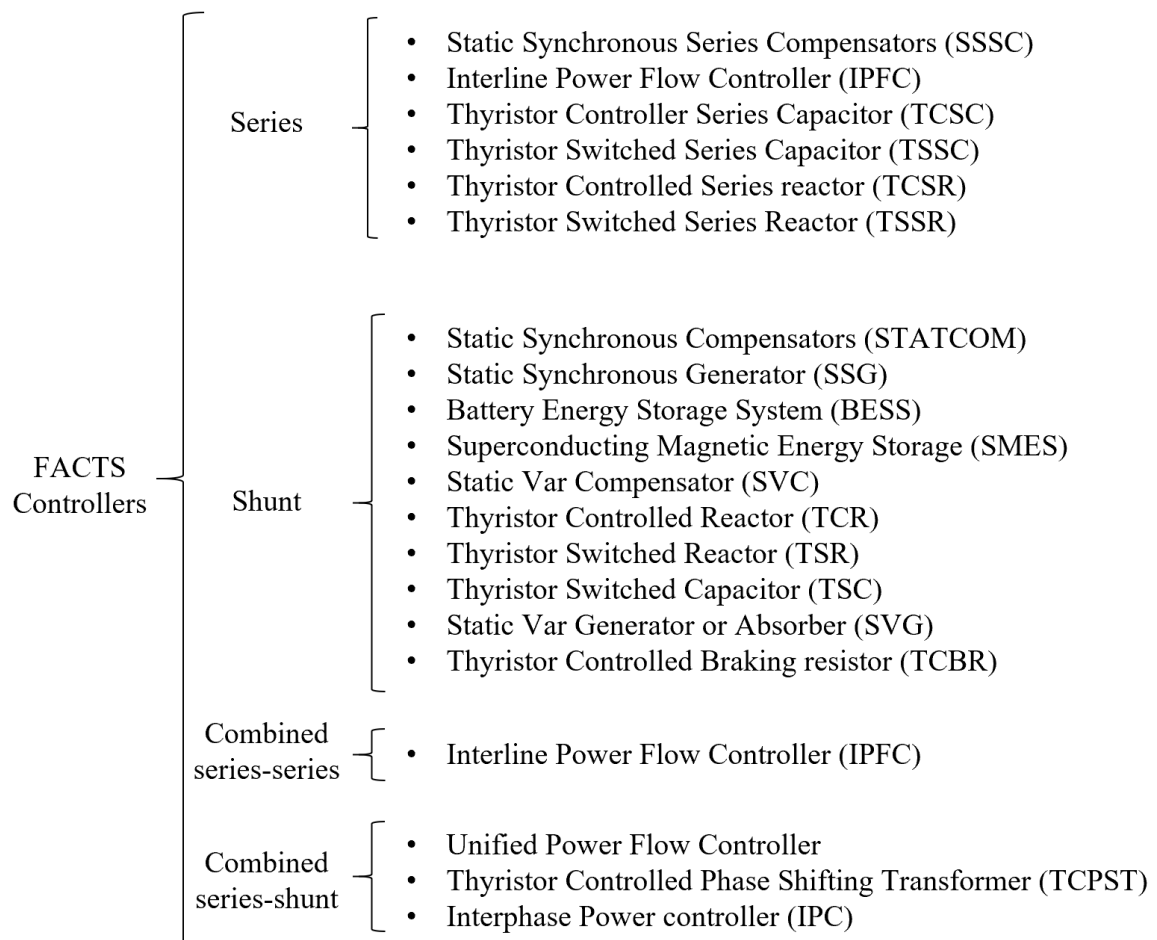


Figure 3.4 FACTS categorization

The SVC and STATCOM involve various components. Nevertheless, Figure 3.6 and Figure 3.8 show that they can be characterized by three fundamental parts. They are: 1. Main Circuit; 2. Auxiliary power supply; and 3. Control system. Each of these presents a failure and repair rate, which are used to create the Markov chain of the system. Figure 3.9, shows the Markov chain that define the reliability model of both compensators. In addition, their transitions rates are presented in Table 3.4 and Table 3.5.

Table 3.3 SVC and STATCOM Electrical Features

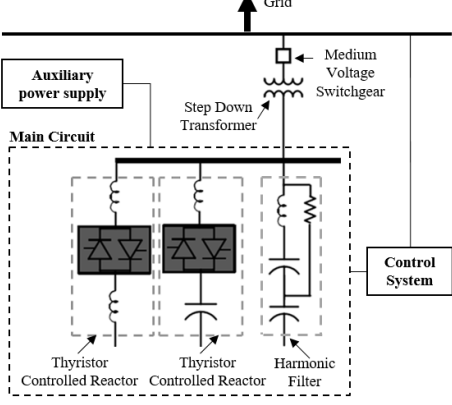
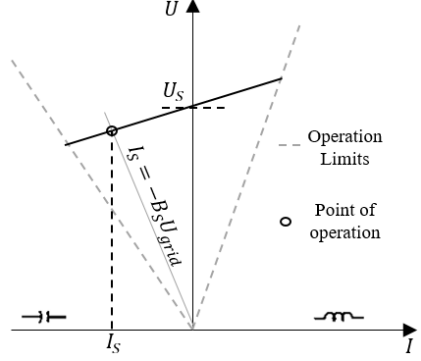
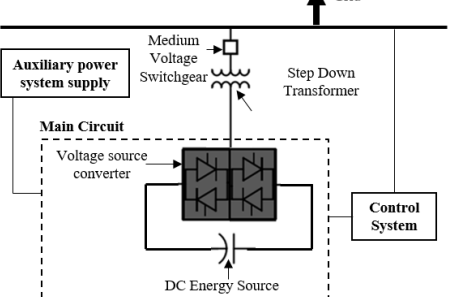
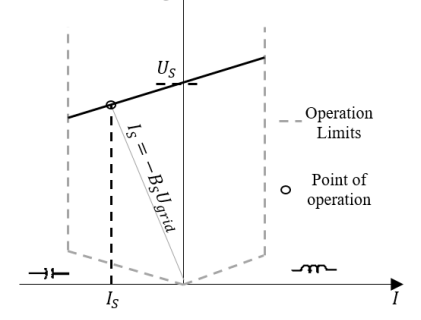
FACT	Electrical Model	Reactive Compensation Model
SVC	 <p>Figure 3.5 SVC electrical circuit [175], [176]</p>	 <p>Figure 3.6 SVC U-I characteristic [177], [178]</p>
STATCOM	 <p>Figure 3.7 STATCOM electrical circuit [179], [180]</p>	 <p>Figure 3.8 STATCOM U-I characteristic [181], [182]</p>

Table 3.4 Static Var Compensator Reliability Features [112], [183]–[186]

Size	System	Failure rate [1/yr]	Repair rate [1/yr]
Small power < 10 MVar	Main circuit	$0.050 \leq \lambda \leq 4.00$	$145 \leq \mu \leq 167$
	Auxiliary power supply	$0.015 \leq \lambda \leq 0.048$	$200 \leq \mu \leq 876$
	Control	$0.0001 \leq \lambda \leq 0.0003$	$995 \leq \mu \leq 4380$
Medium $10 \text{ MVar} \leq \text{power} < 30 \text{ MVar}$	Main circuit	$0.105 \leq \lambda \leq 6.20$	$150 \leq \mu \leq 195$
	Auxiliary power supply	$0.010 \leq \lambda \leq 0.050$	$210 \leq \mu \leq 2190$
	Control	$0.0001 \leq \lambda \leq 0.0004$	$600 \leq \mu \leq 2190$
Large power $\geq 30 \text{ MVar}$	Main circuit	$0.506 \leq \lambda \leq 8.20$	$160 \leq \mu \leq 219$
	Auxiliary power supply	$0.010 \leq \lambda \leq 0.098$	$215 \leq \lambda \leq 1095$
	Control	$0.0001 \leq \lambda \leq 0.0008$	$236 \leq \mu \leq 2190$

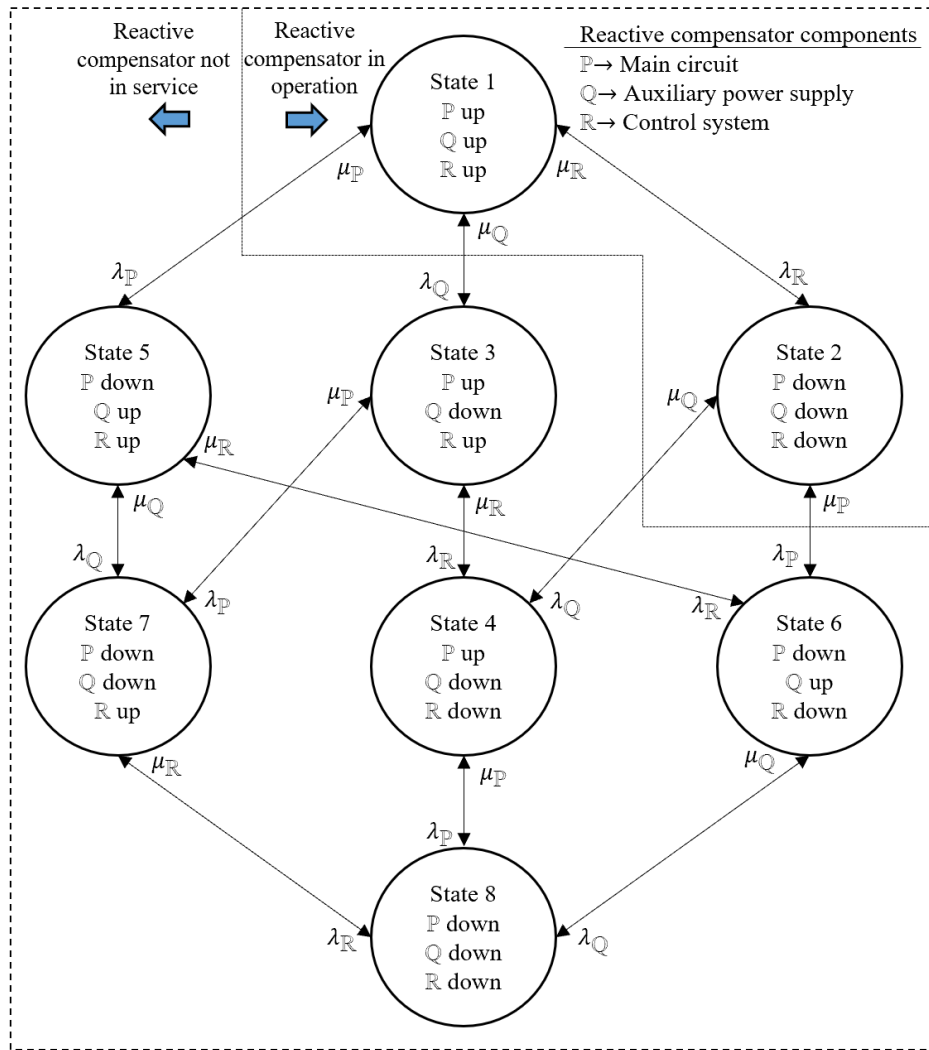


Figure 3.9 SVC/STATCOM reliability model [187]

Table 3.5 Static Synchronous Compensator Reliability Features [186]–[192]

Size	System	Failure rate [1/yr]	Repair rate [1/yr]
Small power < 10 MVA	Main circuit	$1.0 \leq \lambda \leq 6.0$	$130 \leq \mu \leq 180$
	Auxiliary power supply	$0.010 \leq \lambda \leq 0.050$	$205 \leq \mu \leq 900$
	Control system	$0.0001 \leq \lambda \leq 0.0003$	$950 \leq \mu \leq 4280$
Medium $10 \text{ MVA} \leq \text{power} < 30 \text{ MVA}$	Main circuit	$0.23 \leq \lambda \leq 8.60$	$140 \leq \mu \leq 205$
	Auxiliary power supply	$0.012 \leq \lambda \leq 0.070$	$208 \leq \mu \leq 2590$
	Control system	$0.0001 \leq \lambda \leq 0.0004$	$500 \leq \mu \leq 3580$
Large power $\geq 30 \text{ MVA}$	Main circuit	$0.83 \leq \lambda \leq 9.80$	$146 \leq \mu \leq 300$
	Auxiliary power supply	$0.015 \leq \lambda \leq 0.099$	$220 \leq \lambda \leq 1100$
	Control system	$0.0001 \leq \lambda \leq 0.0005$	$205 \leq \mu \leq 3190$

3.5 Reliability Assessment in Power Systems

In all the hierarchical levels, reliability is measured using probabilities, descriptive statistics, operative measures, and deterministic indexes. In the next sections, the required techniques to determine the reliability indices at each hierarchical level are discussed.

3.5.1 Monte Carlo Simulation

Since it is not possible to determine the exact moment when a failure will occur, sampling methods are utilized to estimate the state of the component. Monte Carlo (MC) simulation is the most famous method in reliability field. Literature [193]–[195] reports the method as simple and robust, which makes it feasible for different applications. The method is divided into two: sequential and non-sequential. In the former, the order of the randomized events is relevant in the simulation, while this is not considered in the latter. This causes an increase in the computational burden for sequential MC. Nevertheless, sequential MC presents better accuracy in some applications [196].

Monte Carlo Simulation is applied to power systems to determine the state of each component. The procedure starts by generating a random number between one and zero to every power system component, such that, the state of the σ^{th} component is as given in (3.26).

$$s_{\sigma} = \begin{cases} 1, & \text{Operating} \\ 0, & \text{Not in service} \end{cases} \quad (3.26)$$

The process continues with the calculation of the mathematical expectation of the system state. For this purpose, let define the state of a power system at experiment exp as $S_{exp} = \{s_1, s_2, \dots, s_{NC}\}$. Then, the mathematical expectation of the system state can be expressed as:

$$EXS_{exp} = EXF(S_{exp}) P(S_{exp}) \quad (3.27)$$

where EXF and P represent the experiment function, and the probability event function, respectively. This calculation is repeated for a total number of experiment NE . In every experiment, E_{exp} is recorded.

The procedure finishes at the convergence with the determination of the sample mean value, which can be obtained using (3.28).

$$\widehat{E}XS = \frac{1}{NE} \sum_{exp=1}^{NE} EXS_{exp} \quad (3.28)$$

More details about the method are presented in Algorithm 3.1 [187].

Algorithm 3.1 Monte Carlo Pseudocode

1. **Procedure** of MC
2. **For** $exp = 1$ to total experiment (NE)
3. randomize the states for all components: $S_{exp} = (s_1, s_2, \dots, s_{NC})$
4. define EXF and P
5. evaluate EXF and P in S_{exp}
6. determine EXS_{exp} using (3.27)
7. **Endfor**
8. determine $\widehat{E}XS$ using (3.28)

3.5.2 Generation Adequacy Analysis

The generation adequacy studies the reliability at HLI. The reliability is measured by different indices, such as the loss of load expectation (LOLE) given in hr/yr, loss of energy expectation (LOEE) given in MWh/yr, loss of load probability (LOLP) given in p.u. and expected loss of load (XLOL) given in MW. The determination of these indices required to determine three main metrics: mean time to failure (MTTF), mean time to repair (MTTR), and mean time between failures (MTBF). MTTF is defined as the length of time that a system is in operation between outages; MTTR refers to the amount of time required to repair a component and bring it back to normal operation state; MTBF measures the predicted time that passes between one previous failure of a system to the next failure during normal operation.

The reliability indices calculation starts with simulation of the MTTF, MMTR and MTBF by generating random number a random number for each one-hour time slot sampling during the time analysis TS for each unit generation in the power system. If the generated number is greater than the unavailability, the component goes the operating state, otherwise, the component goes to not in-service state. The next step is to calculate the margin generation by taking the difference between the available hourly power generation and the hourly demand. The sum of the negative margin (area presented in Figure 3.10) determines the energy not supplied ENS_{exp} , while the sum of the time period that this phenomenon occurs determines the loss of load duration LLD_{exp} . These values are saved, and one experiment is completed. The process is repeated NE times. Finally, the reliability indices can be estimated as follows [6], [32]:

$$LOLE = \frac{1}{NE} \sum_{exp=1}^{NE} LLD_{exp} \quad (3.29)$$

$$LOEE = \frac{1}{NE} \sum_{exp=1}^{NE} ENS_{exp} \quad (3.30)$$

$$LOLP = \frac{LOLE}{NE} \quad (3.31)$$

$$XLOL = \frac{LOEE}{LOLE} \quad (3.32)$$

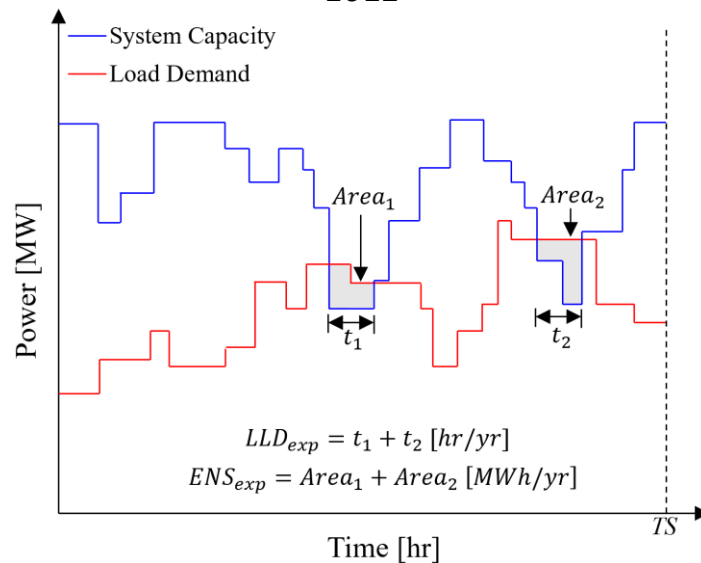


Figure 3.10 Generation-Demand margin model

3.5.3 Composite System Reliability Analysis

The composite system reliability assesses the generation, transmission, and distribution systems adequacy. The reliability is measured by indices, such as the expected number of load curtailments (ENLC) given in occ/yr, expected duration of load curtailments (EDLC) given in hr/yr, probability of load curtailments (PLC) given in p.u. and expected energy not supplied (EENS) given in MWh/yr. Among the described reliability indices, the most used is the EENS [197] attributed to its application in the cost-benefit analysis. It could be used to represent the economic losses due to outages. For its calculation, the analysis starts by conducting Monte Carlo simulation to determine the state of each component of the power system. Then, a generation adequacy assessment that considers load curtailment is performed. The curtailment is carried out by meeting two criteria: 1. curtailed buses which are as close to the elements on outage; 2. loads are categorized by hierarchy relevance [198]. During this step, any load curtailed is added and it becomes the energy not supplied (ENS). Once the generation have satisfied the demand, the process continues with an optimal power flow [199] to determine the voltage and current of the buses. If any voltage constraint is violated or if there is an overloaded line (OL), load curtailment is applied and added to the ENS, otherwise, the experiment finishes. Finally, the whole process is repeated NE times and the EENS is calculated using (3.28). For more details about the study, Figure 3.11 presents a flowchart of the process.

3.6 Risk Quantification

The term risk (\mathfrak{R}) refers to the probability of failure that is caused by external or internal vulnerabilities, and that may be avoided through preventive actions. For the quantification of the risk, the existing literature [95], [194], [200] presents the convolution method (*) as a pathway to calculate it. For instance, let define the probability distribution for the generation and demand as $f_{generation}$ and f_{demand} , respectively. Then, the risk is

assessed by measuring the probability that the available generation in a given time (day, month, and year) is greater than or equal to the maximum demand forecasted.

Mathematically it can be formulated as:

$$Risk = f_{generation}(\wp) * f_{demand}(\wp) = \int_0^{\infty} \int_0^{\wp} f_{generation}(\wp) f_{demand}(\wp) d\wp d\wp \quad (2.1)$$

where \wp is the power given in [MW]. Figure 3.12, presents a schematic representation of the risk.

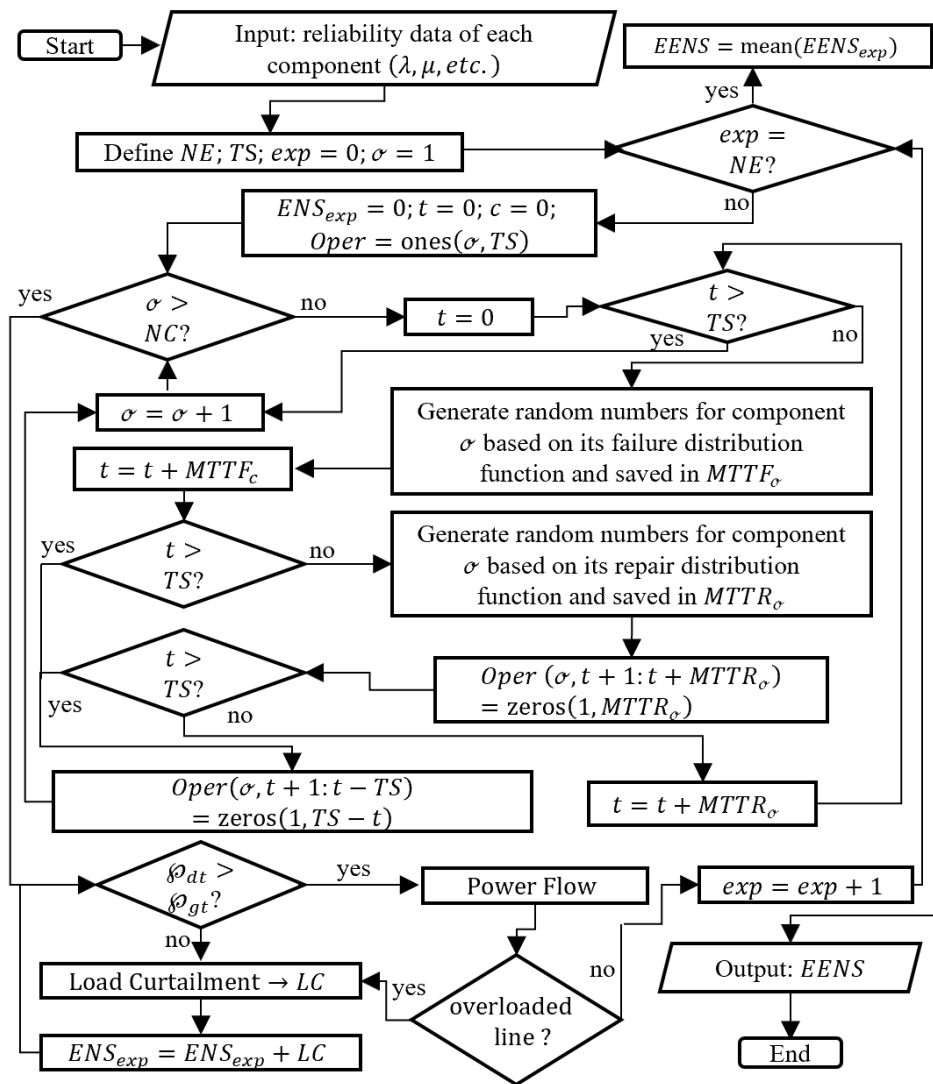


Figure 3.11 Flowchart for a composite system reliability evaluation

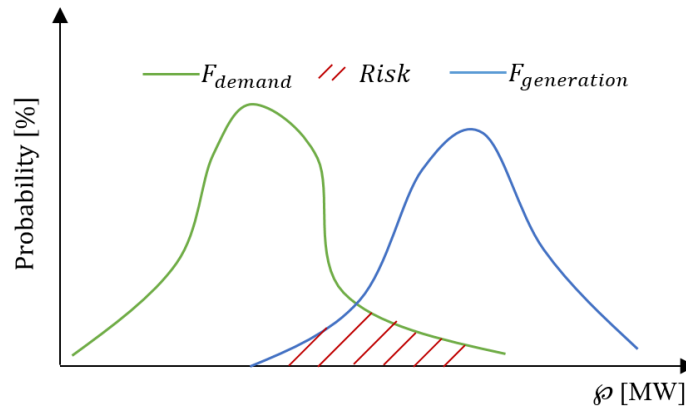


Figure 3.12 Risk of not meeting the predicted maximum demand

3.7 Summary

This chapter presented the existing reliability assessment theories. The parameters that define the reliability of any component are the failure and repair rates, which are determined based on the operational records of the component. If the operational records are known, many analyses can be performed, such as estimate past and future behaviour, and evaluate historical performance. The typical model employed for these aims is the alternating renewal process, which is represented using Markov chains. The chapter also presents the solution of the alternating renewal model.

The chapter continues with the presentation of a data collection of common failure and repair rates of generators. The rates for hydro and thermal unit generation are categorized as a function of the turbine and heat source required to operate the generator, respectively. The data collection is extended to static var compensators and static synchronous generator. The electrical circuit, voltage-current characteristic curve, and Markov chain model of the reactive compensators are also described.

The chapter culminates with the description of the strategies needed to perform a reliability assessment on a power system. This includes Monte Carlo simulation, generation adequacy analysis, composite system reliability analysis, and reliability indices mathematical formulations.

Chapter 4: Reliability Model with Aging Features

Every component in a power system suffers a loss of mechanical and electrical properties (degradation) due to aging. The aging phenomenon is important to consider in a reliability evaluation of power system since it affects the availability of the component. In this chapter a novel reliability model with aging features for repairable components is introduced. The chapter is divided into six sections. Section 4.1 introduces the bathtub curve and the half-arch shape as a Markovian process to define the transition rates of repairable components. Section 4.2 describes the states involved in each stage of transition rates. In section 4.3, the mathematical framework of the proposed reliability model is presented. In section 4.4, the quantification of the degradation is given. Section 4.5 studies the proposed models through a case study. Finally, the last section presents a summary of the chapter.

As a contribution to the state of art, the publications [201], [202] resulted from the research described in this chapter.

4.1 Time Dependent Transitions Rates

A component presents different operational states during its lifetime. The speed associated with various state changes is defined as the transition rate. This can be represented as a function of time, nevertheless, if this takes a constant value the transition rate is considered as time independent. Literature provides several reliability studies [203]–[206] that considers constant transition rates. Nonetheless, components present a tendency to fail, and as time pass by, this tendency increases due to aging phenomenon [201]. Therefore, time-independent transition rates disregard the aging and carry inaccuracies, leading to unrealistic results. To tackle this drawback, it is necessary to incorporate models that consider time-dependent transition rates. For this purpose, the thesis proposes the implementation of the bathtub curve and half-arch shape, which are described as follows.

4.1.1 Bathtub Curve

A milestone in reliability theory is the bathtub curve [94]. This curve describes the behaviour of the failure rate of a reparable component as a function of time t . The literature reports that the curve is divided into three stages [68]. The initial stage corresponds to the infant mortality ($0 \leq t \leq T_U$), in which the component has a high probability of failure in the first instances of operation. This is attributed to undetected or hidden defects during manufacturing. The next stage is the longest period and it is called useful lifetime ($T_U \leq t < T_V$). At this stage, the failure rate takes a constant value. Then, the component transcends to wear out ($T_V \leq t < T_W$). In this stage, the failure rate increases, and the component undergoes to physical deterioration process. Although the literature reports only three stages for the bathtub curve, there is a need to include one more stretch in order to describe the obsolescence of the component. This stage is called end lifetime ($t > T_W$) [201].

There are different distributions functions used to define the bathtub curve. For instance, in [9] employs a Coxian; in [10] uses a nonstandard beta; in [7], [11], [12] use Weibull. In this research, the Gumbel distribution function is suggested since it permits to join the useful lifetime and wear out stages. Hence, the bathtub curve can be formulated as given in (4.1) [2].

$$\lambda(t) = \begin{cases} \lambda_I & ; 0 \leq t \leq T_U \\ a + \alpha e^{\alpha(t-\omega)} & ; T_U < t \leq T_W \\ \infty & ; t > T_W \end{cases} \quad (4.1)$$

where λ_I is the failure rate due to replacement, α is the failure rate scale; a is the failure rate displacement parameter, and ω is the failure rate location parameter.

4.1.2 Half-Arch Shape

The repair rate behaviour is defined by the half-arch shape. As in the bathtub curve, the half-arch shape is divided into four stages. In the infant mortality period, the repair rate mainly depends on how quickly the manufacturer executes the replacement action. During

the useful life, the repair rate of the component takes a constant value. The failures on the component become more intense with time, and the restoration of the component becomes more difficult to execute. Consequently, during the wear out stages, the repair rate decreases fast. The process continues with the end lifetime stage, where restoration cannot be performed, and the repair rate takes a null value. Mathematically, the half-arch shape is as described in (4.2) [202].

$$\mu(t) = \begin{cases} \mu_I & ; 0 \leq t \leq T_U \\ b - \beta e^{\gamma t} & ; T_U < t \leq T_W \\ \infty & ; t \geq T_W \end{cases} \quad (4.2)$$

where μ_I is the repair rate subject to the policy of replacement, β is the repair rate scale; b is the repair rate displacement parameter, and γ is the repair rate power parameter.

4.2 States and Stages

The transitions rates are lanes to different states. Its behaviour depends on where the state takes place within the bathtub curve. For each state, there are corresponding stages which are described below.

4.2.1 States in the Infant Mortality Stage

The infant mortality is defined by the policy of the manufacturer and it corresponds to the period of guarantee. In this stage, the component is in a state denominated as “operation good as new”. Whenever a failure arises, the component goes to a state characterized by the policy of replacement. This process is recurrent, and the component goes to the next stage only if no failures event occurs during the guarantee period ends.

4.2.2 States in the Useful Lifetime and Wear Out Stages

Although the component can operate under different conditions during the infant mortality and wear out stage, this can be summarized in two simple states: 1. Normal operation; 2. Not operating. Other possible states will be discussed in Chapter 6.

4.2.3 State in the End Lifetime Stage

At some point, the unavailability of the component will be so high that a replacement will be required. If that occurs, the component reaches the obsolescence state, which is characterized by the degradation rate ϕ .

Once every state has been recognized and assigned to each stage of the bathtub curve, the Markovian process that describes the reliability model of a repairable component is introduced in Figure 4.1.

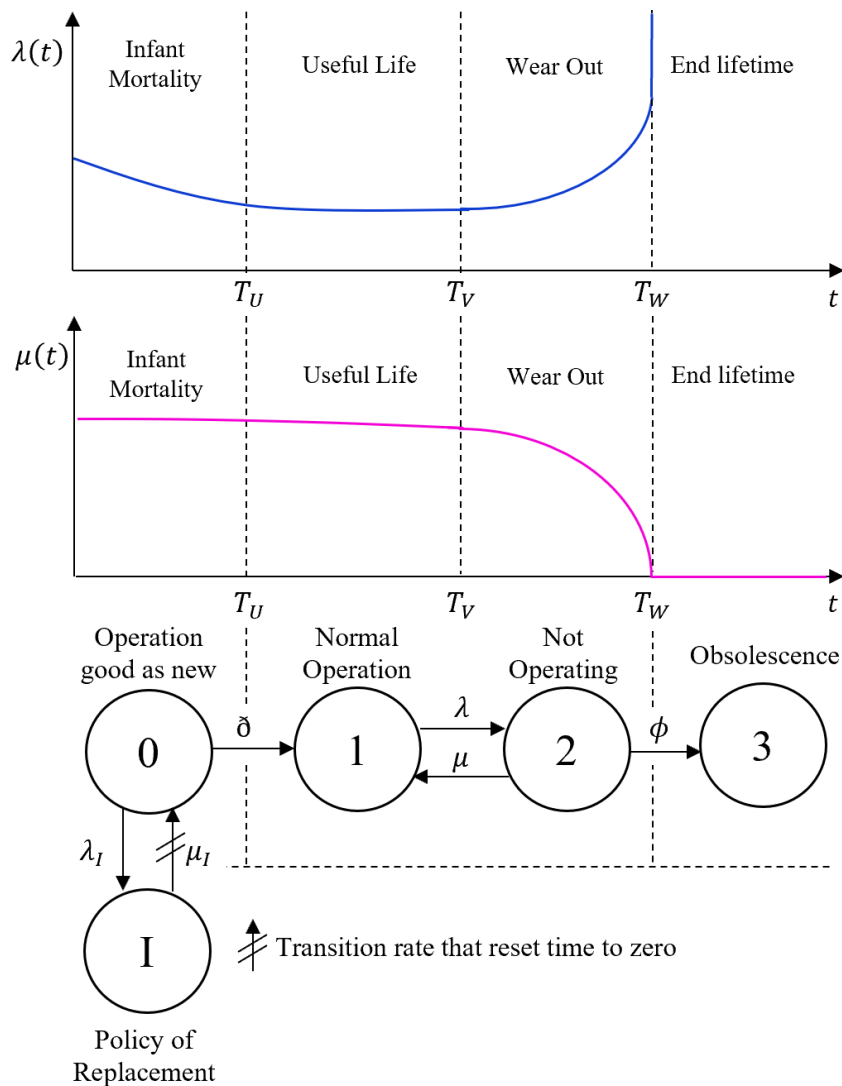


Figure 4.1 State-space diagram based on the Bathtub curve and Half-Arch shape [202].

4.3 Reliability Framework

Although Figure 4.1 shows five possible states, the model can be truncated in three states. This is based on the fact that states “0” and “I” appears only to secure the guarantee, that is, if a failure event takes place during this period, the time is reset to zero. Therefore, the component only goes to the next stage if no failures occur during the guarantee period. Therefore, the model can avoid the states that appear during the infant mortality and the analysis can start from state “1” by considering the end of the guarantee period (T_U) as the initial time analysis. Under these considerations, the process continues as follows.

4.3.1 Probability Vector of States

The stochastic matrix of transition states mathematically represents all possible states in a stochastic process. Its diagonal terms h_{ii} are given by the negative of the sum of the transitions rates that goes out of state i , while the rest of the terms h_{ij} are given by the transition rate that goes from state i to j [201], [202]. Applying this criterion to the model presented in Figure 4.1, the result is:

$$\mathbf{H} = \begin{bmatrix} -\lambda & \phi & 0 \\ \mu & -\mu - \phi & \phi \\ 0 & 0 & 0 \end{bmatrix} \quad (4.3)$$

Later, the eigenvalues, eigenvectors and eigenmatrix of \mathbf{H}^T are given as in (4.4), (4.5) and (4.6), respectively.

$$\chi_1 = 0; \chi_2 = (-\lambda - \mu - \phi - d)/2; \chi_3 = (-\lambda - \mu - \phi + d)/2; \quad (4.4)$$

$$\mathbf{v}_1 = [0 \quad 0 \quad 1]^T$$

$$\mathbf{v}_2 = \left[\frac{(-\lambda - \mu - \phi + d)(\lambda + \mu + \phi + d)}{4\lambda\phi} \quad \frac{-\lambda - \mu - \phi - d}{2\phi} \quad 1 \right]^T \quad (4.5)$$

$$\mathbf{v}_3 = \left[\frac{(\lambda - \mu - \phi - d)(\lambda + \mu + \phi - d)}{4\lambda\phi} \quad \frac{-\lambda - \mu - \phi + d}{2\phi} \quad 1 \right]^T$$

$$\mathbf{Y} = [\mathbf{v}_1 \quad \mathbf{v}_2 \quad \mathbf{v}_3] \quad (4.6)$$

where

$$d = \sqrt{-4\lambda\phi + (\lambda + \mu + \phi)^2} \quad (4.7)$$

The analysis continues with the determination of the c values. At a time $t = 0$ the component is in an operating state ($P_1|_{t=T_u} = 1$; $P_2|_{t=0} = 0$; $P_3|_{t=0} = 0$), therefore:

$$\lim_{t \rightarrow 0} \mathbf{P} = \begin{bmatrix} 1 \\ 0 \\ 0 \end{bmatrix} \quad (4.8)$$

By replacing (4.4), (4.5) and (4.8) in the general solution (3.20):

$$\begin{bmatrix} 1 \\ 0 \\ 0 \end{bmatrix} = c_1 e^{\chi_1(0)} \begin{bmatrix} 0 \\ 0 \\ 1 \end{bmatrix} + c_2 e^{\chi_2(0)} \begin{bmatrix} \frac{(-\lambda - \mu - \phi + d)(\lambda + \mu + \phi + d)}{4\lambda\phi} \\ \frac{-\lambda - \mu - \phi - d}{2\phi} \\ 1 \end{bmatrix} + c_3 e^{\chi_3(0)} \begin{bmatrix} \frac{(\lambda - \mu - \phi - d)(\lambda + \mu + \phi - d)}{4\lambda\phi} \\ \frac{-\lambda - \mu - \phi + d}{2\phi} \\ 1 \end{bmatrix} \quad (4.9)$$

Solving for the c values gives:

$$\begin{aligned} c_1 &= 1; \quad c_2 = \frac{\lambda + \mu + \phi - d}{2d} e^{-0.5T_U(\lambda + \mu + \phi + d)}; \\ c_3 &= \frac{-\lambda - \mu - \phi - d}{2d} e^{-0.5T_U(\lambda + \mu + \phi - d)} \end{aligned} \quad (4.10)$$

Once c , χ and \mathbf{u} are defined in terms of the transitions rates, they can be replaced in (2.20), bringing (4.11) [201], [202]. This formulation determines the probability of each state.

$$\begin{aligned} P_1(t) &= c_1 e^{\chi_1 t} \Upsilon_{11} + c_2 e^{\chi_2 t} \Upsilon_{12} + c_3 e^{\chi_3 t} \Upsilon_{13} \\ P_2(t) &= c_1 e^{\chi_1 t} \Upsilon_{21} + c_2 e^{\chi_2 t} \Upsilon_{22} + c_3 e^{\chi_3 t} \Upsilon_{23} \\ P_3(t) &= c_1 e^{\chi_1 t} \Upsilon_{31} + c_2 e^{\chi_2 t} \Upsilon_{32} + c_3 e^{\chi_3 t} \Upsilon_{33} \end{aligned} \quad (4.11)$$

4.3.2 Degradation Rate

The reliability model requires to know the degradation rate of the component. To get it, let start by defining the term “absorbing state”. This is described as the state in which once reached, there is no possibility to go to any other state. For example, in Figure 4.1 the

obsolescence is an absorbing state. The particularity of this state is that it presents a mean time to absorption (*MTTA*), which can be gotten with the following process [207]:

1. Determine the matrix $\mathbf{G} = \mathbf{H} + \mathbf{I}$. This matrix can be expressed in a canonical form by separating the transient states (TR.) and absorbing states (AB.), as presented in (4.12).

$$\mathbf{G} = \begin{array}{c|c} \text{TR.} & \text{AB.} \\ \hline \mathbf{Q} & \mathbf{L} \\ \hline \mathbf{0} & \mathbf{I} \end{array} \begin{array}{l} \text{TR.} \\ \text{AB.} \end{array} \quad (4.12)$$

2. Obtain the fundamental matrix $\mathbf{N} = [\mathbf{I} - \mathbf{Q}]^{-1}$.

$$\mathbf{N} = \begin{bmatrix} 1 - \lambda & \lambda & 0 \\ \mu & 1 - \mu - \phi & \phi \\ 0 & 0 & 1 \end{bmatrix} \quad (4.13)$$

3. Calculate *MTTA* by adding the terms of \mathbf{N} in the row that corresponds to the started state. In this case, '1' is the initial state, then:

$$MTTA = \frac{\lambda + \mu + \phi}{\lambda\phi} \quad (4.14)$$

In practical terms, the *MTTA* represents the end of lifetime of the component, hence:

$$T_w = \frac{\lambda + \mu + \phi}{\lambda\phi} \quad (4.15)$$

Consequently, from (4.15):

$$\phi = \frac{\lambda + \mu}{T_w\lambda - 1} \quad (4.16)$$

4.3.3 Availability and Unavailability

In a reliability context, the availability quantifies the degree of reliability of a component. It can be obtained from the sum of probabilities of the operating states of the component that are defined in Θ . In contrast, the unavailability is the sum of probabilities of the non-operating states of the component that are defined in Ω . Mathematically, they can be written as shown in (18) and (19), respectively.

$$A(t) = \sum_{s \in \Theta} P_s \quad (4.17)$$

$$U(t) = \sum_{s \in \Omega} P_s \quad (4.18)$$

The set of operational and non-operational states for the proposed model are given in (4.19).

$$\Theta = \{1\}; \Omega = \{2, 3\} \quad (4.19)$$

Hence:

$$A(t) = P_1(t) \quad (4.20)$$

$$U(t) = P_2(t) + P_3(t) \quad (4.21)$$

4.4 Quantification of the Degradation

The degradation is a process that leads to the loss of essential characteristics, and eventually causes a component to fail. In this research, the degradation is a per unit factor defined by the inverse of the product between the lifetime of the component (T_W), and its degradation rate (ϕ_W). Mathematically, it is formulated as given in (4.22) [202].

$$\Lambda = \frac{1}{T_W \phi} \quad (4.22)$$

The degradation must deal with the fact that when the component reaches its end lifetime stage, it must drive the component to the obsolescence state. In order to retain this state, the degradation must be so high, in which case it must satisfy (4.23) [202].

$$\lim_{t \rightarrow T_W} \Lambda = \infty \quad (4.23)$$

4.5 Aging Impact in Reliability Evaluation

To study the impact of the aging effect, a generation adequacy assessment is developed. The system to evaluate is the Roy Billinton Test System (RBTS) [6], with the following assumptions: 1. all generators have a period of guarantee of two years; 2. bathtub curve and half-arch shape of the generators is as shown in Figure 4.2; 3. generators reliability

data is as shown in Figure 4.1; 4. yearly load profile is as shown in Figure 4.3, and it will keep the same for the subsequent years.

Table 4.1 Generators Reliability Data [202]

Unit Generation H:Hydro T:Thermal		H5 Pelton	T10 Oil	H20 Francis	T20 Coal	H40 Kaplan	T40 Coal
# of units		2	1	4	1	1	2
Size [MW]		5	10	20	20	40	40
T_W [yr]		25	20	30	25	40	35
λ [1/yr]	a	2.0	4.0	2.4	5.0	3.0	6.0
	α	0.50	0.40	0.85	0.40	0.88	0.78
	ω	25	20	30	25	40	35
μ [1/yr]	b	198	196	158	195	147	194
	β	0.20	0.10	0.10	0.25	0.30	0.30
	γ	0.28	0.25	0.25	0.27	0.15	0.19

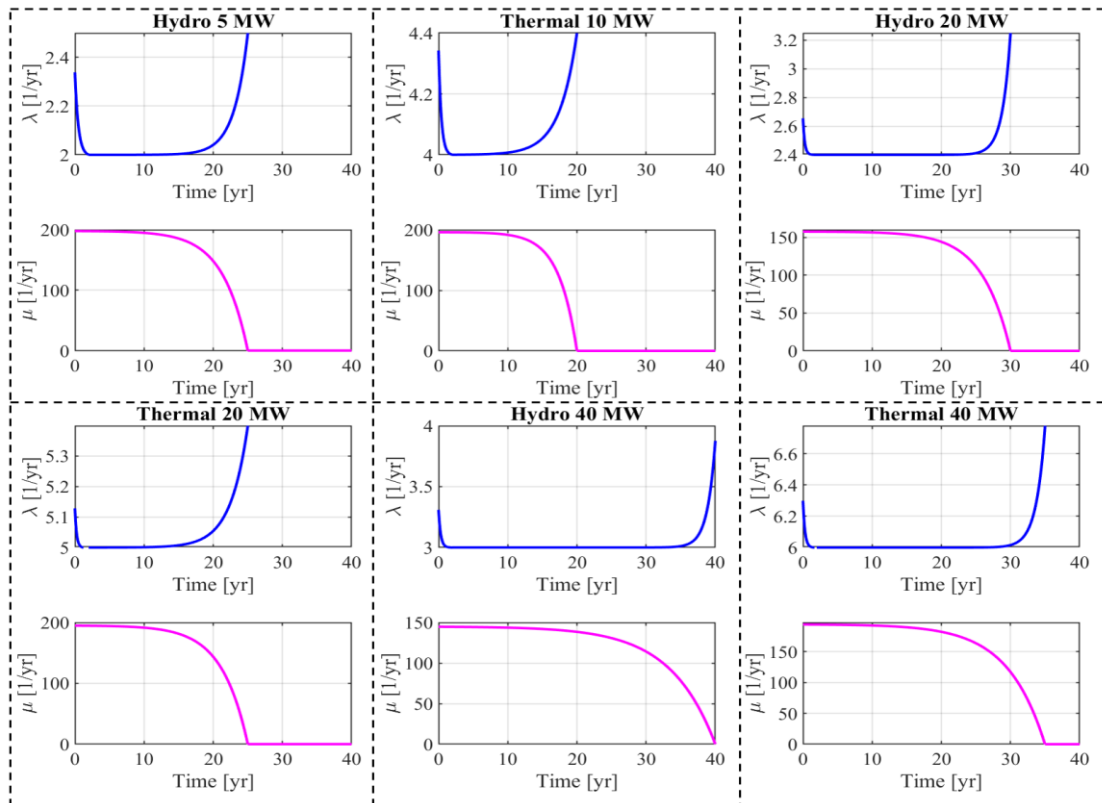


Figure 4.2 Bathtub curve and Half-arch shape for each unit generation [202]

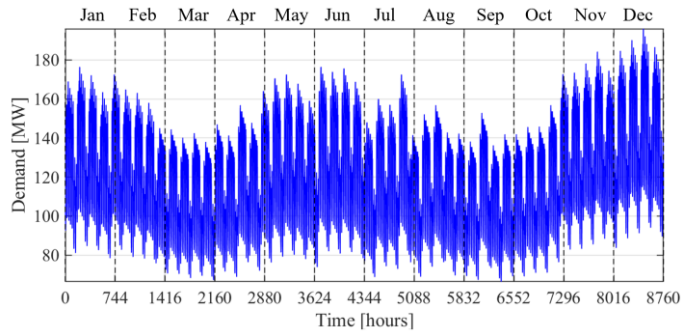


Figure 4.3 Yearly load Profile [201]

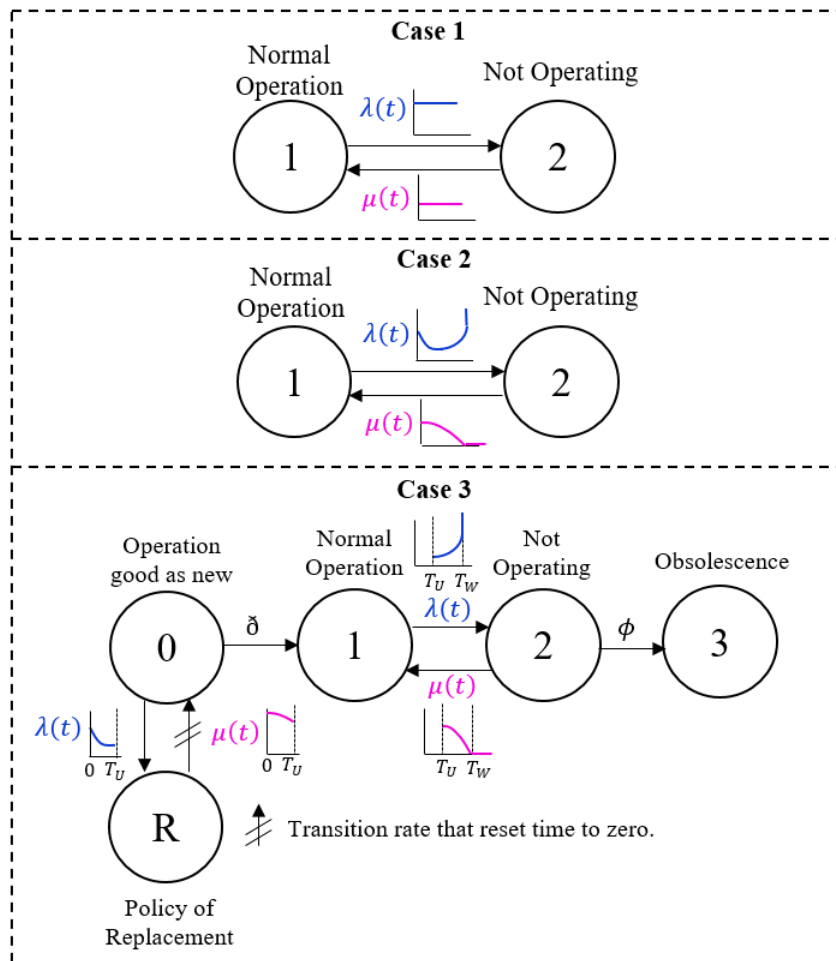


Figure 4.4 State space diagram for each case [202]

In order to show the advantages of the proposed model, three cases are considered.

Figure 4.4 shows the space state diagram for each case and its description is given below.

- Case 1 (classical model no aging): alternating renewal process between state “1” and “2” with constant failure ($\lambda = a$) and repair rate ($\mu = b$).

- Case 2 (classical model with aging): alternating renewal process between state “1” and “2” considering the bathtub curve and half-arch shape.
- Case 3 (proposed model): Markovian process as described in Figure 4.2.

4.5.1 Degradation of the Unit Generation

In this section the first advantage of the proposed model is shown. For the quantification of the degradation, it is required to know the degradation rate ϕ . For case 1 and 2, their space state diagrams do not present the obsolescence state, and so the term ϕ ; therefore, the degradation cannot be calculated in these cases. In contrast, case 3 presents a more comprehensive space state diagram. The model in case 3 incorporates the degradation rate, which can be calculated by replacing the data given in Table 4.1 in (4.16). Then, the degradation is obtained by using (4.22).

Figure 4.5 shows the degradation of each generator. Notice that as time passes by the degradation becomes more intense and when the component reaches its end lifetime ($t = T_W$), the degradation takes an extremely high value, satisfying (4.23).

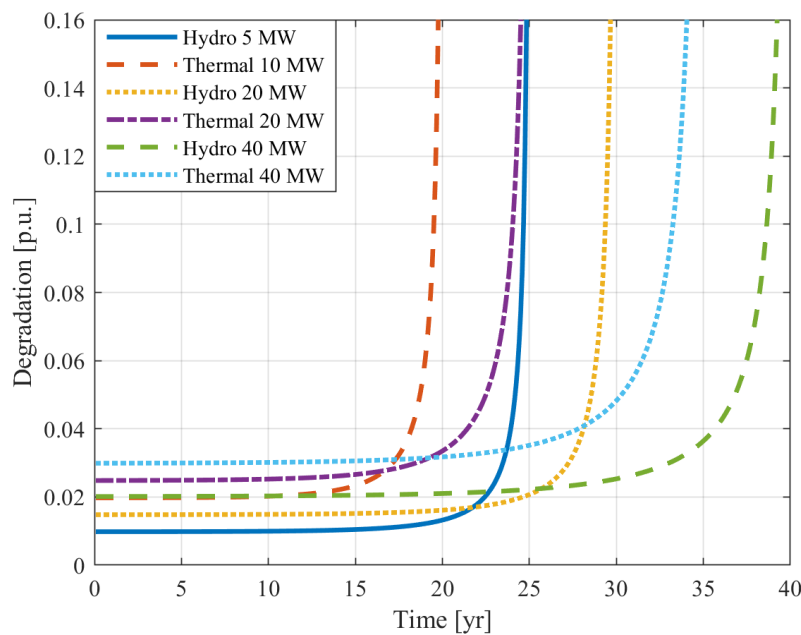


Figure 4.5 Degradation function of each generator [202]

4.5.2 Reliability Model of the Unit generation

The reliability model of a generator is defined by its availability and unavailability, which are described as the sum of the probabilities of being in the operating state or not in-service state, respectively. The reliability model for the case 1 was already discussed in section 3.2, resulting in the functions given by (3.24). Despite the availability and unavailability appear as the sum between a transient and stationary function, Figure 4.6 shows constant values for the availability and unavailability. This is because when replacing the values of λ , μ and t in (3.24), the transient part of the function has a low impact compared to its stationary part, to such an extent that the transient part becomes negligible. Therefore, case 1 disregards the aging phenomenon and carries imprecisions to the reliability assessment.

Case 2 and 3 present time-dependant failure and repair rate, hence, the values c , χ , and \mathbf{u} also become time dependent. Following the process stated in Section 4.3, the probability vector of states for each generator is determined. Then, their availability and unavailability, are obtained applying (4.20) and (4.21), respectively. Figure 4.6 reveals for case 2 that aging influence the generator only at a time close to its end lifetime, resulting in quixotic fact because aging is always acting, and it should be constantly affecting the reliability of the generator. Hence, case 2 brings unrealistic results for reliability evaluation.

Figure 4.6 shows for case 3 that as time passes by, the unavailability increases, while the availability decreases, in such a way that the sum of both is always equal to the unity. It is notable that the degradation due to aging is constantly affecting the reliability of the generator, which results in a more realistic model than the other two previous cases.

Figure 4.6 shows an interception point between availability and unavailability, which appears when the probability is at 50 %. Beyond this point, the generator will start to fail more often because of $U > A$. This point can be considered as an indicator for the

replacement of the generator. Case 1 presents no interception point; therefore, no replacement is required. This is reasonable because the model in case 1 neglects the aging phenomenon, which makes the generator to does not reach the obsolescence state. In case 2, the cross point almost appears at the end of the lifetime of the generator, while for case 3 appears long before. This last one offers more practical reliability behaviour as it shows the continuous impact of the degradation due to aging and not just when it is close to the end of its lifetime as it occurs in case 2.

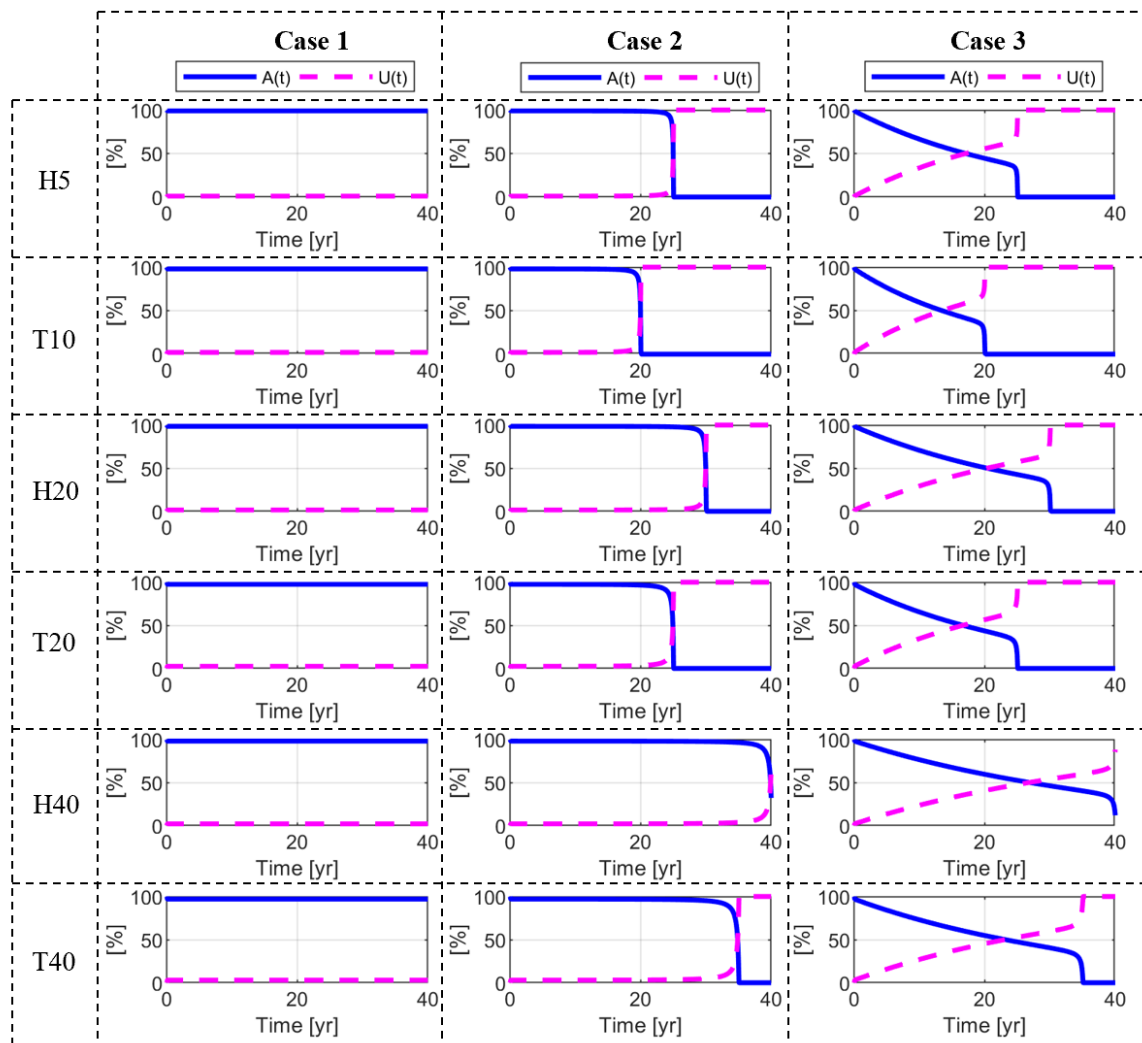


Figure 4.6 Availability and unavailability of each generator [202]

4.5.3 Generation Adequacy with Aging Features

With a view of showing the impact of the different reliability models proposed in each stated case, a generation adequacy assessment for a period of ten years is carried out. The process (flowchart) described in Section 3.4 is implemented in MATLAB 2018 with Monte Carlo simulation experiments of 5000.

Figure 4.7 shows the different reliability indices that characterize the system generation. It can be observed that case 1 and 2 held invariant reliability indices, that is for LOLE, LOLP, LOEE, and XLOL the values are 1.12 [hr/yr], 0.0026 %, 10.32 [MWh/yr] and 6.16 [MW], respectively. Constant reliability indices imply that aging influence is ignored. Thus, case 1 and 2 brings unrealistic results. The case 3 exposes more credible results, the reliability indices exponentially increases with time, reaching values for the tenth year of 866 [hr/yr], 0.99 %, 17213.23 [MWh/yr] and 19.84 [MW], for LOLE, LOLP, LOEE and XLOL, respectively. The results show that as time pass by the power system reliability decreases. This fact is attributed to the aging that produces loss of mechanical and electrical properties of power generators.

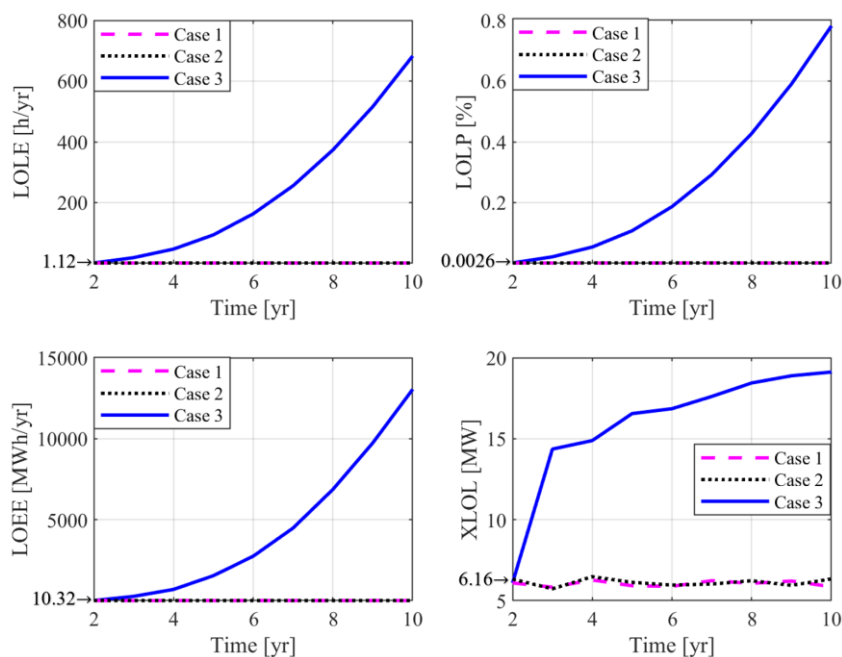


Figure 4.7 Reliability indices [202]

4.6 Summary

This chapter introduces a novel reliability model that considers the aging effect. The model incorporates the bathtub curve and the half-arch shape to describe the failure and repair rates, respectively. Each stage of the curve is described as a Markovian process by defining a state accordingly with the evolution of component lifetime, which is an original contribution to the new knowledge. The chapter also shows the mathematical framework of the proposed model in detail, which is applied to generators. The approach is validated through three different cases. Case 1 analyses the conventional model, that is, an alternating renewal process with constant transition rates. Case 2 is also an alternating renewal process, with the difference that the failure and repair rates follow the bathtub curve and the arc-shape, respectively. Case 3 corresponds to the proposed model, which is presented in Figure 4.1. The results demonstrate the efficacy of the proposed approach since it provides more comprehensive reliability features, leading to more accurate outcomes to the power system reliability evaluation.

Chapter 5: Accelerated Quantum Particle Swarm Optimization

Optimization techniques have become a powerful tool for the diagnosis and solution of multiple engineering problems. For instance, they can be employed to achieve optimum planning and operation of different components installed in a power system. A fact to consider is that a robust optimization technique is required to get an accurate solution in a reasonable time due to the complexity of the power system.

This chapter presents a novel optimization technique called Accelerated Quantum Particle Swarm Optimization (AQPSO). AQPSO introduces the concept of quantum particle position to define a candidate solution to an optimization problem. The optimal solution is obtained via iterative methods that consider concepts of quantum mechanics to simulate the motion of the quantum particle. The novelty of the method lies in the incorporation of the concept of ‘best observation’, which accelerates the motion of the particle and reduce simulation time. The chapter is divided into five sections. Section 5.1 presents the AQPSO methodology. Section 5.2 exposes the mathematical framework that describes the motion of the quantum particle. In section 5.3, AQPSO is employed to reduce the energy not supplied (EENS) of the power system using SVCs. In section 5.4, AQPSO is used to maximize the savings by reducing the cost of power losses in the system. Finally, the last section brings a summary of the chapter.

As a contribution to the state of art, the publications [187], [208] resulted from the research described in this chapter.

5.1 AQPSO Methodology

Quantum Particle Swarm Optimization (QPSO) is an evolutionary computation technique that unlike classical PSO, it does not employ the concept of inertia and velocity (classical physics) to get the optimal solution. Instead, it employs concepts of quantum physics to reach the optimal solution.

AQPSO follows the process described in Figure 5.1. The process starts defining the initial population of the particles SS and total number of iterations It . The position of the particle (x) represents a solution candidate to the optimization problem; thus, it can be used to evaluate the objective function.

The next step is to identify the positions called ‘personal best’ and ‘global best’. In this step is relevant to consider two specific attributes of the particle, which are related to memory and communication. The memory attribute refers to the ability to save the best position of the particle by comparing its actual position with the position after the motion.

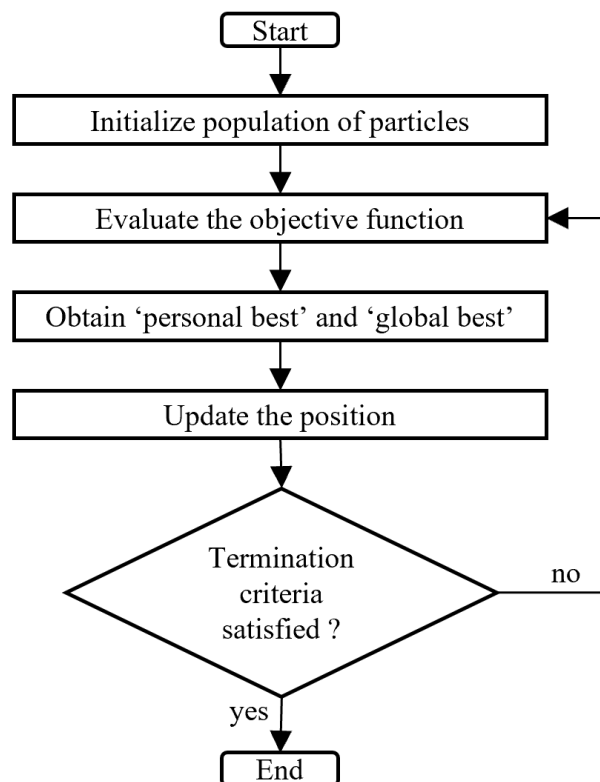


Figure 5.1 AQPSO flowchart

For instance, Figure 5.2 shows two scenarios of particle motion. In scenario 1, the particle has the possibility to move close to the optimum position, therefore, it proceeds to move and saves this position as its best position. In scenario 2, the particle has the possibility to move far from the optimum position, therefore, it will not move and saves its actual position as its best position. The memory attribute is known as ‘personal best’ and denoted by q_ℓ [209], [210].

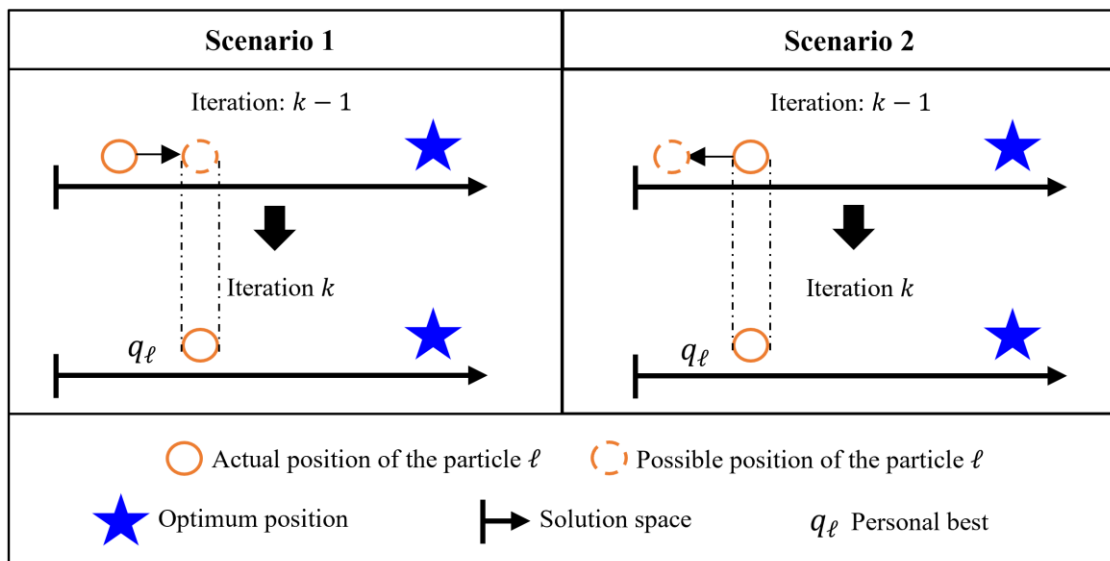


Figure 5.2 Memory attribute of a particle

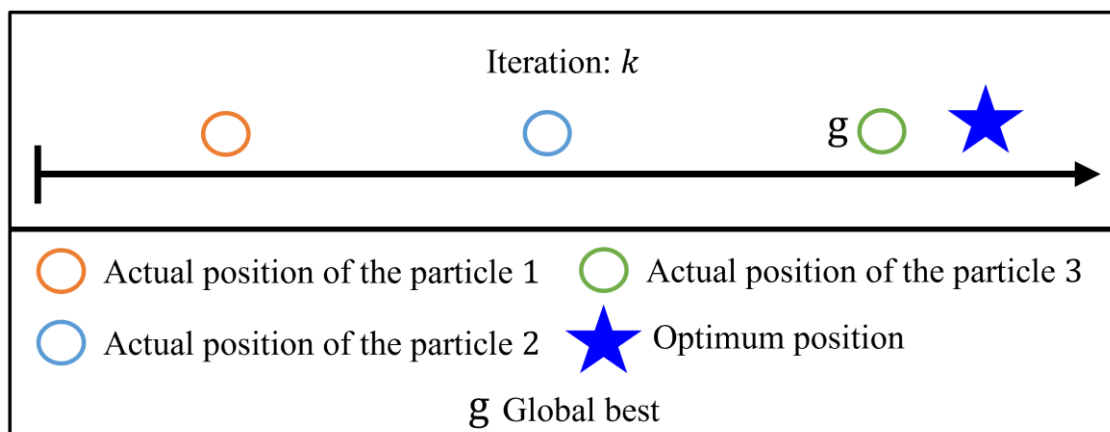


Figure 5.3 Communication attribute of a particle

The communication attribute refers to the ability to save the particle with the best position among the swarm. Figure 5.3 shows a swarm with three particles, resulting in the ‘particle 3’ as the best particle since is the one nearest to the optimum position. The communication attribute is known as ‘global best’ and is denoted by g [209], [210].

The personal best and global best are used to define the local attraction between particles. The authors in [211] conducted a trajectory analysis of a particle and demonstrated that this attraction mainly depends the terms q and g . Mathematically, the local attraction of the particle at search step k is defined as given in (5.1).

$$\begin{aligned} D_\ell(k) &= \varphi q_\ell + (1 - \varphi)g \\ \varphi &= r_1 u_1 / (r_1 u_1 + r_2 u_2) \end{aligned} \quad (5.1)$$

where u is a uniformly distributed random number, and r is a constant of acceleration coefficient such that $0 \leq r \leq 2$. The expression given in (5.1) is important because is needed to describe the motion of the particle.

The process continues with the position update of every particle. The new positions represent an evolution (enhancement) of the actual solutions. The evolution is achieved based on the particle motion mathematical formulations, which are described in the next section. The last step is to verify the termination criterion using the total number of iterations It , and convergence tolerance value ϵ . The process finishes if one of the conditions given in (5.2) is satisfied [212].

$$\text{Convergence Criteria: } \left\{ \begin{array}{l} k = It \\ \left| \sum_{\ell=1}^{SS} q_i(k) - SSg(k) \right| \geq \epsilon \end{array} \right. \quad (5.2)$$

5.2 Mathematical Framework of Quantum Particle Motion

Metaheuristics approaches define different scenarios to describe the motion of a particle. For instance, [211] traditional PSO presents particles with characteristics of classical physics, such as inertia, speed, acceleration, etc. Hence, the motion of the particles

in this scenario is governed by the laws of dynamics and kinematics. Another example is given in [213], which proposes magnetic particles and its motion is described using electromagnetism theory. AQPSO proposes a scenario, where a unidimensional particle lies in a quantum delta potential well. The motion of the particle is driven by quantum mechanics concepts.

To derive the expression that describes the motion of the particle, let define the delta function for a relative position of particle ℓ as $\delta(\Delta x_\ell)$. Then, it can be expressed in terms of the characteristic length l as given in (5.3) [214].

$$\delta(\Delta x_\ell) = 1/l \quad (5.3)$$

Then, probability of finding the quantum particle in a certain region of the space is defined in (5.4) [215].

$$\mathfrak{F}(\Delta x_\ell) = \delta(\Delta x_\ell)u \quad (5.4)$$

By replacing (5.3) in (5.4)

$$\mathfrak{F}(\Delta x_i) = u/l \quad (5.5)$$

Since the particle lies in a delta quantum well, the probability of finding such particle at position x is [214]:

$$\mathfrak{F}(\Delta x_\ell) = e^{-2|\Delta x_\ell|/l}/l \quad (5.6)$$

The expressions given in (5.5) and (5.6) are equal, hence

$$u/l = e^{-2|\Delta x_\ell|/l}/l \quad (5.7)$$

Solving for Δx

$$\Delta x_\ell = (l/2) \ln(1/u) \quad (5.8)$$

The term $l/2$ is a control governed by the contraction-expansion coefficient ε , actual position $x_\ell(k)$ and mean sum of each individual particle of the swarm. Mathematically is defined by [214], [215]:

$$l/2 = \varepsilon \left| x(k) - \frac{1}{SS} \sum_{\ell=1}^{SS} q_{\ell}(k) \right| \quad (5.9)$$

Substituting (5.9) in (5.8)

$$\Delta x_{\ell} = \varepsilon \left| x(k) - \frac{1}{SS} \sum_{\ell=1}^{SS} q_{\ell}(k) \right| \ln(1/u) \quad (5.10)$$

Figure 5.4 shows an illustrative representation of the motion of the quantum particle, from which (5.11) is established

$$\Delta x_{\ell} = D_{\ell}(k) \pm x_{\ell}(k + 1) \quad (5.11)$$

Solving for $x_{\ell}(k + 1)$ and replacing (5.10) in (5.11) [187]

$$x_{\ell}(k + 1) = D_{\ell}(k) \pm \varepsilon \left| x_{\ell}(k) - \frac{1}{SS} \sum_{\ell=1}^{SS} q_{\ell}(k) \right| \ln(1/u) \quad (5.12)$$

The term ‘ \pm ’ indicates that the particle is in a quantum superposition state, that is, its position lies in both sides of the space at the same time (take as reference the Schrödinger cat [216]). The only way to determine its right position is by making an observation, which is defined as $obs = \text{rand}(0,1)$ [217]. At time step $k + 1$, the particle materializes in between the zone $[-x_{\ell}(k + 1), +x_{\ell}(k + 1)]$, then the sign can be assigned following (5.13).

$$\begin{cases} + \text{ if } 1 \geq obs \geq 0.5 \\ - \text{ if } 0 \leq obs < 0.5 \end{cases} \quad (5.13)$$

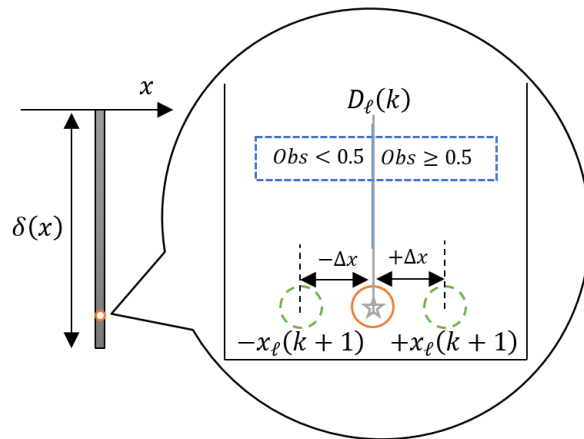


Figure 5.4 Motion of a particle in a quantum delta potential well

In order to improve the robustness of the method, the number of observations NO is increased to an odd number greater than one. Then, the set of observers OBS_1 and OBS_2 are defined below [187]:

$$\begin{aligned} OBS_1 \cup OBS_2 &= \{obs_1, obs_2, \dots, obs_{NO}\} \\ OBS_1 &= \{all\ obs \geq 0.5\};\ OBS_2 = \{all\ obs < 0.5\} \end{aligned} \quad (5.14)$$

The function cardinality (card) establishes the total numbers of elements in a set. This is employed to find the ‘best observation’ \mathcal{B} for the position of the particle, such that [187]

$$\begin{aligned} if\ card(Obs_1) > card(Obs_2) &\Rightarrow \mathcal{B} \geq 0.5 \\ if\ card(Obs_1) < card(Obs_2) &\Rightarrow \mathcal{B} < 0.5 \end{aligned} \quad (5.15)$$

Therefore, (5.12) can be rewritten as given (5.16) [187].

$$x_\ell(k+1) = \begin{cases} D_\ell(k) + \varepsilon \left| x_\ell(k) - \frac{1}{SS} \sum_{\ell=1}^{SS} q_\ell(k) \right| \ln\left(\frac{1}{u}\right), & if\ \mathcal{B} \geq 0.5 \\ D_\ell(k) - \varepsilon \left| x_\ell(k) - \frac{1}{SS} \sum_{\ell=1}^{SS} q_i(k) \right| \ln\left(\frac{1}{u}\right), & if\ \mathcal{B} < 0.5 \end{cases} \quad (5.16)$$

The implementation of AQPSO is presented in Algorithm 5.1.

Algorithm 5.1 Accelerated Quantum Particle Swarm Optimization Pseudocode

<ol style="list-style-type: none"> 1. Procedure of AQPSO 2. For $i = 1$ to swarm size (SS) 3. randomize the position of each particle $x_\ell(0)$; 4. $D_\ell(0) = x_\ell(0)$; 5. Evaluate the objective function $OF(x_\ell(0))$; 6. Endfor 7. $\min OF(x_\ell(0)) \rightarrow g$; $k = 0$; $\epsilon = 1 \times 10^{-6}$ 8. While $k \neq (It)$ & $\sum_{\ell=1}^{SS} q_i(k) - SSg(k) \geq \epsilon$ 9. For $\ell = 1$ to SS 10. calculate $D_\ell(k)$ with (5.1); 11. Get obs based on (5.15); 12. update $x_\ell(k)$ with (5.16); 13. Evaluate the objective function $OF(x_\ell(k))$; 14. If $OF(x_\ell(k)) < OF(D_\ell(k))$ 15. $D_\ell(k) = x_\ell(k)$; 16. If $\min OF(x_\ell(k)) \rightarrow g(k)' < g(k)$ 17. $g(k) = g(k)'$ 18. Endif 19. Endif 20. $k = k + 1$; 20. Endwhile 21. Endfor

5.3. Composite System Reliability Evaluation with Reactive Compensation Using AQPSO

In this section, the first application of AQPSO is presented. The optimization technique is employed to maximize the reliability of a power system by incorporating SVCs into the power system. The description of the case study, problem formulation, proposed algorithm, and results are as given in the following sections.

5.3.1 Case Study

The study incorporates the IEEE 24 bus reliability test system [163], with the following assumptions: 1. All components start operating at time $t = 0$; 2. Reliability model of the SVC [148], [185] is as shown in Figure 3.9; 3. Table 5.1 shows the features of the available SVCs; 4. Bus voltage must meet IEEE Standard 1860-2014 [218] that is $0.95 p.u. \leq V_{bus} \leq 1.05 p.u.$

Table 5.1 Static Var Compensators Available for AQPSO First Case Study [187]

Capacity [MVar]	SVC in Stock					
	5	10	20	30	40	50
λ_P [1/yr]	0.0906	0.1283	0.5789	1.0580	2.045	2.5480
λ_Q [1/yr]	0.0200	0.0250	0.0250	0.0300	0.040	0.0450
λ_R [1/yr]	0.0001	0.0001	0.0002	0.0002	0.0002	0.0003
μ_P [1/yr]	150	160	162	180	188	200
μ_Q [1/yr]	250	300	155	190	170	199
μ_R [1/yr]	999	999	732	652	428	357

5.3.2 Problem Formulation

The objective is to maximize the reliability of the system by incorporating the SVC in the most suitable locations. The expected energy not supplied (*EENS*) is used to measure power system reliability. By defining the slot index t , real power P , and reactive power Q , the optimization problem can be written as [187]:

$$\text{minimize } (EENS) \tag{4.24}$$

Subject to [187]

$$\sum_{gen=1}^{NG} P_{gen}(t) = \sum_{load=1}^{NLo} P_{load}(t) + \sum_{line=1}^{NLi} P_{line}(t) \quad (5.17)$$

$$\sum_{gen=1}^{NG} Q_{gen}(t) + \sum_{SVC=1}^{NSVC} Q_{SVC}(t) = \sum_{load=1}^{NLo} Q_{load}(t) + \sum_{line=1}^{NLi} Q_{line}(t) \quad (5.18)$$

$$P_{min_{gen}} \leq P_{gen}(t) \leq P_{max_{gen}} \quad (5.19)$$

$$Q_{min_{gen}} \leq Q_{gen}(t) \leq Q_{max_{gen}} \quad (5.20)$$

$$Q_{min_{SVC}} \leq Q_{SVC}(t) \leq Q_{max_{SVC}} \quad (5.21)$$

$$V_{min_{bus}} \leq V_{bus}(t) \leq V_{max_{bus}} \quad (5.22)$$

$$I_{line}(t) \leq I_{max_{line}} \quad (5.23)$$

$$0 \leq N_{bus} \leq NSVC \quad (5.24)$$

where $\{gen, load, line, t\} \in \mathbb{N}$.

The restriction (5.17) states that the active power injected by all generators (P_{gen}) must satisfy the power losses in the transmission lines (P_{line}) plus the active power demanded by all the loads (P_{load}). The restriction (5.18) states that the reactive power injected by all generators (Q_{gen}) plus the reactive power injected by all SVC installed in the power system (Q_{SVC}) must satisfy the power losses of the transmission lines (Q_{line}) plus the reactive power demanded by all loads (P_{load}). The constraint (5.19) regulates the minimum ($P_{min_{gen}}$) and maximum ($P_{max_{gen}}$) active power that the generator can inject. The constraint (5.20) regulates the minimum ($Q_{min_{gen}}$) and maximum ($Q_{max_{gen}}$) reactive power that the generator can inject. The restriction (5.19) attributes the minimum ($Q_{min_{SVC}}$) and maximum ($Q_{max_{SVC}}$) power that the SVC can generate. The voltage in the buses is regulated by a minimum and maximum, which is defined by (5.22). The maximum current that the transmission line can carry ($I_{max_{line}}$) is controlled by (5.23). The last constraint (5.24) is to assure that the number of SVC ($NSVC$) does not exceed the number of bus in the system (N_{bus}).

5.3.3 Proposed Algorithm

To get the solution to the formulated problem, the algorithm shown in Figure 5.5 is employed and implemented using MATLAB 2018. The algorithm is divided into five main stages, which are described below.

- Stage 1: The algorithm starts by loading the power system data, such as impedances of the lines, capacity of the generators, failure and repair rates of the lines and generators, and active and reactive power consumed by each load. In addition, the size of the swarm SS and total number of iterations It are also defined.
- Stage 2: The first particles $x_\ell(0)$ are randomly generated. Each particle represents a different combination of installing the available SVC into the power system. Every combination is saved in x_ℓ . $\sigma(0)$. In addition, the particle also contains the maximum and minimum reactive power of every SVC, which given by x_ℓ . $Q_{SVC}(0)$. Then, the information of the particle is added to the power system. Then, a composite system reliability assessment takes place following the procedure previously described in Section 3.5.3. As a result, $EENS$ is calculated for every particle and saved in x_ℓ . $EENS(0)$. The stage finishes with the identification of the ‘global best’ particle, which is obtained by looking for the particle with the minimum value of $EENS$. The value is saved in g . On the other hand, notice that the ‘best personal’ q_ℓ is equal to the actual position $x_\ell(0)$ since the particles have not started their motion.
- Stage 3: The first iteration takes place, and the particles start their motion. The attraction parameter $D_\ell(k)$, and best observation \mathcal{B} are obtained using (5.1) and (5.15), respectively. Then, the new position of the particle is computed using (5.16). The updated position of the particle represents a new SVC combination that may lead to a better $EENS$. The composite system reliability assessment described in Section 3.5.3 takes place to obtain a new $EENS$ value, which is saved in x_ℓ . $EENS(k)$.

- Stage 4: The *EENS* values before $x_{\ell}.EENS(k-1)$ and after $x_{\ell}.EENS(k)$ the motion of the particle is compared. A reduction of *EENS* value implies that the particle is getting closer to objective function since the algorithm is looking for the minimum *EENS*. Therefore, if $x_{\ell}.EENS(k) < x_{\ell}.EENS(k-1)$ then the particle updates its position. In addition, the ‘personal best’ of the particle is also updated and saved in q_{ℓ} . This is followed by a second comparison in which the ‘global best’ is considered. For this purpose, it is required to find the best $x_{\ell}(k)$ among the swarm such that brings the minimum *EENS*. The best particle is saved in the variable g'_{op} . If the $g'.EENS < g.EENS$ then the $x_{\ell}(k)$ becomes the ‘global best’, otherwise the ‘global best’ is not replaced. In case that $x_{\ell}.EENS(k) \geq x_{\ell}.EENS(k-1)$ then the process continues with the next particle.
- Stage 5: The process in stage 3 and stage 4 are repeated until one of the convergence criteria presented in (5.2) is satisfied. Consider for the convergence criteria a $|\sum_{\ell=1}^{SS} q_{\ell}.EENS(k) - SS g.EENS(k)| \leq 10^{-6}$. Finally, the outcome is the particle with the best SVC combination and location, as presented in Figure 5.6.

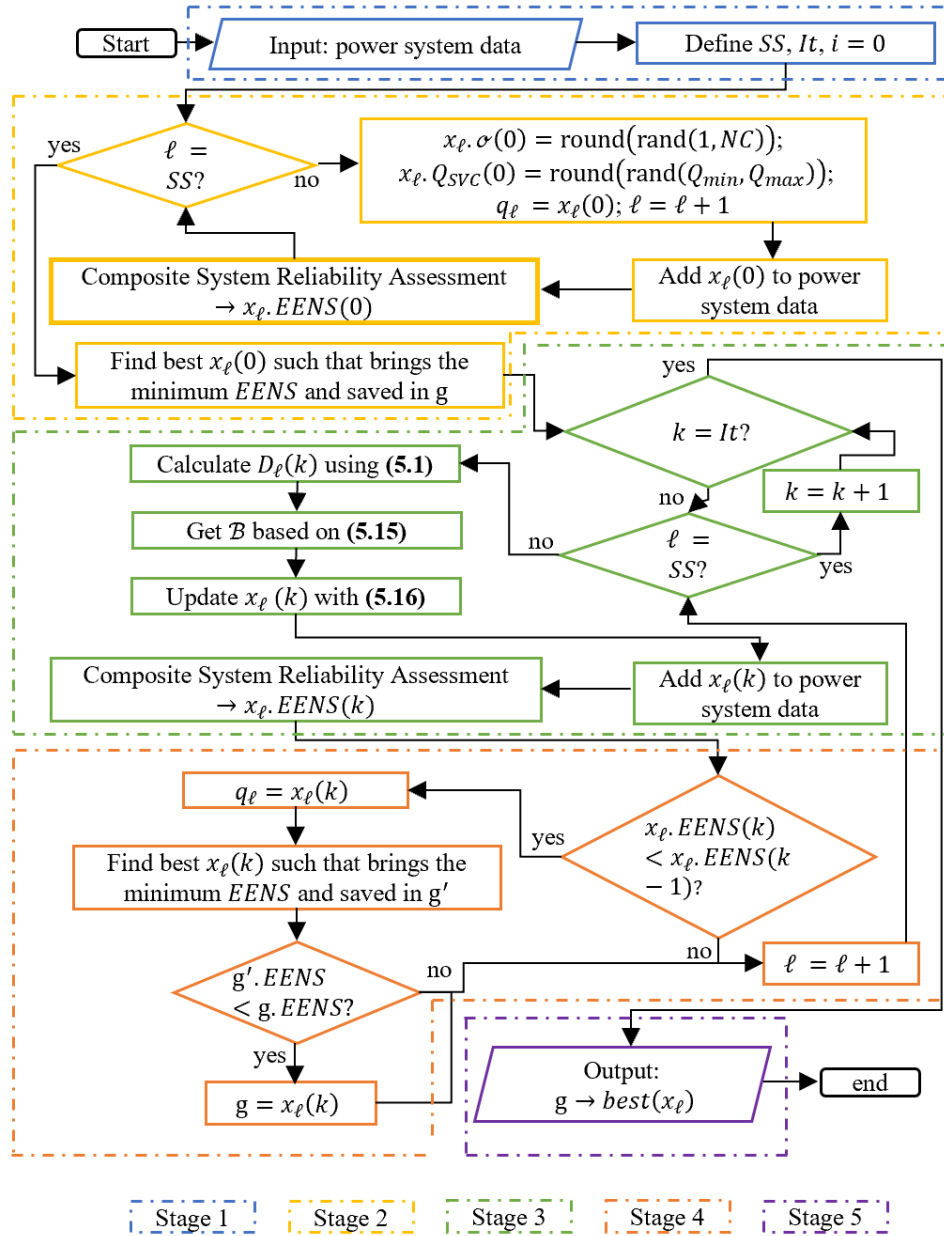


Figure 5.5 Flowchart for optimum reliability assessment through VAr compensation [187]

Figure 5.6 shows that the optimal placement and sizing of the SVCs that minimize the *EENS*, is as follows:

- SVC of size 5 [MVar] installed at bus 5.
- SVC of size 10 [MVar] installed at bus 4.
- SVC of size 30 [MVar] installed at bus 3.
- Three SVCs of size 40 [MVar] installed at bus 10, 11 and 19, respectively.
- SVC of size 50 [MVar] installed at bus 13.

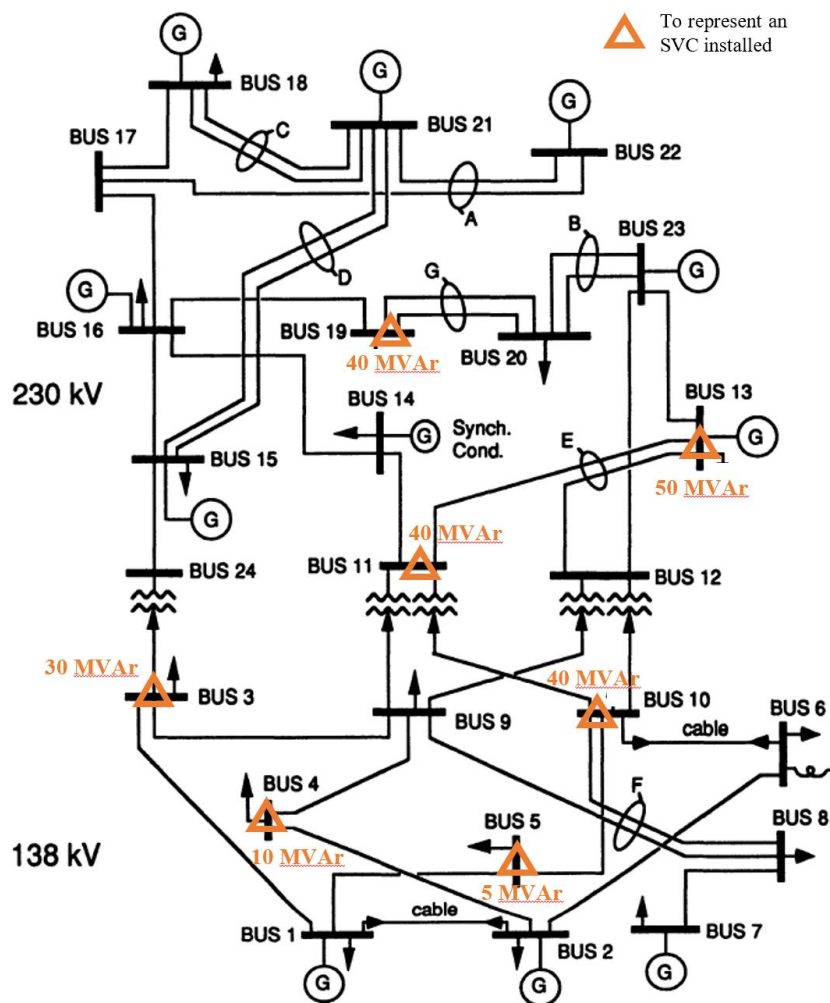


Figure 5.6 SVC placement and sizing that minimize *EENS* [187]

5.3.4 Results and Discussion

To perceive the impact of the SVC installation, Table 5.2 presents the *EENS* values in two different scenarios: 1. No SVC installed; 2. Optimum SVC installation. In the first scenario, *EENS* takes a value of 12.9×10^4 MWh/year, and this value is used as a benchmark to measure the reliability of the power system. In the second scenario, *EENS* takes a value of 7.18×10^4 MWh/year. The results reveal that the expected energy not supplied is less in the case where SVCs are employed, which implies reliability enhancement in the power system. This is attributed to the ability of the SVC to deal with the problems of bus voltage instability and overloaded line, which are produced in case of line outages. Consequently, load shedding strategy is less required and expected energy not supplied is

reduced. The optimal installation of the SVC is an adequate reactive power reserve to maintain system integrity.

With a view to show the computational efficiency of the proposed optimization technique, AQPSO was executed with three (AQPSO3), five (AQPSO5) and seven (AQPSO7) observers. In addition, the same optimization problem was solved using other two different optimization techniques, these are PSO and QPSO. It is relevant to highlight that a total of 20 particles and 50 iterations are used for every optimization technique with Monte Carlo simulation experiments of 5000. The computer employed for this purpose possesses a RAM of 8.00 GB and processor Intel Core i7-6700 of 3.40 GHz. Figure 5.7 shows the convergence behaviour for each optimization technique.

Figure 5.7 depicts that as the number of observers increases, the faster is the convergence. This is because the probability of finding the position of the quantum particle within the solution space increases with the number of observers [219]. Another important fact to discuss in the time simulation, which is presented in Table 5.3. Among the existing optimization techniques, PSO presents the highest time simulation. This is attributed to the velocity parameter that PSO requires to update the position the particles. The calculation of the velocity increases time simulation in every iteration. On the other hand, the smallest time simulation corresponds to AQPSO, followed by AQPSO3, AQPSO5 and AQPSO7. This is understandable, the mathematical operations during the optimization process to determine the position of the quantum particle within a certain region of the solution space increases with the number of observers. Consequently, the time simulation increases.

Table 5.2 Impact of the SVC on power system reliability [187]

Scenario:	No SVC installed	Optimum SVC installation
<i>EENS</i> :	12.9×10^4 MWh/year	7.18×10^4 MWh/year

Table 5.3 Optimization Technique Robustness for AQPSO first case study [187]

Optimization Technique	Average time simulation per experiment [s]	Convergence iteration
PSO	11.67	34
QPSO	11.04	37
AQPSO3	11.20	36
AQPSO5	11.25	30
AQPSO7	11.26	30

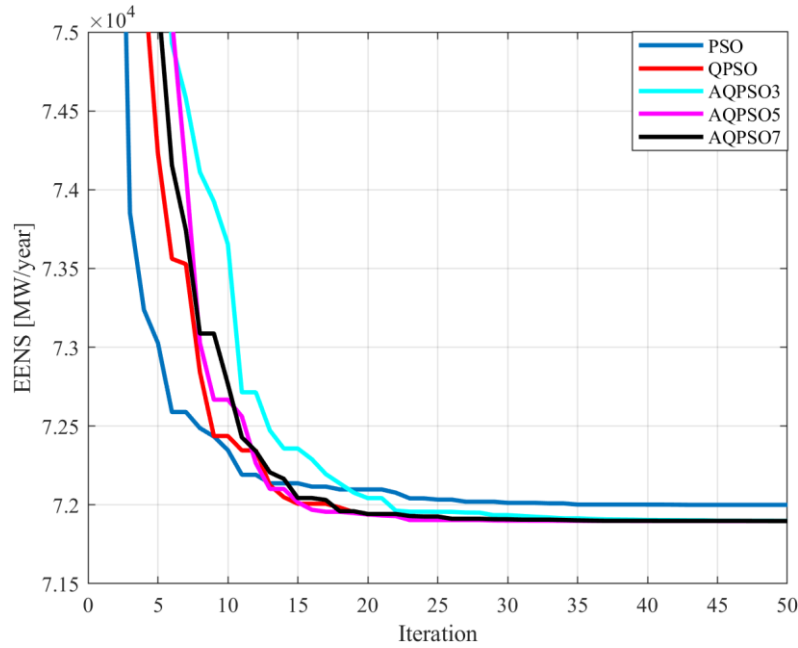


Figure 5.7 Optimization Technique Convergence [187]

5.4 Planning and Operation of Static Var Compensators

The second application of AQPSO is presented in this section. AQPSO is used to determine the optimum planning and operation of the SVCs that minimize power losses in the transmission lines. The description of the case study, problem formulation, proposed algorithm, and results are as given in the following sections.

5.4.1 System Layout Description

The study incorporates the IEEE 24 bus reliability test system [163], with the following assumptions: 1. All components start operating at time $t = 0$. 2. Energy and SVC price constants are $wL = 0.08$ [£/kWh] and $wSVC = 4 \times 10^4$ [£/MVar] [208]; 3. Normalized demand profile during weekdays and weekends is as shown in Figure 5.8 [208];

4. Table 5.4 shows the features of the SVC in stock [208]; 5. Bus voltage must meet IEEE Standard 1860-2014 [218] that is $0.95 \text{ p.u.} \leq V_{bus} \leq 1.05 \text{ p.u.}$

Table 5.4 Static Var Compensators Available for AQPSO Second Case Study [208]

	Capacity [MVar]					
SVC in Stock	10	20	50	100	120	150

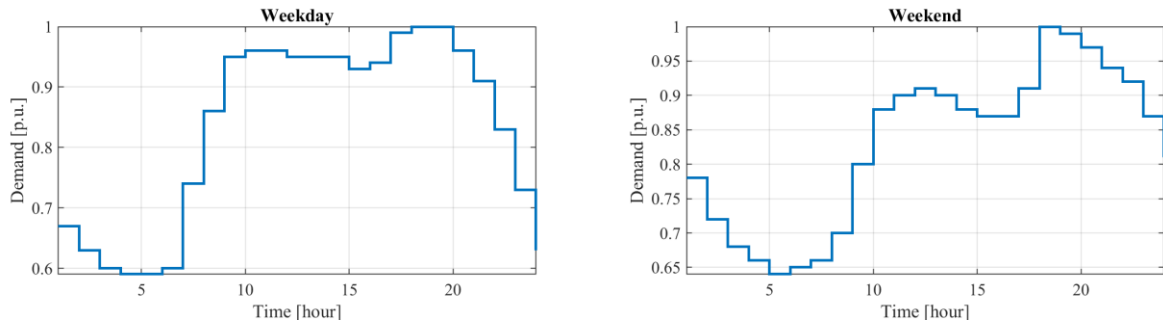


Figure 5.8 Load profiles for AQPSO Second Case Study [208]

5.4.2 Problem Formulation

SVC is employed in the power system in order to maximize the savings by reducing the cost of power losses in the system. The SVC injects reactive power, which causes a reduction on the conductor current magnitude [110]. Consequently, it produces a reduction of power losses that are described as shown below [208]:

$$\Delta L_{line} = (I_{line}^2 - I'_{line}{}^2)R_{line} \quad (5.25)$$

where I_{line} is the current flow without the installation of the SVC, I'_{line} is the current flow considering the installation of the SVC, and R_{line} represents the resistance of the conductor. Then, the savings due to power losses reduction can be obtained using the following formulation [208]:

$$SavingL = e \sum_{line=1}^{NLi} \Delta L_{line} \quad (5.26)$$

where e represents the energy cost function and NL_i is the total number of lines of the power system.

The acquisition and installation of the SVC imply a costly investment, which appears as a function of the price per MVar (w). This cost is given by (5.27) [208].

$$CostSVC = \sum_{SVC=1}^{NSVC} w_{SVC} Q_{SVC} \quad (5.27)$$

Then, the optimization problem can be defined as follows [208]:

$$maximize (SavingL - CostSVC) \quad (5.28)$$

which is subject to the constraints presented in (5.17) to (5.24).

5.4.3 Proposed Algorithm

The optimization problem cannot be addressed using a simple AQPSO since the solution involves the optimization of two types of particles. The first type of particles is used for the planning of the SVCs, while the second type of particles deals with the operation of the SVCs. Thus, a Bi-Level Accelerated Quantum Particle Swarm Optimization (BL-AQPSO) is employed. The first level is called AQPSO_{sp}, which focuses on the determination of the effective placement and sizing of the SVC (SVCs planning). The second level is called AQPSO_{op} and is used to determine the optimal strategy dispatch for each SVC (SVCs operation). AQPSO_{sp} and AQPSO_{op} are presented in Figure 5.9 and Figure 5.10, respectively. Both algorithms are implemented using MATLAB 2018. Every level of the algorithm presents different stages. Stage 2 to stage 5 correspond to AQPSO_{op}, while the rest of the stages belongs to AQPSO_{sp}. Each stage is described as follows.

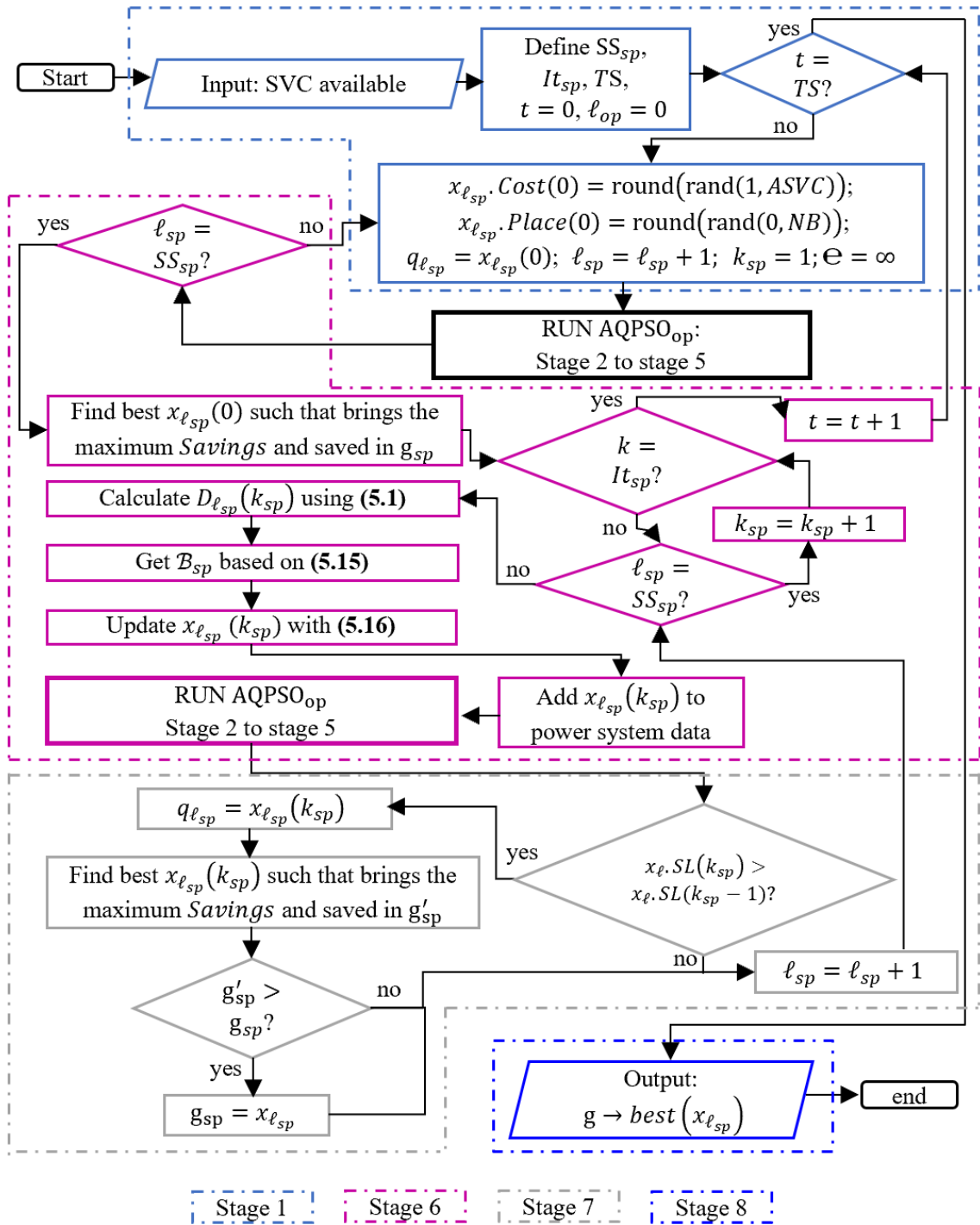


Figure 5.9 AQPSO_{sp} flowchart for optimum SVC planning [208]

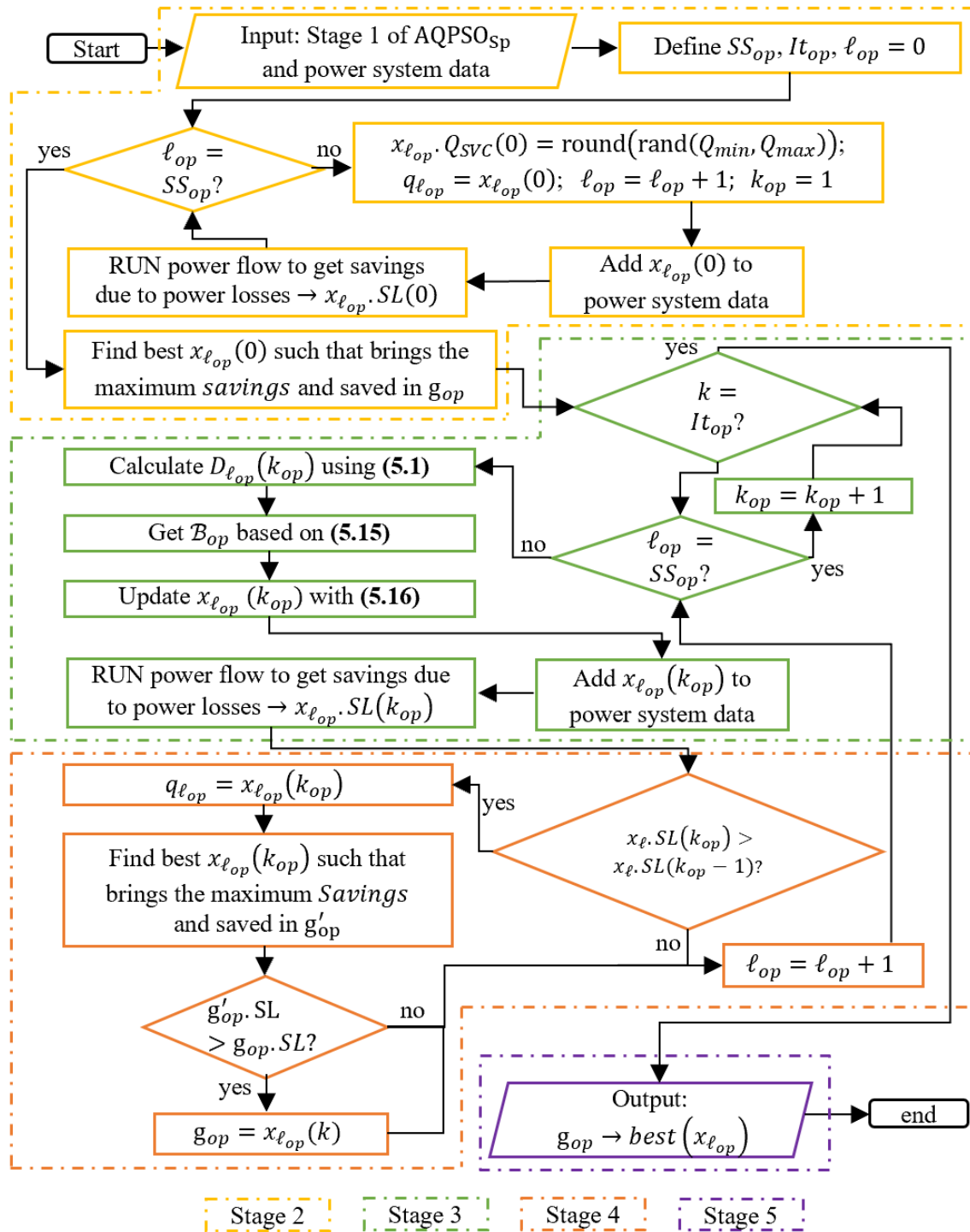


Figure 5.10 AQPSO_{op} flowchart for optimum SVC operation [208]

- Stage 1: The algorithm starts by taking as data input the size of the SVCs available, swarm size SS_{sp} , the total number of iterations It_{sp} and simulation time TS . This is followed by the random generation of the first particles $x_{\ell_{sp}}(0)$. Each particle represents a different combination of installing the available SVC into the power system. The SVC placement is saved in $x_{\ell_{sp}}.Place(0)$, while its total acquisition cost is saved in $x_{\ell_{sp}}.Cost(0)$.
- Stage 2: This stage takes as input the power system data, specifically the impedances of the lines, the capacity of the generators, and active and reactive power consumed by each load. In addition, a second swarm size SS_{op} and the total number of iterations It_{op} are defined. Next, a strategy dispatch (within the limits of the SVC) is set for every particle, which is saved in the variable $x_{\ell_{op}}.Q_{SVC}(0)$. In order to get the power losses, a power flow based on Newton Raphson method is computed. The savings are obtained and the particle with the highest savings becomes the ‘global best’ and is saved in g_{op} . In addition, notice that the ‘best personal’ $q_{\ell_{op}}$ is equal to the actual position $x_{\ell_{op}}(0)$ since the particles have not started their motion.
- Stage 3: The first AQPSO_{op} iteration takes place, and the particles of the swarm SS_{op} start their motion. The attraction parameter $D_{\ell_{op}}(k_{op})$, and best observation B_{op} are obtained using (5.1) and (5.15), respectively. Then, the new position of the particle is computed using (5.16). The updated position of the particle represents a new strategy dispatch for every SVC that may lead to a better saving value.
- Stage 4: The savings before $x_{\ell_{op}}.SL(k_{op} - 1)$ and after $x_{\ell_{op}}.SL(k_{op})$ the motion of the particle are compared. The higher the savings implies that the particle is getting closer to objective function since the algorithm is looking to maximize savings.

Therefore, if $x_{\ell_{op}}.SL(k_{op}) > x_{\ell_{op}}.SL(k_{op} - 1)$ then the particle updates its position. The ‘personal best’ is also updated and saved in $q_{\ell_{op}}$. This followed by a second comparison in which the the ‘global best’ is considered. For this purpose, it is required to find best $x_{\ell_{op}}(k_{op})$ among the swarm such that brings the maximum savings. The best particle is saved in the variable g'_{op} . If the $g'_{op}.SL > g_{op}.SL$ then the $x_{\ell_{op}}(k_{op})$ becomes the ‘global best’, otherwise the ‘global best’ is not replaced. In case that $x_{\ell_{op}}.SL(k_{op}) \leq x_{\ell_{op}}.SL(k_{op} - 1)$ then the process continues with the next particle.

- Stage 5: The process in stage 3 and stage 4 are repeated until one of the convergence criteria given in (5.2) is satisfied. Consider for the convergence criteria $|x_{\ell}.SL(k) - x_{\ell}.SL(k - 1)| < 10^{-6}$. The outcome is the particle with the best SVC strategy dispatch at time simulation t . The next step is to verify if the SVC location is optimum.
- Stage 6: The first AQPSO_{sp} iteration takes place, and the particles of the swarm SS_{sp} starts their motion. The attraction parameter $D_{\ell_{sp}}(k_{sp})$, and best observation \mathcal{B}_{sp} are obtained using (5.1) and (5.15), respectively. Then, the new position of the particle is computed using (5.16). The updated position of the particle represents a new location for every SVC. Then, AQPSO_{sp} is used to obtain the optimal SVC strategy dispatch.
- Stage 7: In this stage the particles compete between them to determine the best SVC placement. If $x_{\ell_{sp}}.SL(k_{sp}) > x_{\ell_{sp}}.SL(k_{sp} - 1)$ then the particle updates its position. The ‘personal best’ is also updated and saved in $q_{\ell_{sp}}$. This is followed by a second comparison in which the ‘global best’ is considered. For this purpose, it is

required to find best $x_{\ell_{sp}}(k_{sp})$ among the swarm such that brings the maximum savings. The best particle is saved in the variable g'_{sp} . If the $g'_{sp} \cdot SL > g_{sp} \cdot SL$ then the $x_{\ell_{sp}}(k_{sp})$ becomes the ‘global best’, otherwise the ‘global best’ is not replaced. In case that $x_{\ell_{sp}} \cdot SL(k_{sp}) \leq x_{\ell_{sp}} \cdot SL(k_{sp} - 1)$ then the process continues with the next particle.

- Stage 8: The process in stage 6 and stage 7 are repeated until one of the convergence criteria given in (5.2) is satisfied. Consider for the convergence criteria $|\sum_{\ell=1}^{SS} q_{\ell} \cdot SL(k) - SS \cdot g \cdot SL(k)| \leq 10^{-6}$. The outcome is the particle that contains the SVC with the best location and strategy dispatch.

5.4.4 Results and Discussion

There are many combinations in which the available SVCs can be installed within the power system. Nevertheless, there is a combination that leads to the maximum reduction of power losses and hence the maximum savings. Figure 5.11 shows that the optimal placement and sizing of the SVCs that maximize the savings, is as follows:

- SVC of size 100 [MVar] at bus 3.
- SVC of size 50 [MVar] at bus 8.
- Two SVC of size 10 [MVar] at bus 11 and 19, respectively.

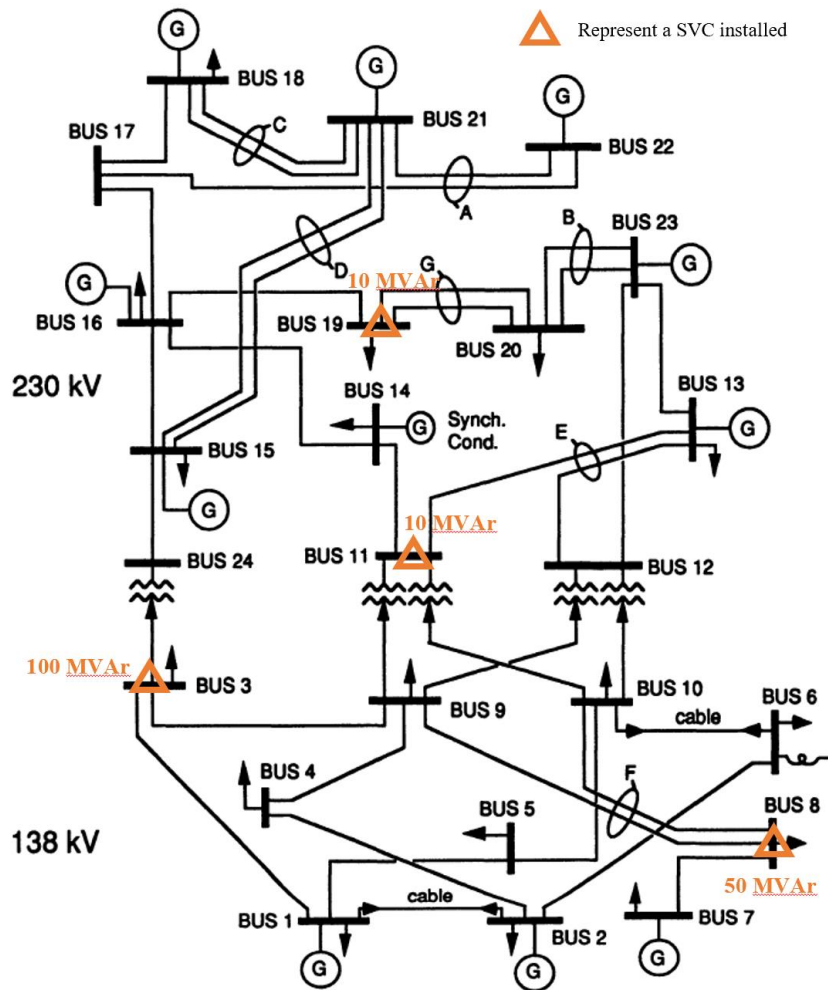


Figure 5.11 SVC optimal placement and size for AQPSO second case study [208]

Even though the SVCs optimal sizing and placement are known, the challenge is to set the strategy dispatch for each SVC. The reactive power injected by each SVC cannot be constant since the load demand is a time-dependent function. Figure 5.12 shows the operation for each SVC during weekday and weekend.

Once the optimal planning and operation of the SVC are obtained, it is required to verify that the solution does not violate voltage restrictions. Figure 5.13 presents a box plot that contains the voltages values for each bus in the power system. As can be perceived in Figure 5.13, the median voltage value in all buses $1.02 p.u.$, with a maximum and minimum of $1.04 p.u.$ and $0.97 p.u.$ Therefore, the voltages values in all buses follow the IEEE Standard 1860-2014 [218] which establishes $0.95 p.u. \leq V_{bus} \leq 1.05 p.u.$

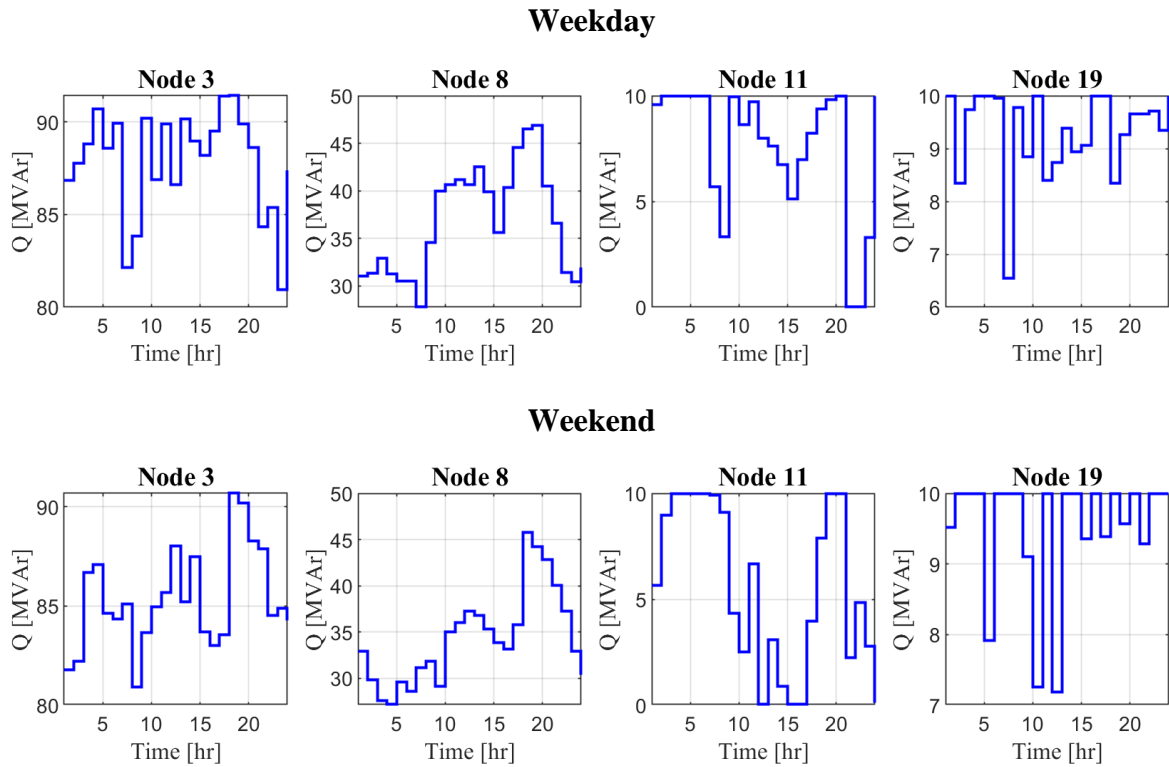


Figure 5.12 Optimal dispatch strategy for each SVC [208]

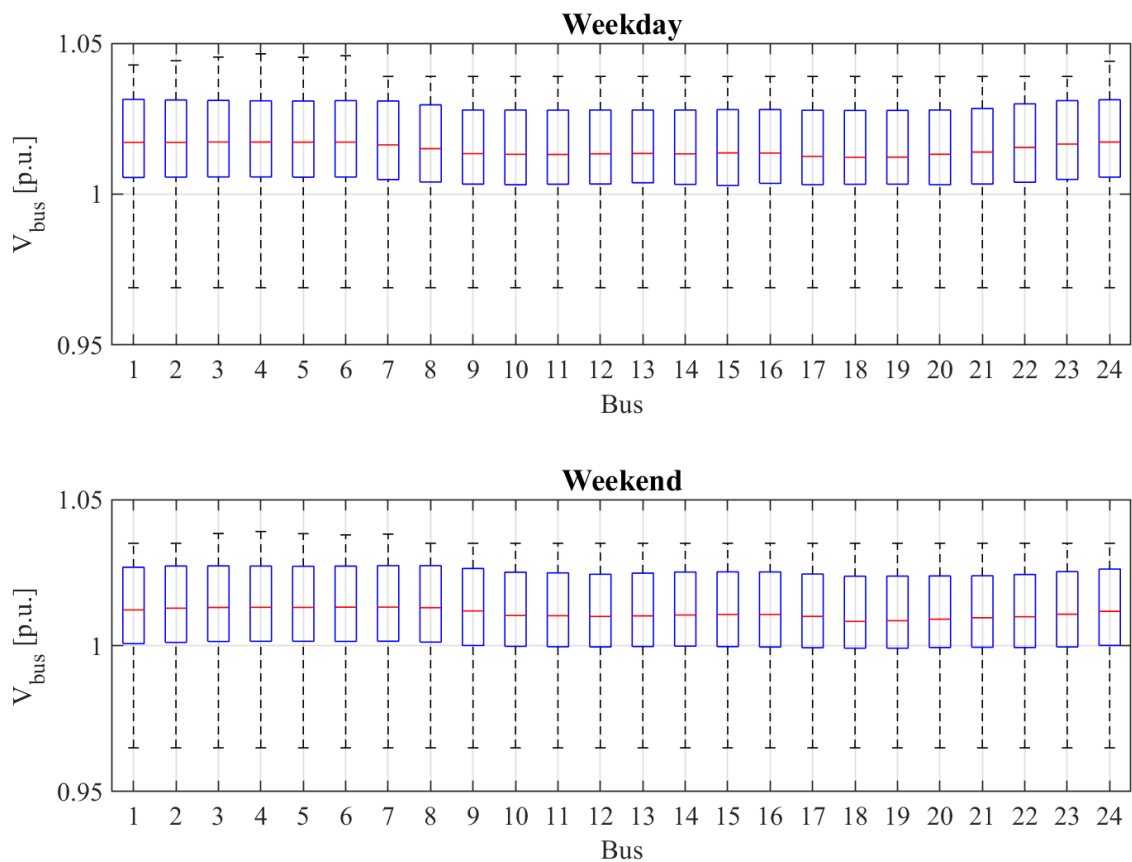


Figure 5.13 Voltage profile for AQPSO second case study [208]

Regarding the savings, over the initial period of analysis, the cost exceeds the savings due to the high upfront investment required for the installation and acquisition of the SVCs. However, as time pass by, the savings increases and by the year 12 the total savings is 4.40×10^5 [£]. To verify that this value is the maximum saving, the same optimization problem is solved using two different algorithms. The former is called Bi-level Particle Swarm Optimization (BPSO) and it employs 20 particles and 30 iterations in each level with Monte Carlo simulation experiments of 5000 per level; the second is called Bi-level Genetic Algorithm (BLGA) and it employs a population of 20 chromosomes and 30 iterations with Monte Carlo simulation experiments of 5000 per level. Table 5.5 shows the results for each optimization technique and it can be appreciated that the total savings obtained from BPSO and BGA coincide with the value obtained from BAQPSO.

Another relevant fact to consider in the analysis is the average time simulation, which is given by the time average simulation and number of iterations for convergence of each optimization technique. Table 5.5 reveals that BAQPSO presents the lowest average time simulation by 3.98 [s] and 3.09 [s] in comparison to BPSO and BGA, respectively. Additionally, BAQPSO also presents the fastest convergence by 34.3 % and 37.5 % in comparison to BPSO and BGA, respectively. This is attributed to physical theories that describe the motion of the particles. BPSO and BGA employ particles that move following the principles of classical physics and biology, respectively. Their convergence is defined by deterministic equations. Consequently, the particles in both algorithms move towards the solution with a specific rate in each iteration. In contrast, BAQPSO employs quantum particles and their motion is given by principles of uncertainties (Quantum Mechanics), which establishes that the particle can appear at any position within the solution space. Nevertheless, this is controlled by observers that leads the particle closer to the optimal

solution. Hence the probability of convergence for BAQPSO may increase drastically in each iteration.

Table 5.5 Optimization Technique Robustness for AQPSO second case study [208]

Algorithm	Average time simulation [s]	Number of iterations to reach convergence	<i>SavingL – CostSVC</i> (after 12 years)
BAQPSO	10.69	20	4.40×10^5
BPSO	14.67	32	4.40×10^5
BGA	13.78	30	4.40×10^5

5.5 Summary

This chapter presents an advance optimization technique called Accelerated Quantum Particle Swarm Optimization (AQPSO). AQPSO uses the concept of quantum particle position to define a candidate solution to an optimization problem. The mathematical formulation that describes the motion of the quantum particle is derived from quantum mechanics theories. The novelty of the proposed AQPSO is the incorporation of the ‘best observation’ parameter, which is determined by performing several observations. This parameter increases the probability of finding the particle close to the optimal solution, which accelerates the convergence to the near-optimal solution. To prove the performance of the proposed approach, two different optimization problems in power systems are solved using AQPSO. In the first case, the AQPSO is employed to determine the size and location of SVCs that minimize the expected energy not supplied. In the second case, the technique is applied to maximize the savings due to power losses reduction by optimal planning and operation of SVCs. In addition, to show the computational efficiency of AQPSO in comparison to other optimization techniques, the same optimization problems are solved using standard PSO and genetic algorithm. The results reveal that AQPSO proved to be superior in convergence, accuracy and time simulation.

Chapter 6: Smart Maintenance Scheme for Generators

In order to provide a reliable service and being able to supply the electricity demand, all power system components should be subjected to an effective maintenance plan. Such maintenance plan is vital to limit failures and downtime of the components. The smarter the maintenance performed could potentially result in a better performance of the power system. In this context, periodic preventive maintenance (PPM) and reliability-centered maintenance (RCM) are the most popular in power system industry and recommended by many standards [128], [220], [221]. Nevertheless, these plans do not consider the different operational states and optimum maintenance, which brings inaccuracies to the reliability evaluation.

Several researchers proposed the vision of smart maintenance with the inclusion of smart-inspections [25], smart-devices [26] and smart-services [27], giving a scheduled and proactive maintenance schemes. The current literature in this area provides limited transparency of mathematical frameworks that can effectively capture the maintenance paradigms for the economic benefit of planning and operating power systems.

This chapter presents a reliability-based smart maintenance approach of generators to compute the net-maximum economic benefit. The chapter is divided into four sections. Section 6.1 exposes the reliability and risk concepts employed to define the SM scheme. Section 6.2 describes SM general process. In Section 6.3, SM is employed to get the maximum net benefit from the system generation. Finally, the last section brings a summary of the chapter.

As a contribution to the state of art, the publications [222]–[224] resulted from the research described in this chapter.

6.1 Smart Maintenance Mathematical Framework

Smart maintenance (SM) is an advanced maintenance framework that incorporates operational risk and reliability models of the components to set an effective maintenance plan that maximize the generation adequacy economic benefits. Figure 6.1 presents the reliability and risk concepts needed to formulate the smart maintenance mathematical framework.

Firstly, Kijima model [225] is employed to characterize the impact of maintenance over the virtual age of the component. Secondly, Markov chain is used to describe the probability of being in the different operational states of the component. Thirdly, fuzzy logic is applied to quantify the maintenance exertion degree (maintenance effort). This is required to measure the impact of maintenance over the magnitude of the failure rate of the component.

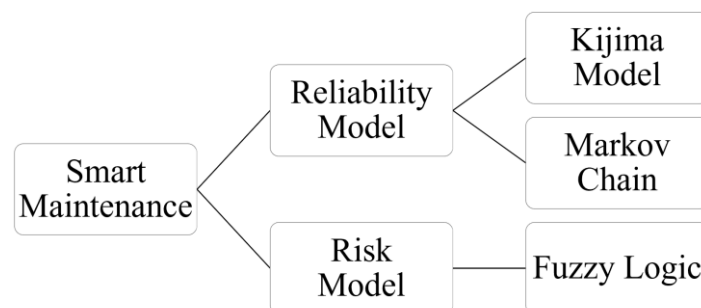


Figure 6.1 Smart maintenance concepts

6.1.1 Kijima Model: Virtual Age, Actual Age and Maintenance

Maintenance produces a rejuvenation effect on the lifetime of a component. To quantify its impact the Kijima model type I is employed [225] since is simple and bring accurate results. It assumes that the repairs can be fixed only by the damage incurred during the period of operation since the last repair. For its formulation, let the real age be time t in which the component is in operation. Then, the virtual age Γ of the component can be defined using a linear function of its real age, in such a way that the virtual age varies by an amount

proportional to the time elapsed from the $n - 1^{\text{th}}$ maintenance to the n^{th} maintenance, as is presented in (6.1). Mathematically, the virtual age is as follows [225]:

$$\Gamma_n = \Gamma_{n-1} + q_n \Delta\tau_n \quad (6.1)$$

where q represents the degree of maintenance.

By expanding the formulation given in (6.1):

$$\begin{aligned} \text{No maintenance} &\Rightarrow \Gamma_0 = 0 \\ \text{1}^{\text{st}} \text{ maintenance} &\Rightarrow \Gamma_1 = \Gamma_0 + q_1 \Delta\tau_1 = q_1 \Delta\tau_1 \\ \text{2}^{\text{nd}} \text{ maintenance} &\Rightarrow \Gamma_2 = \Gamma_1 + q_2 \Delta\tau_2 = q_1 \Delta\tau_1 + q_2 \Delta\tau_2 \\ &\vdots \\ \text{n}^{\text{th}} \text{ maintenance} &\Rightarrow \Gamma_n = \Gamma_{n-1} + q_n \Delta\tau_n = q_1 \Delta\tau_1 + \dots + q_n \Delta\tau_n \end{aligned} \quad (6.2)$$

Generalizing for the two types of maintenance, (6.2) can be rewritten as in (6.3).

$$\begin{aligned} \Gamma_n &= \sum_{CM=1}^{NCM} q_{CM} \Delta\tau_{CM} + \sum_{PM=1}^{NPM} q_{PM} \Delta\tau_{PM}; \\ n &= NPM + NCM \end{aligned} \quad (6.3)$$

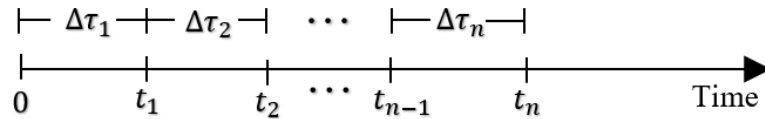


Figure 6.2 Virtual age evolution

6.1.2 Markov Chain: Probability Vector of all Possible States

Table 6.1 presents the seven operational stages of generators used to create the Markov chain. Figure 6.3 shows each operational state based on the stages of the bathtub curve and half-arch shape [14]. Each state and stage are described as follows:

- **Operation Good as New and Policy of Replacement:** The infant mortality is considered as a period of guarantee given by the manufacturer's policy. In this stage, the component is in a state denominated by 'operation good as new'. If an event failure occurs, the component is subjected to the policy of replacement and the

component's lifetime is reset to start from zero. This process is repeated until the guarantee period ends.

- Non-operating, derated, and rated operation:** In order to evaluate the reliability, it is common to represent the components of the system in two basic states: 1. Operating (On); 2. Non-Operating (Off). Although this model is simple to use, it lacks completeness of modelling a real system. There are systems that present $n+1$ redundancy between their components, and if a failure occurs in a certain component, such systems may be partially operating, in which case it is said that the component is in a derated operation. For example, thermal unit generation is designed with a main and auxiliary circuits working in parallel. Whenever the auxiliary circuit fails, the output power of the system is reduced by a certain amount, resulting in a derated state of power [6]. A schematic diagram of the given example is presented in Fig. 2. Table I shows the individual impact of the states between the main and auxiliary unit of a thermal power generator. Consequently, the derated state open a pathway to define the term 'semi availability'. The semi-availability (\dot{A}) is described by the sum of probabilities of the derated states of the component that belongs to the set Ξ . Mathematically, semi availability is given by (6.4).

$$\dot{A}(t) = \sum_{s \in \Xi} P_s \quad (6.4)$$

Hence, the semi availability for the model presented in Figure 6.3 is given by (6.5).

$$\dot{A}(t) = P_4 \quad (6.5)$$

- Overloaded operation:** This operation can be executed after the infant mortality stage. In contrast to the states already presented, this state is based on decision-making, that is, if at τ_{ov} an overloaded operation is programmed, then the transition

rate automatically conducts the component to that state. Mathematically, it can be formulated as:

$$q(t) = \begin{cases} \infty; & t = \tau_{ov} \\ 0; & t \neq \tau_{ov} \end{cases} \Rightarrow P_{II}(t_{ov}) = 1.0 \quad (6.6)$$

It is considered that under overloaded operation the component will not exceed its permitted limits of time ($\Delta\tau_{ov}$) operation and output power. Therefore, no failure will occur and the only state to return is to state I. Mathematically, it can be expressed as:

$$\lim_{t \rightarrow \tau_{ov} + \Delta\tau_{ov}} P_1(\theta(t)) = 1.0 \quad (6.7)$$

- **Obsolescence:** At some point, the component's unavailability could be high, and a replacement is required. If that occurs, the component can be treated as having reached the obsolescence state. The transition rate that leads to this state is the component's degradation rate ϕ [202], which can be determined following the procedure described in Section 4.3.2. Mathematically, the degradation rate can be expressed as given in (6.8).

$$\phi = \frac{\lambda_K + 2\mu_K}{\Gamma_n \lambda_K - 1} \quad (6.8)$$

Notice that the impact of maintenance is considered within the degradation rate since the real age (T_W) of the component is replaced by the virtual age (Γ_n). Then, as described in Section 4.4, the degradation of the component can be defined as:

$$\Lambda = \frac{1}{\Gamma_n \phi} \quad (6.9)$$

Table 6.1 Operational States Labels

State	Name
0	Operation good as new
1	Rated operation
2	Derated operation
3	Obsolescence
4	Not in Operation
I	Policy of replacement
II	Overloaded operation

Table 6.2 Thermal Unit Power Output

Main	Auxiliary	System	State
Off	Off	Off $P_{out} = 0$	Not in service
Off	On	Off $P_{out} = 0$	Not in service
On	Off	On $P_{out} = \zeta P_{out}$ $0 < \zeta < 100\%$	Derated Operation
On	On	On $P_{out} = 100\% P_{out}$	Rated Operation

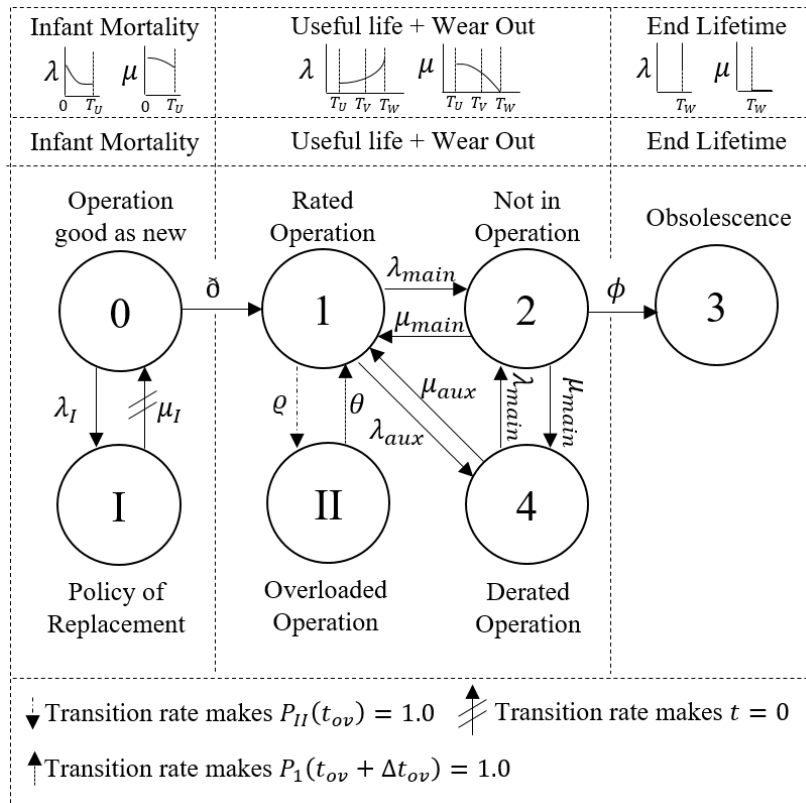


Figure 6.3 Markov chain of the operational states

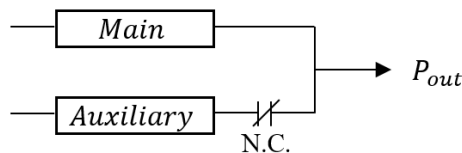


Figure 6.4 Design of a thermal unit with auxiliary support

Even though Figure 6.3 shows seven possible states, the Markov chain model can be reduced to four states. In the first instance, failures being occurred during the guarantee period does not correspond to the customer. The state “0” and “1” are to secure the guarantee, that is, if a failure occurs during this period, then time count is reset to zero and this process is repeated until guarantee period ends. Therefore, the model can avoid the states that appear during the infant mortality and the analysis can starts from the state “1” by considering the end of the guarantee period (T_U) as the initial time analysis. On the other hand, the overloaded operation is a based-decision-making state, hence once the decision is made the probability of being in this state becomes to the unit. Under these considerations, the stochastic matrix of transitions states is determined following the procedure given in Section 4.3.1. The stochastic matrix of transitions of the model presented in Figure 6.3 is given by (6.10).

$$\mathbf{H} = \begin{bmatrix} -\lambda_{main} - \lambda_{aux} & \lambda_{main} & 0 & \lambda_{aux} \\ \mu_{main} & -2\mu_{main} - \phi & \phi & \mu_{main} \\ 0 & 0 & 0 & 0 \\ \mu_{aux} & \lambda_{main} & 0 & -\lambda_{main} - \mu_{aux} \end{bmatrix} \quad (6.10)$$

where the λ_{main} and μ_{main} are the transitions rates of the main circuit of the component and λ_{aux} and μ_{aux} represent the transitions rates of the auxiliary circuit, respectively. Then, the probabilities of being in each state are [226]:

$$\begin{aligned} P_1(t) &= c_1 Y_{11} e^{\chi_1 t} + c_2 Y_{12} e^{\chi_2 t} + c_3 Y_{13} e^{\chi_3 t} + c_4 Y_{14} e^{\chi_4 t} \\ P_2(t) &= c_1 Y_{21} e^{\chi_1 t} + c_2 Y_{22} e^{\chi_2 t} + c_3 Y_{23} e^{\chi_3 t} + c_4 Y_{24} e^{\chi_4 t} \\ P_3(t) &= c_1 Y_{31} e^{\chi_1 t} + c_2 Y_{32} e^{\chi_2 t} + c_3 Y_{33} e^{\chi_3 t} + c_4 Y_{34} e^{\chi_4 t} \\ P_4(t) &= c_1 Y_{41} e^{\chi_1 t} + c_2 Y_{42} e^{\chi_2 t} + c_3 Y_{43} e^{\chi_3 t} + c_4 Y_{44} e^{\chi_4 t} \end{aligned} \quad (6.11)$$

where χ represent the eigenvalues of \mathbf{H}^T , Y is the element of the matrix formed by the eigenvectors of \mathbf{H}^T , and c is a constant given by the initial conditions; T indicates the transpose of the matrix.

6.1.3 Fuzzy Logic to Quantify Maintenance Effort

During the manufacturing process, components are subject to operational strength-toughness test. Based on this, the operational risk (Ω) is defined as the probability of failure due to danger events [97]. The operational risk Ω is closely associated with the maintenance exertion degree z . Mathematically, their relationship is as follows:

$$z \propto \Omega \quad (6.12)$$

The exertion degree represents the efficacy of maintenance, which can be perfect, imperfect and minimal. The term perfect ($z = 1$) refers to the restoration of the component as ‘good as new’, the imperfect ($0 < z < 1$) implies a restoration of the component between ‘good as new’ and ‘bad as old’, and in the case where maintenance is developed with limited effort, is called minimal ($z = 0$) [227]. Concerning the imperfect maintenance, it can be fuzzified as follows: ‘*Negligible*’, ‘*Minor*’, ‘*Moderate*’ and ‘*Major*’. Its quantification and description are exhibit in Table 6.3.

There are two fundamental risk parameters used to assess the exertion degree. The first one is the availability (A), which determines the frequency of failures in a certain time period. It can be classified using five linguistic variables, these are: ‘*Extremely Low*’, ‘*Low*’, ‘*Medium*’, ‘*High*’ and ‘*Extremely High*’. The quantification and description of each grade are presented in Table 6.4. The other parameter that defines the risk is the factor of operation (Op), which determines the magnitude of operation of the component. Four linguistic variables are defined to describe it, these are: ‘*Light*’, ‘*Marginal*’, ‘*Regular*’ and ‘*Forced*’. The quantification of each grade is as presented in Table 6.5.

Linguistic variables are used to describe different types of fuzzy membership functions according to the situation of an interested area, and these are critically defined by experts. After an exhaustive interview with the experts in the field of power generator maintenance [228]–[232], the membership functions for each risk parameter is established

and presented in Table 6.6. With this information, the next step is to process the fuzzy dataset by defining the control rules. These are based on an antecedent and consequence, in such a way that for every action associated with the input variables, there is a response related to the output variables. After verification with the experts in the field [228]–[232], the control rules are defined and presented in Table 6.6. Such control rules are used to determine the maintenance exertion degree as a function of the availability and factor of operation. This can be appreciated in Figure 6.6.

Table 6.3 Maintenance Exertion Degree Qualitative Descriptors

Qualitative Descriptors	Description	Range [p.u.]
Negligible	Risk is insignificant and can be controlled by with a simple inspection	0.00-0.25
Minor	Risk is low; therefore, a low maintenance effort is required	0.00-0.50
Moderate	Risk is medium bringing the need of a medium maintenance effort	0.25-0.75

Table 6.4 Availability Qualitative Descriptors

Qualitative Descriptors	Description	Range [%]
Extremely Low	Failure is almost unavoidable	0.00-50.0
Low	Failure to happen frequently	50.0-77.0
Medium	Risk is medium bringing the need of a medium maintenance effort	62.0-87.0
High	Occasional failure	72.0-95.0
Extremely High	Failure is unlikely to occur but possible	92.0-100

Table 6.5 Factor of Operation Qualitative Descriptors

Qualitative Descriptors	Description	Range [%]
Light	Most of the time the component was not in operation	0.00-50.0
Marginal	Most of the time the component was in derated operation	50.0-92.0
Regular	Most of the time the component was in rated operation	90.0-105
Forced	Most of the time the component was in overloaded operation	105-115

Table 6.6 Maintenance Exertion Degree Control Rules

Rule	Statement
1	If (<i>A</i> is <i>Extremely Low</i>) & (<i>Op</i> is <i>Light</i>) \Rightarrow (<i>z</i> is <i>Negligible</i>)
2	If (<i>A</i> is <i>Extremely Low</i>) & (<i>Op</i> is <i>Marginal</i>) \Rightarrow (<i>z</i> is <i>Negligible</i>)
3	If (<i>A</i> is <i>Extremely Low</i>) & (<i>Op</i> is <i>Regular</i>) \Rightarrow (<i>z</i> is <i>Negligible</i>)
4	If (<i>A</i> is <i>Extremely Low</i>) & (<i>Op</i> is <i>Forced</i>) \Rightarrow (<i>z</i> is <i>Negligible</i>)
5	If (<i>A</i> is <i>Extremely High</i>) & (<i>Op</i> is <i>Light</i>) \Rightarrow (<i>z</i> is <i>Negligible</i>)
6	If (<i>A</i> is <i>Extremely High</i>) & (<i>Op</i> is <i>Marginal</i>) \Rightarrow (<i>z</i> is <i>Minor</i>)
7	If (<i>A</i> is <i>Extremely High</i>) & (<i>Op</i> is <i>Regular</i>) \Rightarrow (<i>z</i> is <i>Moderate</i>)
8	If (<i>A</i> is <i>Extremely High</i>) & (<i>Op</i> is <i>Forced</i>) \Rightarrow (<i>z</i> is <i>Moderate</i>)
9	If (<i>A</i> is <i>Medium</i>) & (<i>Op</i> is <i>Light</i>) \Rightarrow (<i>z</i> is <i>Minor</i>)
10	If (<i>A</i> is <i>Medium</i>) & (<i>Op</i> is <i>Marginal</i>) \Rightarrow (<i>z</i> is <i>Minor</i>)
11	If (<i>A</i> is <i>Medium</i>) & (<i>Op</i> is <i>Regular</i>) \Rightarrow (<i>z</i> is <i>Moderate</i>)
12	If (<i>A</i> is <i>Medium</i>) & (<i>Op</i> is <i>Forced</i>) \Rightarrow (<i>z</i> is <i>Major</i>)
13	If (<i>A</i> is <i>Low</i>) & (<i>Op</i> is <i>Light</i>) \Rightarrow (<i>z</i> is <i>Moderate</i>)
14	If (<i>A</i> is <i>Low</i>) & (<i>Op</i> is <i>Marginal</i>) \Rightarrow (<i>z</i> is <i>Moderate</i>)
15	If (<i>A</i> is <i>Low</i>) & (<i>Op</i> is <i>Regular</i>) \Rightarrow (<i>z</i> is <i>Major</i>)
16	If (<i>A</i> is <i>Low</i>) & (<i>Op</i> is <i>Forced</i>) \Rightarrow (<i>z</i> is <i>Major</i>)
17	If (<i>A</i> is <i>High</i>) & (<i>Op</i> is <i>Light</i>) \Rightarrow (<i>z</i> is <i>Minor</i>)
18	If (<i>A</i> is <i>High</i>) & (<i>Op</i> is <i>Marginal</i>) \Rightarrow (<i>z</i> is <i>Minor</i>)
19	If (<i>A</i> is <i>High</i>) & (<i>Op</i> is <i>Regular</i>) \Rightarrow (<i>z</i> is <i>Moderate</i>)
20	If (<i>A</i> is <i>High</i>) & (<i>Op</i> is <i>Forced</i>) \Rightarrow (<i>z</i> is <i>Moderate</i>)

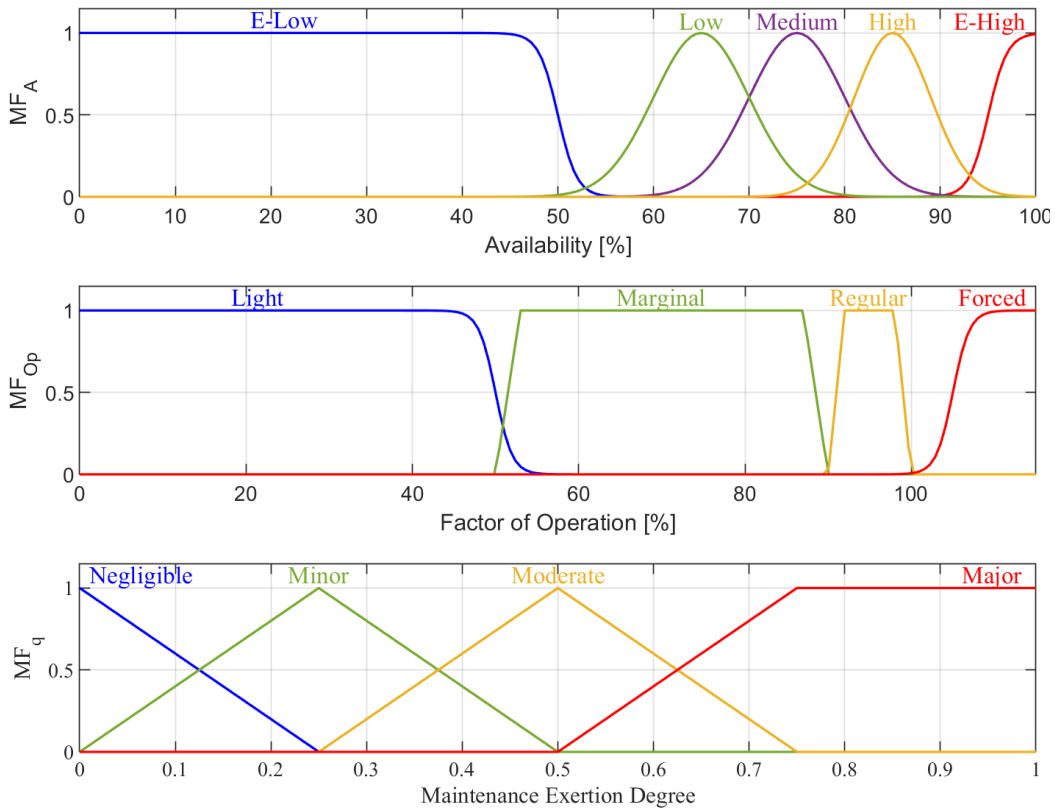


Figure 6.5 Membership functions

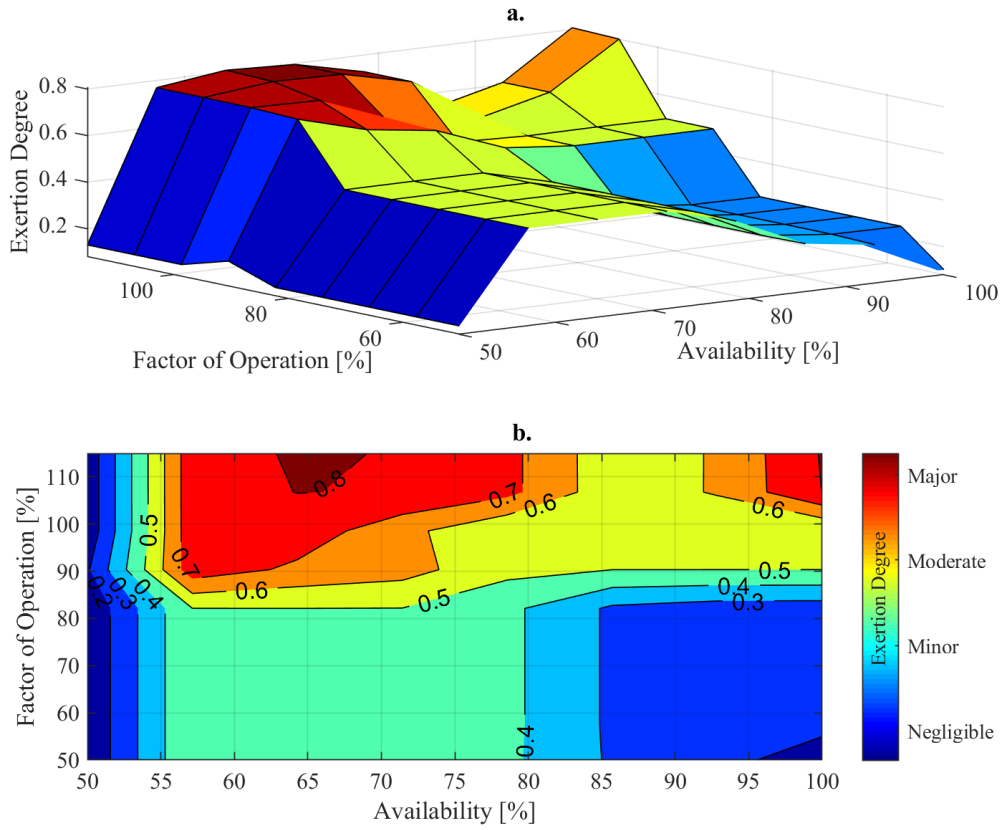


Figure 6.6 Maintenance Exertion Degree: a) 3d plot; b) contour plot

6.1.4 Maintenance Effort Impact on Failure Rate

In order to measure the impact of the maintenance on the failure rate, the maintenance exertion degree is required. Figure 6.7 shows that the failure rate varies by a proportional amount z , such that [225]:

$$\begin{aligned}
 \text{No maintenance} &\Rightarrow \lambda_0(t) \\
 \text{1}^{\text{st}} \text{ maintenance} &\Rightarrow \lambda_1(t) = z\lambda_0(t - \Delta\tau_1) + (1 - z)\lambda_0(t) \\
 \text{2}^{\text{nd}} \text{ maintenance} &\Rightarrow \lambda_2(t) = z\lambda_1(t - \Delta\tau_2) + (1 - z)\lambda_1(t) \\
 &\vdots \\
 \text{}^n \text{ maintenance} &\Rightarrow \lambda_n(t) = z\lambda_{n-1}(t - \Delta\tau_{n-1}) + (1 - z)\lambda_{n-1}(t)
 \end{aligned} \tag{6.13}$$

where $\Delta\tau_n$ represents the time elapsed between the n^{th} and $n^{\text{th}} - 1$ maintenance.

Since there are two types of maintenance, (6.13) can be generalized as follows:

$$\lambda_n(t) = \begin{cases} z_{CM}\lambda_{n-1}(t - \Delta\tau_{n-1}) + (1 - z_{CM})\lambda_{n-1}(t), & \text{if CM is performed} \\ z_{PM}\lambda_{n-1}(t - \Delta\tau_{n-1}) + (1 - z_{PM})\lambda_{n-1}(t), & \text{if PM is performed} \end{cases} \tag{6.14}$$

To simplify the model, the maintenance type factor ϑ is incorporated into the model. Depending on the type of maintenance, ϑ can be: One, if CM is performed; 2. Zero, if PM is performed. Hence, (6.14) can be rewritten as in (6.15).

$$\lambda_n(t) = z_{CM}^\vartheta z_{PM}^{1-\vartheta} \lambda_{n-1}(t - \Delta\tau_{n-1}) + (1 - z_{CM}^\vartheta z_{PM}^{1-\vartheta}) \lambda_{n-1}(t);$$

$$\vartheta = \begin{cases} 1, & \text{if CM is performed} \\ 0, & \text{if PM is performed} \end{cases} \quad (6.15)$$

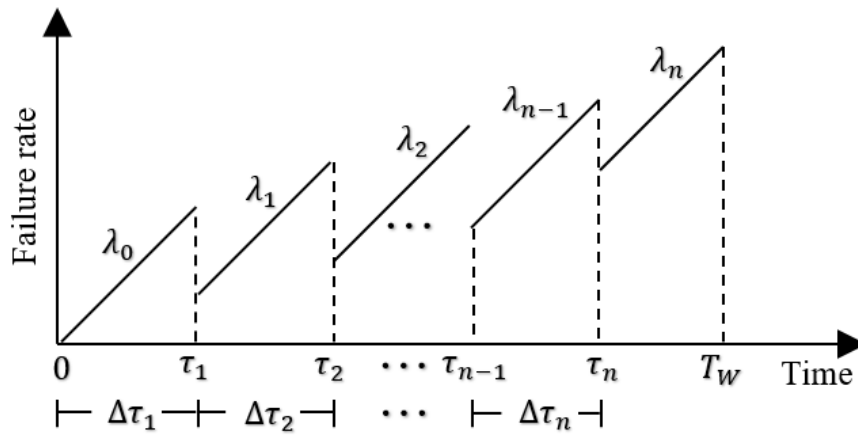


Figure 6.7 Maintenance impact on failure rate

6.2 Smart Maintenance Procedure

Smart maintenance (SM) is an evolutionary maintenance strategy that proposes a maintenance schedule optimization problem, of which the objective is to minimize the maintenance cost while keeping adequate reliability of the system. Consequently, SM leads to a comprehensive and effective preventive maintenance schedule that indicates when (time to perform the maintenance), which (component that receives the maintenance) and how (effort required during maintenance) the maintenance actions should be performed in order to maximize the economic benefits. Although SM can incorporate smart devices, SM is not limited to it since SM can be achieved using the historical operational records of the component following the process described in Figure 6.8.

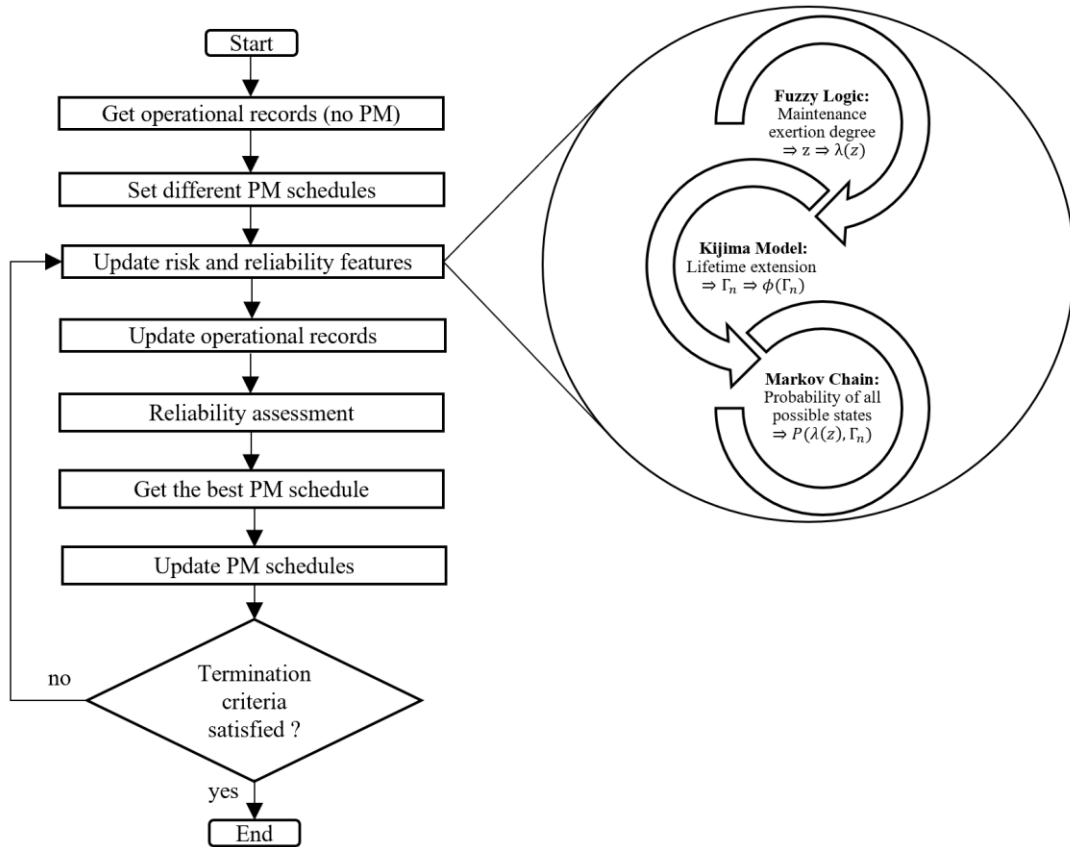


Figure 6.8 Smart Maintenance flowchart

- Get initial operational records (no PM):** SM starts by determining the initial operational records of the components of the system. The operational records are obtained from the base case in which no PM is considered. This is done in order to get a benchmark and be able to measure the impact of the preventive maintenance schedule. From this analysis, the availability and factor of operation of the components are obtained.
- Set different PM schedules:** SM takes as input different PM schedules. During the optimization process, the PM schedules candidates will evolve (enhance) based on the PM schedule with the highest economic benefit. It is suggested that among the PM schedules to consider periodic preventive maintenance (PPM). This is in virtue that PPM is highly recommended by many standards [128], [220], [221] and is simple to incorporate as a candidate solution into the SM process.

- **Update reliability and risk features:** Maintenance actions bring many impacts on the risk and reliability features of the component. Firstly, the maintenance exertion degree is determined based on fuzzy logic (section 6.1.3), by using the operational records of the component that were initially obtained. Then, the failure rate of the component is updated as described in section 6.1.4. Secondly, the virtual age of the component is calculated by using the Kijima Model described in Section 6.1.2. Subsequently, the degradation rate is updated. Finally, the probabilities vector of all possible states (influenced by PM) can be estimated following the process described in section 6.1.1.
- **Update operational records:** New operational records are generated in this stage. This is due to the impact of the maintenance actions over the reliability model of the component. The updated operational records are obtained by using the updated reliability model of the components in combination with sampling techniques. In this research the Sequential Median Latin Hypercube sampling technique is suggested to reduce the computational burden.
- **Reliability assessment:** In order to quantify the system performance due to maintenance, a reliability assessment is conducted.
- **Get the best PM schedule:** In this stage, the economic benefits of the proposed PM schedules are compared. The best PM schedule is the one that presents the highest economic benefits.
- **Update PM schedules:** In order to assure the optimum economic benefits among the PM schedules candidates, PM schedules evolve (enhance) based on the rules set by the optimization technique employed. Notice that SM involves a complex optimization problem (non-linear equations), which can be solved using robust

optimization techniques. For this reason, SM incorporates the AQPSO into the model. Therefore, the PM schedules evolve following the expression given in (5.16).

- **Termination criteria:** The termination criteria mainly depend on the optimization technique employed to solve the optimization problem. Since SM employs AQPSO, SM finishes if one of the conditions given in (5.2) is satisfied.

6.3 Generation Adequacy using Smart Maintenance

SM is employed to define an effective maintenance plan that maximizes the net benefit from the system generation. The description of the case study, problem formulation, proposed algorithm, and results are as given in the following sections.

6.3.1 Case Study

The study incorporates the Roy Billinton Test System (RBTS) [6]. Four scenarios are evaluated: 1. No PM (NPM); 2. Yearly periodic PM with $z = 0.80$ (PPM); 3. Reliability-centred maintenance using PSO with $z = 0.80$ (RCM). 4. Smart maintenance (SM). The assumptions are the following: 1. Generators reliability features are as shown in Table 4.1; 2. Generators cost data is as given in Table 6.7; 3. Energy price is $e = 0.082$ [£/kWh] with a yearly increment of 3%; 4. Only thermal generators are subjected to a derated operation and it cost half of the CM to restore the component to rated operation; 5. Overloaded operation maximum time for all generators is one hour with a maximum power output of 115%; 6. Yearly load profile is as shown in Figure 4.3 with a yearly increment of 0.5 %; 8. The cost increases every year by 2%. 8. PM cost is as shown in Figure 6.9.

Table 6.7 Generators Maintenance Cost

Unit Generation H: Hydro T: Thermal	H5 Pelton	T10 Oil	H20 Francis	T20 Coal	H40 Kaplan	T40 Coal
Acquisition Cost [M£]	40	40	80	60	160	80
Operation Cost [k£/yr]	12.5	600	50	680	100	790
CM Cost [k£]	156	625	375	1250	750	1375

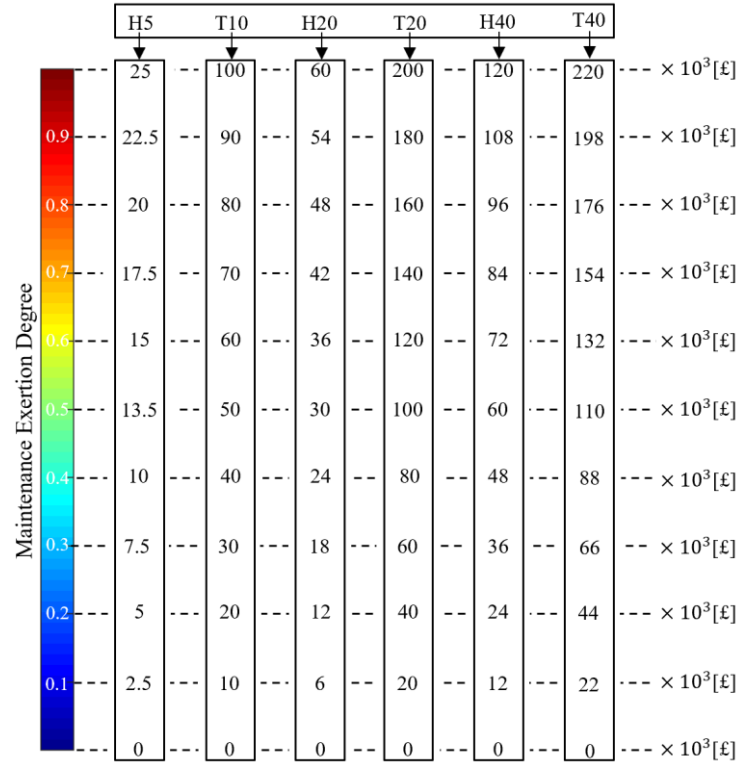


Figure 6.9 PM cost as a function of the exertion degree

6.3.2 Problem Formulation

The annual reliability index under consideration is the loss of energy expectation (*LOEE*) in MWh/yr. This index is calculated using the Sequential Median Latin Hypercube (SMLH). SMLH is a statistical method for generating a near-random sample of parameter values from a multidimensional distribution. The key idea of SMLH is the stratification of the input probability distribution function. This is divided into equal intervals that coincide with the total number of experiments NE . Then, the set G is formed with the intervals, such that:

$$G = \{G_1, G_2, \dots, G_{NE}\} \quad (6.16)$$

where

$$G_1 = \left[0, \frac{1}{NE}\right); G_2 = \left[\frac{1}{NE}, \frac{2}{NE}\right); \dots; G_{NE} = \left[\frac{NE-1}{NE}, 1\right] \quad (6.17)$$

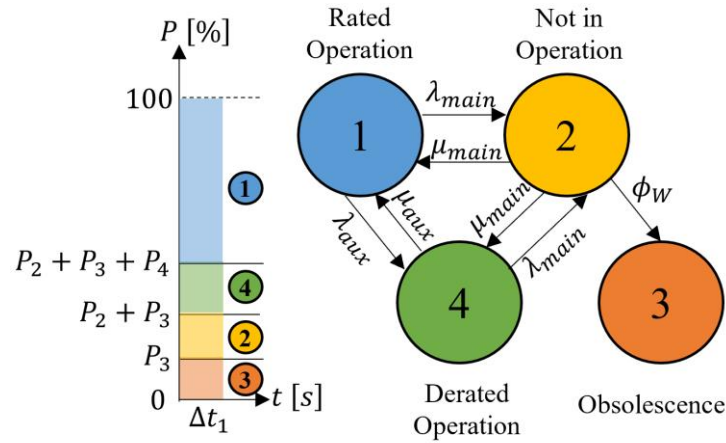


Figure 6.10 State estimation rule using SMLH

When the experiment ex takes place, the median value (u) of each equiprobable interval G_i is selected by comparing with the probability state of the component as presented in Figure 6.10. Then, the operational state s of the component is given by the rule in (12) [6].

$$s = \begin{cases} \text{State 1, if } u > P_2 + P_3 + P_4 \\ \text{State 2, if } P_2 + P_3 + P_4 \leq u \leq P_2 + P_3 \\ \text{State 3, if } P_2 + P_3 \leq u < P_3 \\ \text{State 4, if } P_3 \leq u \end{cases} \quad (6.18)$$

Once the state of each generator is identified, the energy not supplied due to interruptions of the service (ENS_{ex}) is obtained by calculating the available energy margin. That is, if the demand is greater than the total generation (negative margin), then its difference becomes the ENS_{ex} . This value is saved, and the experiment is completed. The process is repeated for NE experiments during the period of study TS . Finally, the reliability index is calculated by using (6.19).

$$LOEE = \frac{1}{NE} \sum_{exp=1}^{NE} ENS_{exp} \quad (6.19)$$

Then, the unit generation benefit is obtained by multiplying the energy price times the energy supplied. Mathematically, the generation adequacy benefit can be written as

$$Benefit = e \left(\sum_{t=1}^{TS} E(t) - LOEE \right) \quad (6.20)$$

where $E(t)$ represents the demanded energy at time t .

On the other hand, maintenance cost is the price paid for the actions taken to preserve or restore the generator to rated operational state. In the case of corrective maintenance (CM), the cost is related to the repair or substitution of the failed part in the component. In the case of preventive maintenance (PM) action, the cost is related to the resources needed to perform inspection and reduce the occurrence failure. By defining gen as the slot index for generators, $CostPM$ as the price of performing one PM, $CostCM$ as the price of performing one CM, NPM as the total number of PM performed, and NCM as the total number of CM. Then, the maintenance cost can be formulated as given in (6.21) Hence, the total maintenance cost in the interval $(0, TS]$ can be expressed as

$$CostM = \sum_{gen=1}^{NG} (CostPM_{gen} NPM_{gen} + CostCM_{gen} NCM_{gen}) \quad (6.21)$$

Another cost to consider is the $CostAc$, which represent the capital required to buy the generators. The last cost involves the operation of the generator defined as $CostOp$. Therefore, the total cost is:

$$CostTotal = CostM + \sum_{gen=1}^{NG} (CostAc_{gen} + CostOp_{gen}) \quad (6.22)$$

With the obtained expressions, the net benefit can be mathematically formulated as:

$$NB = Benefit - CostTotal \quad (6.23)$$

The main goal is to maximize the net benefit by obtaining the optimum PM scheduling for each generator. Hence, the optimization problem can be defined as follows:

$$maximize (NB) \quad (6.24)$$

Subject to (6.18), (6.25), (6.26) and (6.27).

$$(NPM_{Gen} \& NCM_{Gen}) \in \mathbb{N} \quad (6.25)$$

$$tPM_{gen} \in \mathbb{N} \quad (6.26)$$

$$\exists f \in F \Rightarrow \exists CM: t < T_W \quad (6.27)$$

The formulation given in (6.18) determines the operational state of each generator. The restriction shown in (6.25) establishes that the number of CM and PM must be positive integers. Restriction (6.26) indicates that the time to perform PM must be an integer in the interval $(0, T_S]$. The last restriction (6.27) states that in case that the failure f (element of the set of failures events F) is detected, a CM will immediately take place, as long as, component's end lifetime is not reached.

6.3.3 Proposed Algorithm

To get the solution to the formulated problem, the SM algorithm shown in Figure 6.11 is employed and implemented using MATLAB 2018. The algorithm is based on AQPSO and is divided into five main stages, which are described below.

- Stage 1: The algorithm starts by loading the power system load profile and reliability generators' reliability data such as failure and repair rates, capacity, costs of acquisition, operation and maintenance. In addition, the size of the swarm SS and total number of iterations It are also defined.
- Stage 2: The first particles $x_\ell(0)$ are randomly generated. Each particle represents a different PM schedule. The generators subjected to PM are saved in $x_\ell.gen(0)$, while the time when PM is performed is saved in $x_\ell.tPM(0)$. In addition, the maintenance exertion degree for each maintenance is calculated using Figure 6.6 and saved in $x_\ell.z(0)$. This is followed by the determination of the degradation rate and failure rate (updated) of the generators, which are saved in $x_\ell.\phi(0)$ and $x_\ell.\lambda(0)$, respectively. The probability vector of all possible states is obtained using Markov

Chain and used to conduct generation adequacy using SMLH. As a result, $LOEE$ is calculated for every particle and saved in $x_p.LOEE(0)$. The stage continues with the calculation of the total cost and net benefit using (6.22) and (6.23); these values are save these values in $x_p.cost(0)$ and $x_p.NB(0)$, respectively. The stage finishes with the identification of the ‘global best’ particle, which is obtained by looking for the particle with the maximum net benefit. The value is saved in g . It is relevant to mention that the ‘best personal’ q_p is equal to the actual position $x_p(0)$ since the particles have not started their motion.

- Stage 3: The first iteration takes place, and the particles start their motion. The attraction parameter $D_p(k)$, and best observation \mathcal{B} are obtained using (5.1) and (5.15), respectively. Then, the new position of the particle is computed using (5.16). The updated position of the particle represents a new PM schedule that may lead to a better net benefit. Then, generation adequacy is computed to obtain a new net benefit value, which is saved in $x_p.NB(k)$.
- Stage 4: In this stage, the particles compete between them to determine the best PM schedule. If $x_p.NB(k) > x_p.NB(k - 1)$ then the particle updates its position. The ‘personal best’ is also updated and saved in q_p . This is followed by a second comparison in which the ‘global best’ is considered. For this purpose, it is required to find the best $x_p(k)$ among the swarm such that brings the maximum savings. The best particle is saved in the variable g' . If the $g'.NB > g.NB$ then the $x_p(k)$ becomes the ‘global best’, otherwise the ‘global best’ is not replaced. In case that $x_p.NB(k) \leq x_p.NB(k)$ then the process continues with the next particle.
- Stage 5: The process in stage 3 and stage 4 are repeated until one of the convergence criteria presented in (5.2) is satisfied. Consider for the convergence criteria a

tolerance value of 10^{-6} . Finally, the outcome is the particle with the best PM schedule.

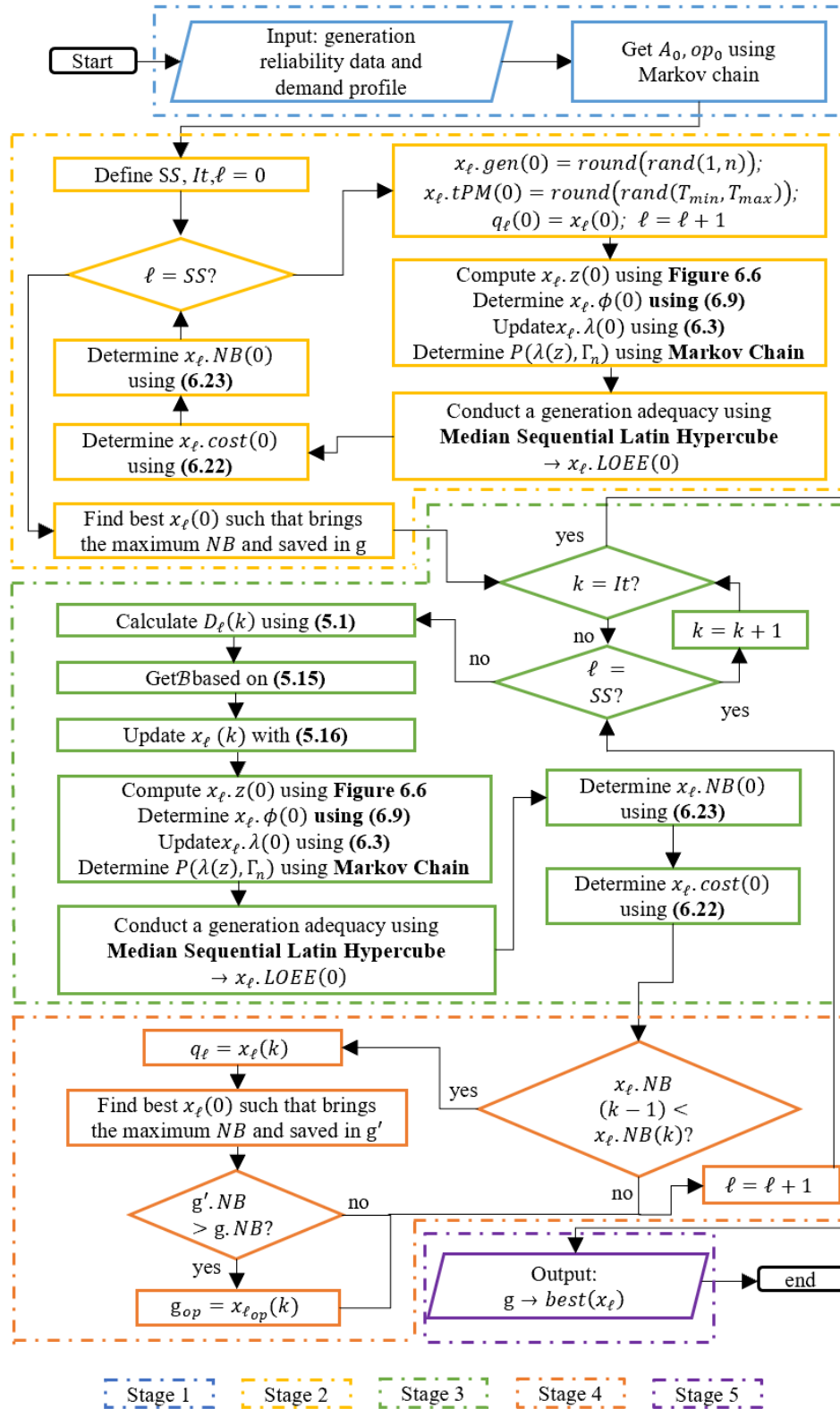


Figure 6.11 Flowchart for effective maintenance plan through SM

6.3.4 Smart Maintenance Schedule

In order to consider the impact of maintenance in the long term, the analysis is conducted for the next 50 years. Figure 6.12 and Figure 6.13 present the SM schedule for hydro and thermal unit generation (UG), respectively. To understand these graphs, a symbol is defined for every UG. Then, the time when the PM takes place is given by the interception point formed from the figure axis, that is, the month is determined by the x-axis and the year is given by the y-axis. The colour on the symbol indicates the maintenance exertion degree. For example, the first PM (with $z \approx 0.37$) to execute on H20 (●) is in February of the third year. Notice that the PM cost is given by the colour, as shown in Figure 6.9.

The maintenance displays different patterns depending on the UG. The first pattern appears in H5 and T10, in which the exertion degree increases with the time until reaching the maximum of 0.95. This is attributed to their low capacity of power that leads to a small contribution to the demand in comparison to other UG. On the other hand, H40 and T40 show the highest number of maintenances. These UGs are the most relevant in the system as they produce the highest amount of power. Focusing on H20 and T20, their exertion degree also increases with time until reaching values around 0.94 and 0.77, respectively.

Independently of the UG, SM scheme suggests performing PM after the second and a half year of acquisition of the generator. In the subsequent years, SM recommends in an average of one, one and a half, and two maintenances per year during the useful lifetime for high (H40 and T40), medium (H20 and T20), and low (H5 and T10) UGs, respectively. In addition, SM acclaims for all UGs not to perform any maintenance for three and a half years before the generator reaches its obsolescence state.

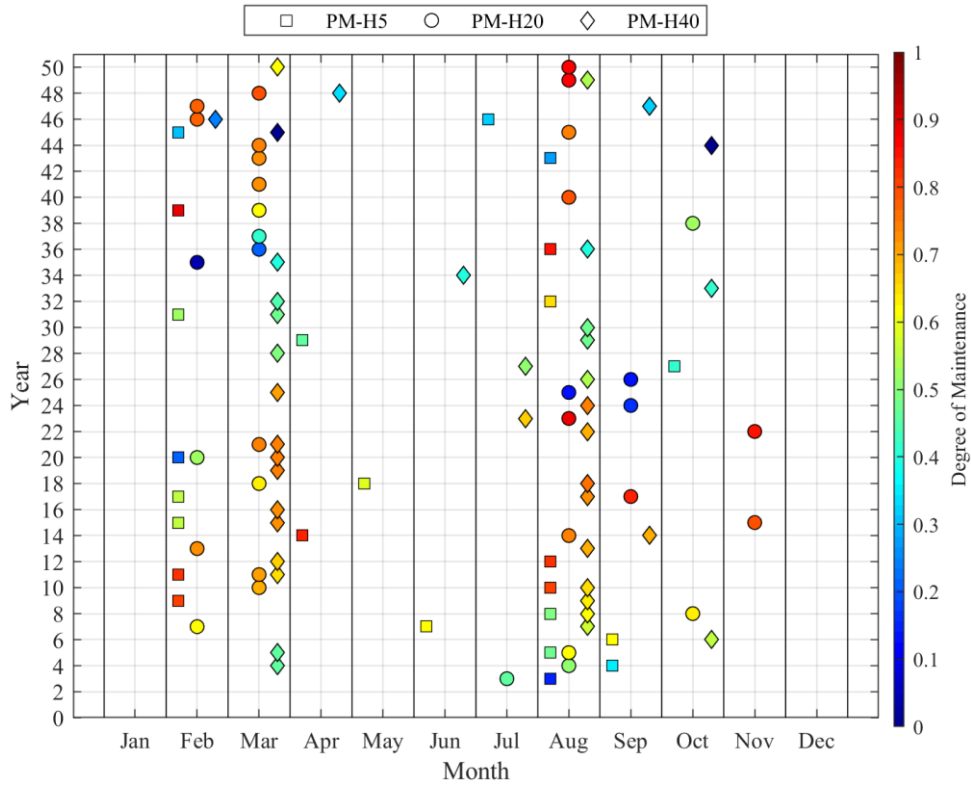


Figure 6.12 SM plan for hydro unit generation

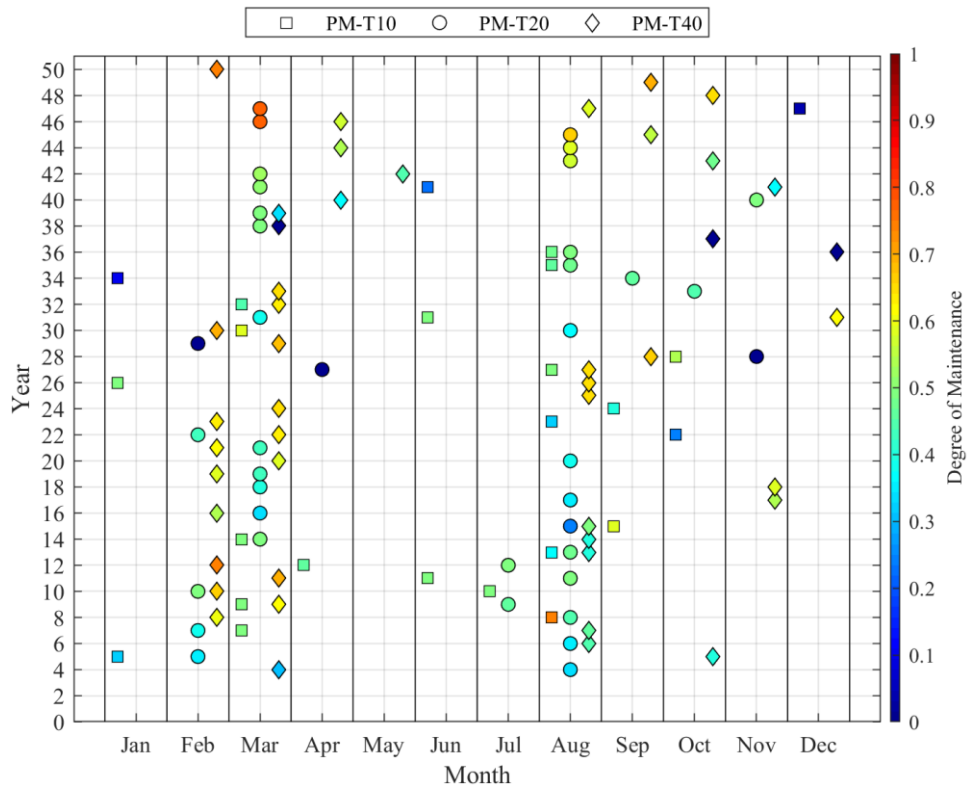


Figure 6.13 SM plan for thermal unit generation

Figure 6.12 and Figure 6.13 show a tendency during the months of February, March, and August. These are the months on which most PMs are performed. This is due to the strategy established by SM, which takes advantage of the months with demand of lowest peaks (March and August, as presented in Figure 4.3) to be prepared and supply the demand during the month of high peaks (January, May, June and November, and December as presented in Figure 4.3). The impact of the schedules generated by the SM scheme is discussed in the next sections.

6.3.5 Operation and Number of Maintenances

During the next 50 years, every generator will be subjected to different operating conditions. Table 6.8 shows a summary of the operation of every UG with different maintenance strategies. It can be observed that scenario NPM presents the lowest and highest values of percentage for 'rated operation' and 'not in operation' states. This is because in this scenario the failures are recurrent due to the absence of maintenance. In contrast, the highest values of percentages for the rated operation state belongs to PPM, followed by RCM and SM. Regarding the overloaded operation, in all the cases the values do not exceed the five per cent. This is attributed to the condition of operation which establishes that the generators cannot operate under this condition for more than one hour, therefore the overloaded operation is very limited. On the other hand, the percentage of derated operation corresponds to NPM followed by SM, RCM and PPM scenario. This last point is relevant since it reveals that SM uses the derated state as a strategy for planning PM, at the difference with RCM and PPM.

Table 6.8 Summary of the Operational States of each UG

Unit Generation	Case	Operation within 50 years [%]			
		Rated	Derated	Overloaded	Not in Operation
H5	NPM	83.28	0	3.72	13
	PPM	93.16	0	3.3	3.54
	RCM	93.66	0	3.13	3.21
	SM	89.8	0	4.49	5.71
T10	NPM	77.2	16.76	1.25	4.79
	PPM	93.1	3.65	0.81	2.44
	RCM	92.71	3.76	1.04	2.49
	SM	84.84	13.06	1.25	0.85
H20	NPM	85.19	0	4.24	10.57
	PPM	96.44	0	1.85	1.71
	RCM	95.16	0	2.66	2.18
	SM	93.57	0	3.08	3.35
T20	NPM	78.53	17.88	1.57	2.02
	PPM	94.66	3.54	0.65	1.15
	RCM	92.36	4.59	1.52	1.53
	SM	87.62	10.34	0.86	1.18
H40	NPM	85.27	0	4.9	9.83
	PPM	94.88	0	1.8	3.32
	RCM	92.82	0	2.71	4.47
	SM	92.71	0	2.74	4.55
T40	NPM	78.12	14.25	2.07	5.56
	PPM	94.25	3.19	1.7	0.86
	RCM	93.39	4.64	1.26	0.71
	SM	84.41	11.03	1.24	3.32

Table 6.9 Summary of the Maintenances performed to each UG

Unit Generation	Number of PM within 50 years				Number of CM within 50 years			
	NPM	PPM	RCM	SM	NPM	PPM	RCM	SM
H5	0	50	31	24	125	57	69	71
T10	0	50	36	24	151	77	85	88
H20	0	50	42	34	134	57	60	65
T20	0	50	46	38	176	84	88	91
H40	0	50	46	40	142	63	70	73
T40	0	50	47	45	180	96	99	104

In order to get an insight into the numbers of PM and CM executed to every UG, Table 6.9 presents a maintenance summary. It can be appreciated that under the SM scheme, the thermal UGs require more attention than hydro UGs. This is in virtue of the derated operation that just thermal generators possess, which reduces the probabilities of being in the rated operation.

Concerning the number of PM and CM, NPM scenario shows the highest number of CM, which makes this scenario the least reliable. In contrast, PPM shows the lowest and highest number of CM and PM, respectively. Therefore, PPM is the scenario with the lowest occurrence of failures, and the most reliable scenario. Nevertheless, it is important to consider that there should be a balance between the reliability and the cost maintenance in order to maximize the net benefit. Consequently, PPM may not lead to the optimum net benefit since is the most expensive among the strategies. This is discussed in detail in the next sections.

6.3.6 Unit Generation Degradation

In order to get the degradation, the reliability data of each generator is used in (6.9). Figure 6.14 shows the degradation as a function of time for every UG under different PM strategies. It can be observed that the degradation tends to be more intense as time passes by. Nevertheless, PM actions influence degradation. The results reveal that since PPM presents the highest number of maintenances followed by RCM and SM, the degradation is reduced. This fact brings repercussion over the reliability of the UG, and therefore in the net benefit.

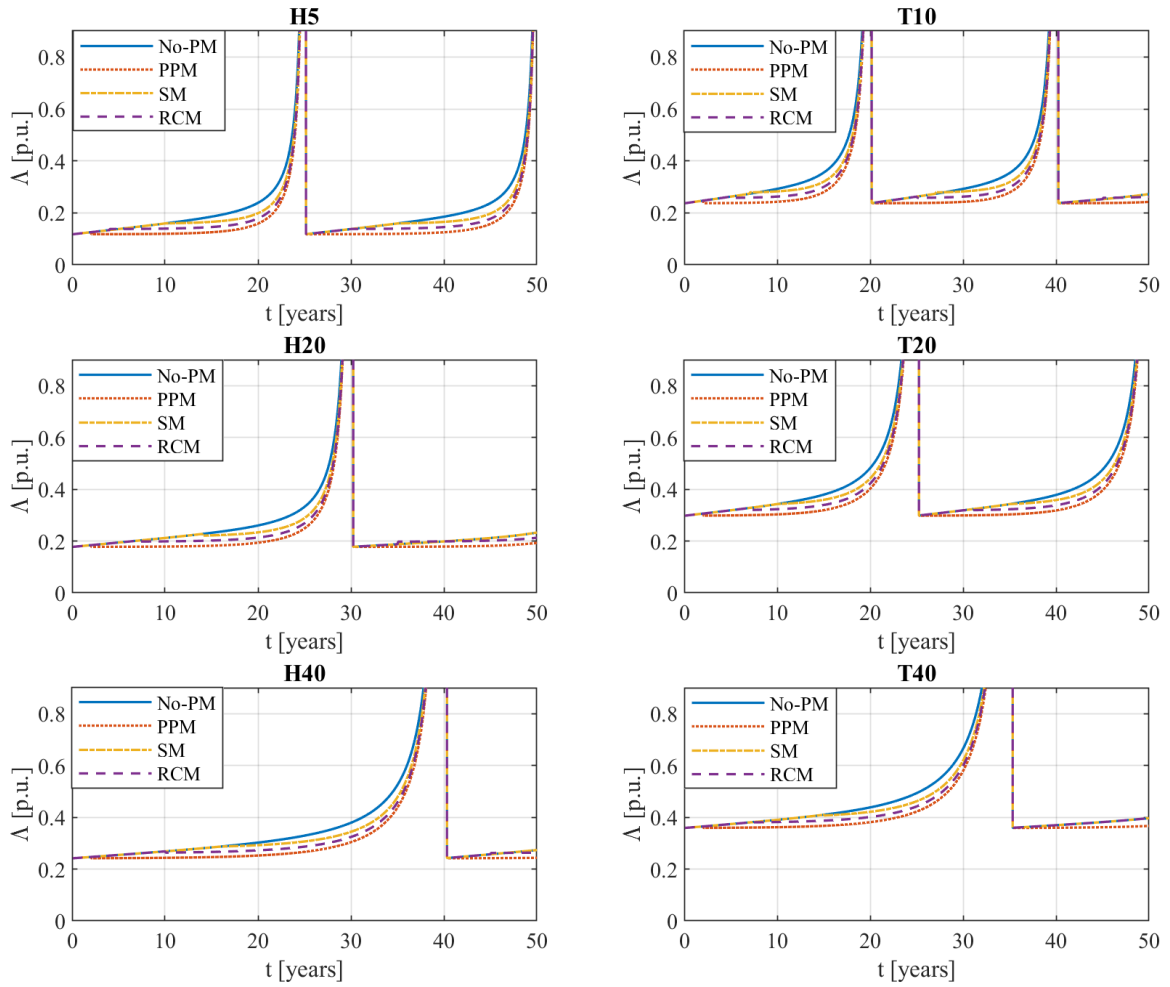


Figure 6.14 Degradation of each unit generation under different PM strategies

6.3.7 Unit Generation Reliability Model

Following the process described in Section 6.1.2, the probability vector of each possible state is obtained. Then, the availability, unavailability, and semi-availability are determined using (4.20), (4.21) and (6.5), respectively.

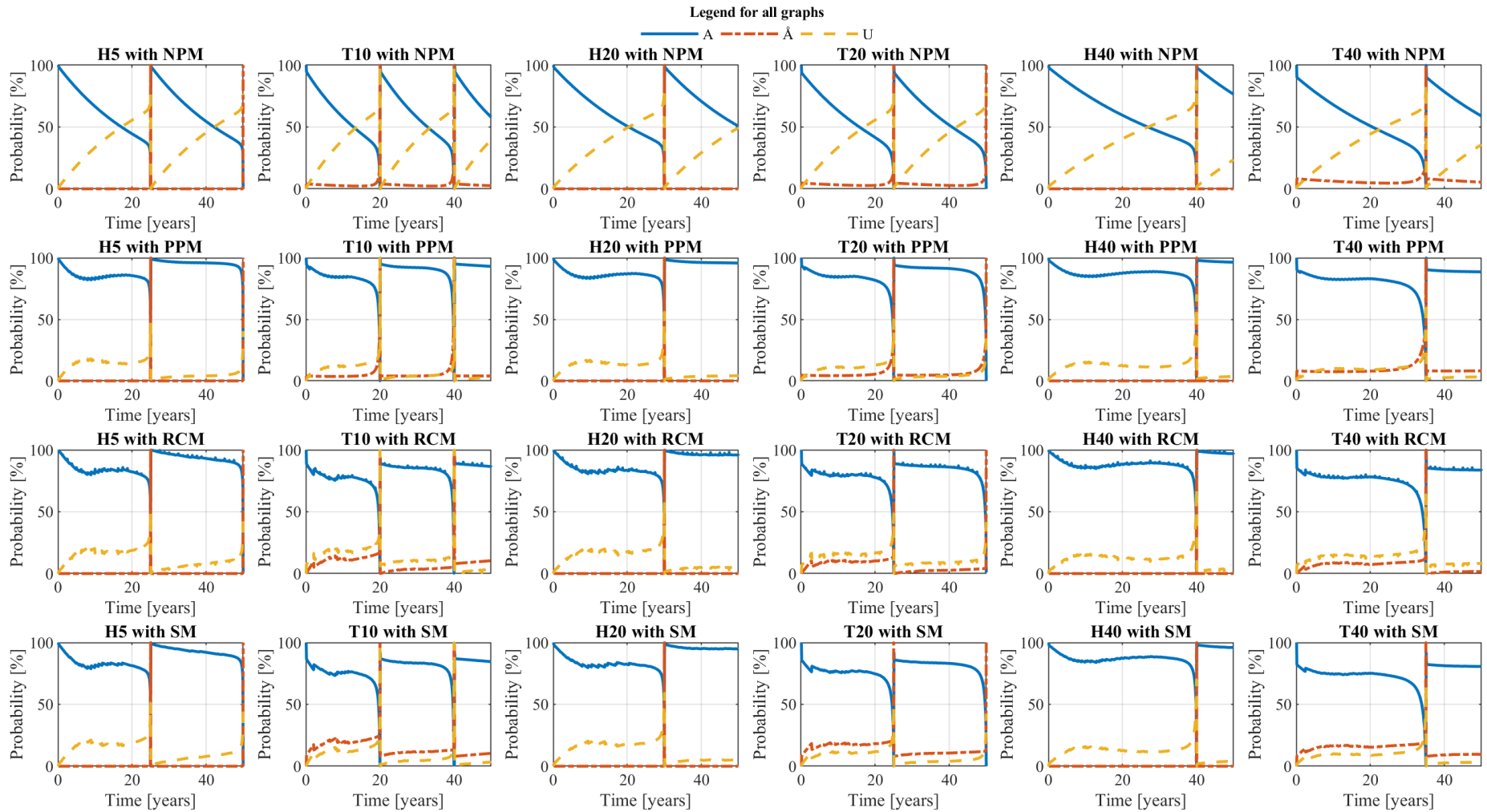


Figure 6.15 Reliability model for each UG under different PM strategies

Figure 6.15 shows for every scenario the reliability behaviour of each unit generation. It is notable that at some point the availability and semi-availability go to zero while the unavailability takes a value of 100%. This phenomenon indicates that the component had reached its end lifetime, then a replacement takes place. The figure also depicts that when no PM (NPM) is executed, the availability decreases, while the unavailability increases, both at a fast rate. In contrast, PPM, RCM and SM schemes present a more stable and higher value of availability than NPM. In addition, PPM, RCM and SM schemes present a more stable and lower value of availability than NPM. This fact demonstrates the strong influence of PM on the reliability of generators.

The availability with the highest value is given by the PPM scenario. This is reasonable, as previously presented, the PPM scenario presents the highest number of PM. Therefore, PPM is the most reliable, but also, the one with the highest maintenance cost. On the other hand, RCM presents a slightly highest value of availability than SM. Nevertheless, SM compensates this difference with the semi-availability. This instance has implications on the net benefit as shown in the next section.

6.3.8 Smart Maintenance Maximum Net Benefit

Figure 6.16 presents the behaviour of the net benefit every five years. Figure 6.16 shows that independently of the scenario, a negative net benefit appears at time zero. This is reasonable, in the beginning, the net benefit corresponds to the UGs acquisition cost. During the next years until the twenty-fifth, the net benefit increases and still negative for all cases, showing the lowest value for NPM. Between the twenty-fifth and fortieth year, the net benefit increases at a low rate in comparison to previous years. This is because by the fortieth year all the UGs have reached their end lifetime, which increases the cost due their renewal requirement. In the subsequent years the net benefit for NPM increases at a lower rate than the

other two scenarios. By the fifth year SM presents the highest net benefit, followed by the RCM, PPM and the NPM.

Even though PPM and RCM show a slightly better reliability performance than SM, it does not necessarily superior to SM in an economic context. The reason is being that the optimization process of SM defines a hierarchical level, based on the power output, reliability features and operation behaviour of every UG. This leads to a proactive PM plan that contains the optimum time and maintenance exertion degree for each UG.

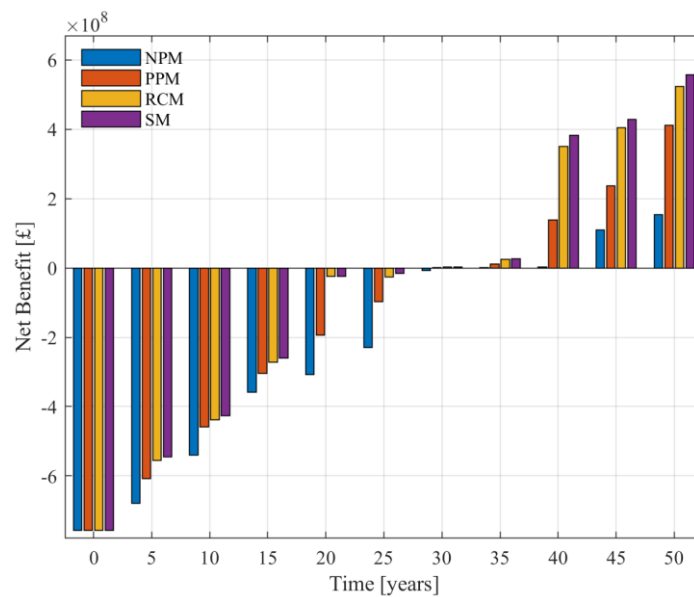


Figure 6.16 Net benefit evolution

6.3.9 Smart Maintenance Computational Efficiency

With a view to show the computational efficiency of AQPSO for SM, the same preventive maintenance schedule optimization problem is solved using traditional PSO and genetic algorithm (GA). It is relevant to mention that a total of 50 particles and 100 iterations are used for each optimization technique with Sequential Median Latin Hypercube experiments of 5000. A computer with a RAM of 16.0 GB and processor Intel Core i7-6700 of 3.40 GHz is employed to run the algorithms.

The proposed case study given in Section 6.3.1 employs the Roy Billinton test system. Such system is considered as a small-scale power system (6 bus). For this reason, the IEEE 73-

bus reliability test system (RTS) [163] is used to investigate the robustness of the proposed approach for a large-scale system.

Figure 6.17 shows the convergence behaviour of each optimization technique. For the RBTS, the convergence is reached at iteration 21, 23 and 25 for AQPSO, PSO and GA, respectively. Even though AQPSO presents the fastest convergence, the convergence speed difference in comparison to PSO and GA is not significant. On the other hand, for the RTS, the convergence is reached at iteration 75, 85 and 89 for AQPSO, PSO and GA, respectively. In this case, AQPSO presents again the fastest convergence with a notable difference in comparison to PSO and GA. It is relevant to highlight that independently of the size of the power systems, at some iteration number all the employed optimization techniques reached the same net benefit, which guarantees the accuracy of the results.

Another important aspect to analyse is the simulation time. Table 6.10 presents the simulation time values per experiment for each optimization technique. Table 6.10 reveal that for the RBTS, the simulation time difference among the optimization techniques does not exceed 0.4 %. Nevertheless, for the RTS, such difference is outstanding since PSO and GA simulation time exceeds by 22.1 % and 18.1 % to AQPSO, respectively. Therefore, AQPSO presents the best efficiency in terms of simulation time, which makes AQPSO the most suitable optimization technique to be used in the Smart-Maintenance model.

Table 6.10 SM Optimization Techniques Robustness

Power System	Algorithm	Simulation time per iteration [s]
RBTS (6 buses)	PSO	10.05
	GA	10.03
	AQPSO	10.01
RBT (73 buses)	PSO	124.3
	GA	120.2
	AQPSO	101.8

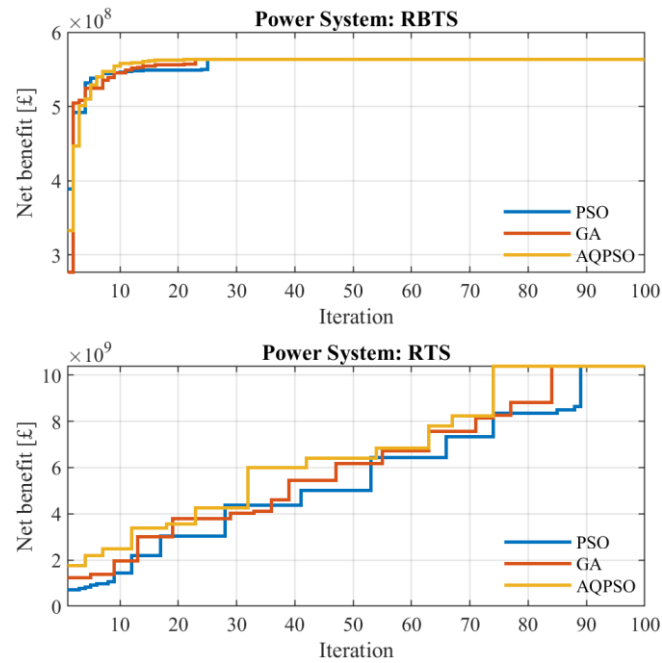


Figure 6.17 SM Optimization technique convergence

6.4 Summary

This chapter focuses on an innovative mathematical approach for SM of generators that maximizes generation adequacy net benefit. The main difference between the proposed SM with other advanced maintenance strategies is that SM considers the maintenance exertion degree and the composite operation of every component in the system to formulate an effective maintenance plan. SM is based on reliability and risk concepts including Markov chain to get the probability vector of states, Kijima model to quantify the virtual age of the component, and fuzzy logic to determine the maintenance effort during maintenance action. The SM scheme involves an optimization problem which is solved using AQPSO in combination with SMLH. To prove the efficacy of the proposed approach four scenarios are evaluated: 1. No preventive maintenance (NPM), 2. Periodic preventive maintenance (PPM); 3. Reliability-centered maintenance (RCM); 4. Smart maintenance (SM).

The results show that PM actions have a strong impact on the reliability of the component, deriving in the lowest economical net benefit for NPM scenario. In contrast, the SM scenario presents the highest economical net benefit. This fact is attributed to the effective

maintenance schedule that SM brings, which includes the effort required in each PM. Even though PPM and RCM are highly recommended by many standards, this may not lead to maximum net benefit as evidenced by the presented work in this chapter.

Chapter 7: Closure

This chapter presents the conclusions from the key findings of the research. It is followed by an outline of potential applications of the proposed approach that might be of interest to the power industry and others.

7.1 Conclusions

Electrical power system components are constantly affected by failures, which can be due to meteorological phenomena, technical causes, and human errors. The occurrence of failures can be reduced by performing proper maintenance actions at the right time. This research proposes a novel Smart Maintenance (SM) scheme that optimises the economic benefits, while maintaining adequate level of reliability of the system.

SM takes the failure and repair rates of the components as inputs to formulate a system reliability model. A more rigorous reliability model provides more accurate reliability indices. Chapter 4 proposed a novel reliability model with aging features. The advancement of the model is the incorporation of the obsolescence state that is used to describe the degradation of generators due to aging. The accuracy of the proposed model is further improved by modelling the failure and repair rates of the components using the bathtub curve and half-arch shape, respectively. The efficacy of the approach is validated by a case study that considers three different reliability models. The results reveal that the existing models (first and second) produce imprecise availability functions. For instance, in the first model, the availability of generators is constant over all stages of the bathtub curve. In the second model, the availability decreases exponentially when a generator is within the wear-out stage. However, the availability should decrease over time since generators degrade throughout their entire lifecycle due to mechanical and electrical stresses. To incorporate the aging process in all stages of the bathtub curve, the proposed model (third) adds the obsolescence state. The obsolescence state

enables the quantification of the degradation rate of the generators, which exponentially reduces the availability over all stages of the bathtub curve. The proposed model offers a more realistic estimation of the generator availability than traditional models, providing a more comprehensive alternative for generation adequacy assessments.

SM formulates a preventive maintenance (PM) schedule optimization problem, in which the objective is to maximize the maintenance economic benefits. In order to obtain the optimum solution in an adequate time, the optimization technique must be robust and reliable. Chapter 5 proposes an advanced optimization technique named as Accelerated Quantum particle Swarm Optimization (AQPSO). AQPSO is an evolutionary computation technique that, unlike traditional PSO, does not employ the classical physics concepts to get the optimal solution. Instead, it associates the motion of particle based on quantum mechanics theories. The innovation of the approach lies in the incorporation of the ‘best observation’, which is obtained by using more than one observer into the experiment. Applicability, stability and robustness of AQPSO are validated by applying it for two different case studies.

In the first case study, the proposed optimization technique was used to determine the optimal sizing and placement of SVCs such that the expected energy not supplied (EENS) is minimized. The results argue that the presence of SVC produces an improvement in power system reliability by 44.3%. To assure the accuracy of the results, the same optimization problem is solved using different number of observers, emerging in the same EENS value. A finding is that as the number of observers increases, faster convergence is achieved. This is because the probabilities of finding the quantum particle near the optimal solution increases with the number of experiments (observations).

In the second case study, the objective was to maximize the savings due to the reduction in power losses. The strategy is based on the proficient planning and operation of SVCs. The optimization problem is solved using three different methods: Bi-Level Genetic Algorithm

(BLGA), Bi-Level Particle Swarm Optimization (BPSO) and Bi-Level Accelerated Quantum particle Swarm Optimization (BAQPSO). The case study was carried out for the next 12 years and all methods generated savings of £440,000. This result indicates the potential economic benefits of installing SVCs into the power transmission system. Even though all the optimization techniques reached the same outcome, their computational efficiency differs. The fastest convergence corresponds to BAQPSO by 34.3% and 37.5% in comparison to BPSO and BGA, respectively. Furthermore, BAQPSO exhibits the lowest time simulation with a reduction of time by 27.1% and 22.4% in comparison to BPSO and BGA, respectively. Therefore, AQPSO demonstrates to be the most robust technique in comparison to the conventional GA and PSO.

The greater number of preventive maintenances could potentially lead to a considerable level of the improvement in the reliability of power system. Nevertheless, it is vital to consider the operational risk of the components and perform preventive maintenance (PM) at the benefit horizons to avoid superseding the cost over benefit. Under this context, Chapter 6 presented an innovative smart maintenance scheme that incorporates reliability and risk concepts to maximize economic benefits. From the reliability perspective, SM considers Kijima model to calculate the virtual age of the component after PM is performed and Markov chain to describe the probability of being in the different operational states of the component. From the risk perspective, SM considers the fuzzy logic to quantify the maintenance effort based on the operational records and availability of the component. In addition, SM formulates a PM schedule optimization that is solved using AQPSO in combination with the Mean Sequential Latin Hypercube (MSLH). In this way, SM achieves a comprehensive schedule that indicates where, when and how the PM should be executed.

The proposed maintenance strategy is applied to a case study to maximize the economic benefits due to the reduction of occurrence of failures of power generators. In order to show

the efficacy of the proposed approach, the case study considers two more maintenance strategies: yearly periodic preventive maintenance (PPM) and reliability-centre maintenance (RCM). The case study results suggest that during the optimization process, SM defines a hierarchical level for each generator based on its failure rate, capacity and lifetime. For instance, generators with higher failure rate, lower lifetime and lower capacity, require more maintenance than the ones with lower failure rate, higher lifetime and higher capacity. For this reason, the SM schedule does not present a common pattern as in the PPM in which the PM is performed every year. On the other hand, the maintenance strategy with the lowest degradation belongs to PPM, followed by RCM and SM. This fact is associated with the number of preventive maintenances. The more PM executed, the slower the degradation process. Consequently, PPM presents the highest availability, but also, the one with the highest maintenance cost. Thirdly, the predominance of SM over the PPM and RCM is corroborated. Even though PPM and RCM are highly recommended by many standards, it does not contemplate a comprehensive reliability and risk operational analysis of the component. This fact heads to a maintenance plan that may not carry the maximum net benefit.

The research presented in this thesis provides significant contributions to the knowledge in the field of power system reliability. Firstly, a more accurate relationship between maintenance, degradation due to aging, and operational risk is achieved. Such relationship is useful to quantify the impact of maintenance on the reliability parameters of power generators, bringing more realistic reliability assessment results. Secondly, a detailed Smart-Maintenance mathematical framework for power generators is proposed. The application of these mathematical formulations leads to the net-maximum economic benefit engendered from the improved reliability performance of generators, resulting in an approach that might be of interest to the power industry. Thirdly, an advanced SM algorithm that combines the AQPSO with SMLH for the scheduling of proactive maintenance of generators in a power system is

proposed. Such algorithm demonstrates to be efficient in terms of convergence speed and simulation for small and large power systems. Therefore, the proposed algorithm could be considered as an effective optimization technique for the optimization of generators in a PM schedule.

Thus, it is relevant to highlight that PM is essential to keep a high-reliability level in the power system. However, a more important fact to consider is to perform PM based on the reliability performance and operational risk of the components such that the maintenance cost does not supersede the economic benefit. Further, the approach is beneficial for planning PM schedules with the aim of improving the reliability performances in the long run. Although this research employs the SM scheme for generators, the model can be extended for other power system components, providing a range of opportunities for the operational planning of modern power systems.

7.2 Future Research

The proposed research includes several aspects related to the improvement of power system reliability. These aspects focus on the reactive compensation and the impact of smart maintenance over aging of power generators. Nevertheless, there are other fields that can be explored, leading to new trends in power system reliability. The following is a list of the possible future directions:

- To incorporate the aging of power generators in reliability modelling, this thesis proposes the use of the bathtub curve and half-arch shape. However, other equipment installed in the power system contain unique features, which impact the aging process. For instance, wind turbines and transmission lines are constantly affected by weather conditions, and the bathtub curve and half-arch shape may not represent the true behaviour of their failure and repair rates. Thus, it would of interest to develop a holistic framework that considers aging due to climate conditions such as humidity,

temperature, solar radiation, and wind speed. These considerations could result into a more comprehensive power system reliability assessment.

- To enhance the performance of the power system reliability, this research proposed an innovative smart maintenance model for power generators. Nevertheless, brand new maintenance models for other power system components are needed since the proposed model is limited to system generation adequacy. For instance, advanced maintenance planning for transmission lines and power transformers requires researchers to consider parameters such as the maximum potential of insulators, electrical stress due to short circuits failures, and extreme weather conditions. These considerations could result in more effective maintenance planning.
- To show the real-world applications of the proposed approach, it will be advantageous to perform simulations using the manufacturers' datasheet for the different power system components. Moreover, the consideration of a real power system (i.e. the UK national grid) could result in a practical evolution of the proposed approach, bringing new reliability models to be considered.

Appendix

A.1 Roy Billinton Test System (RBTS)

The Roy Billinton Test System (RBTS) [6] is a 230 kV transmission system that has 9 buses, two generator, four load buses, nine transmission lines, and eleven generating units. Figure A.1 shows the RTBS single line diagram. The normalized yearly load demand is presented in Figure A.2. Reliability data regarding the generation units and transmission lines are presented in Table A.1 and Table A.2, respectively.

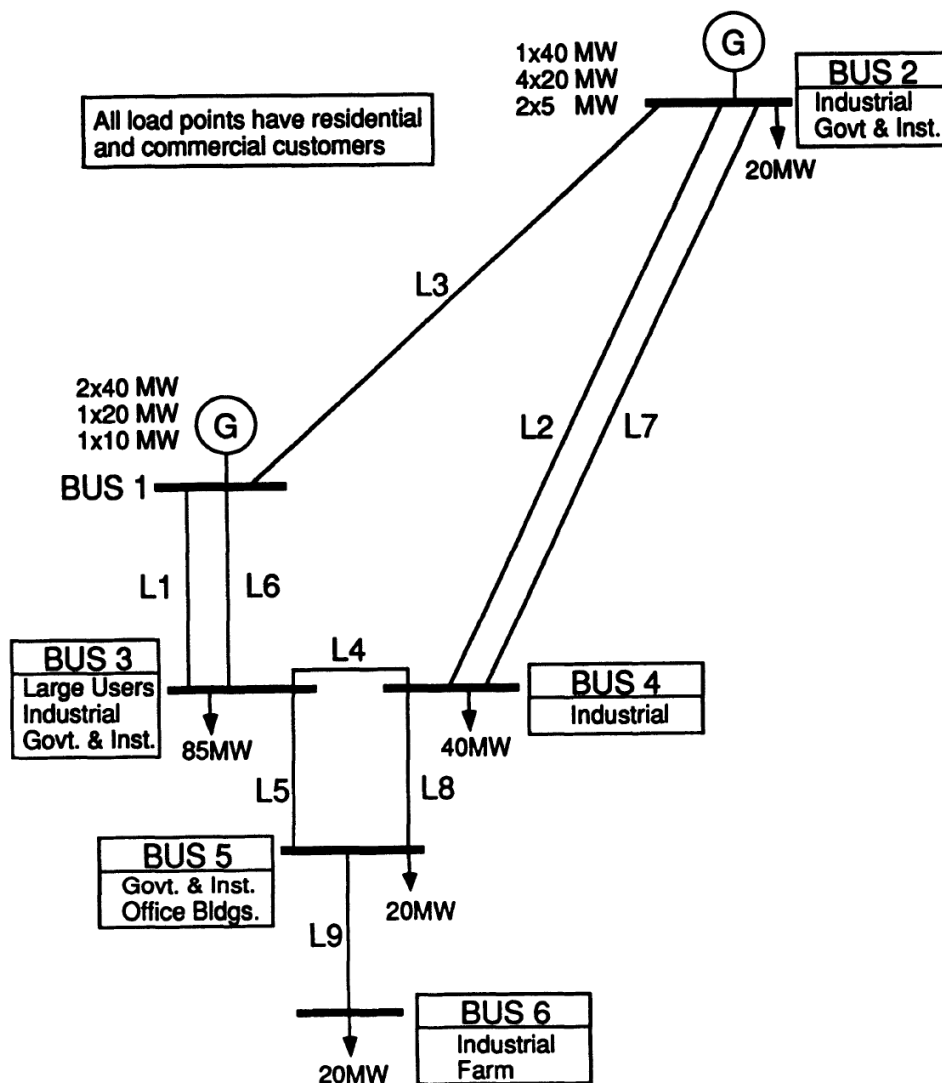


Figure A.1 RBTS single line diagram [6]

Table A.1 RBTS Unit Generation Reliability Data [6]

Unit size [MW]	Type	# of units	Forced outage rate	Failure Rate [1/yr]	Repair Rate [1/yr]
5	Hydro	2	0.010	2.0	198.0
10	Thermal	1	0.020	4.0	196.0
20	Hydro	4	0.015	2.4	157.6
20	Thermal	1	0.025	5.0	195.0
40	Hydro	1	0.020	3.0	147.0
40	Thermal	2	0.030	6.0	194.0

Table A.2 RBTS Transmission Lines Reliability Data [6]

From	To	R [p.u.]	X [p.u.]	Outage rate [occ/yr]	Repair time [1/yr]
1	2	0.0342	0.180	1.5	10.0
2	4	0.1140	0.600	5.0	10.0
1	2	0.0912	0.480	4.0	10.0
3	4	0.0228	0.120	1.0	10.0
3	5	0.0028	0.120	1.0	10.0
1	3	0.0342	0.180	1.5	10.0
2	4	0.1140	0.600	5.0	10.0
4	5	0.0228	0.120	1.0	10.0
5	6	0.0028	0.120	1.0	10.0

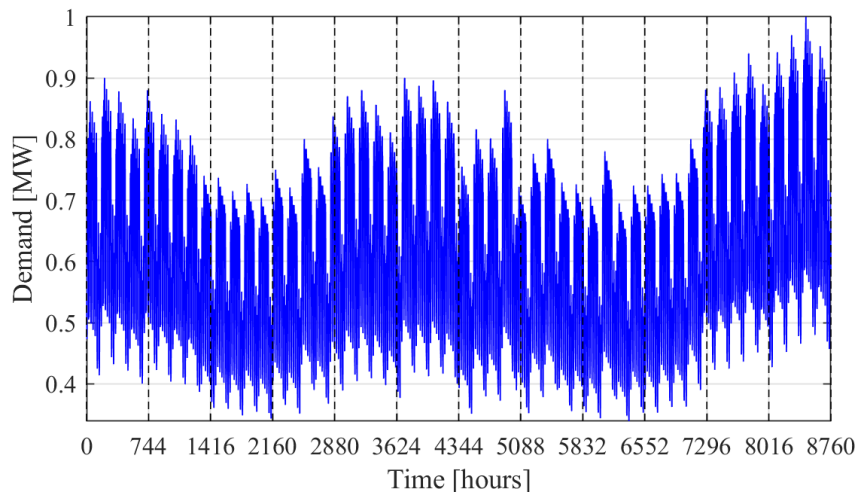


Figure A.2 Normalized yearly load profile [6]

A.2 IEEE Reliability Test System (RTS)

The IEEE Reliability Test System (RTS) [163] is a transmission system that is divided in three areas. Each area presents the same electrical topology, having 24 bus, 38 lines, and five transformers, as shown in Figure A.3. The normalized yearly load demand is presented in Figure A.2. Reliability data regarding the bus, generation units, and transmission lines are presented in Table A.1 and Table A.2, respectively.

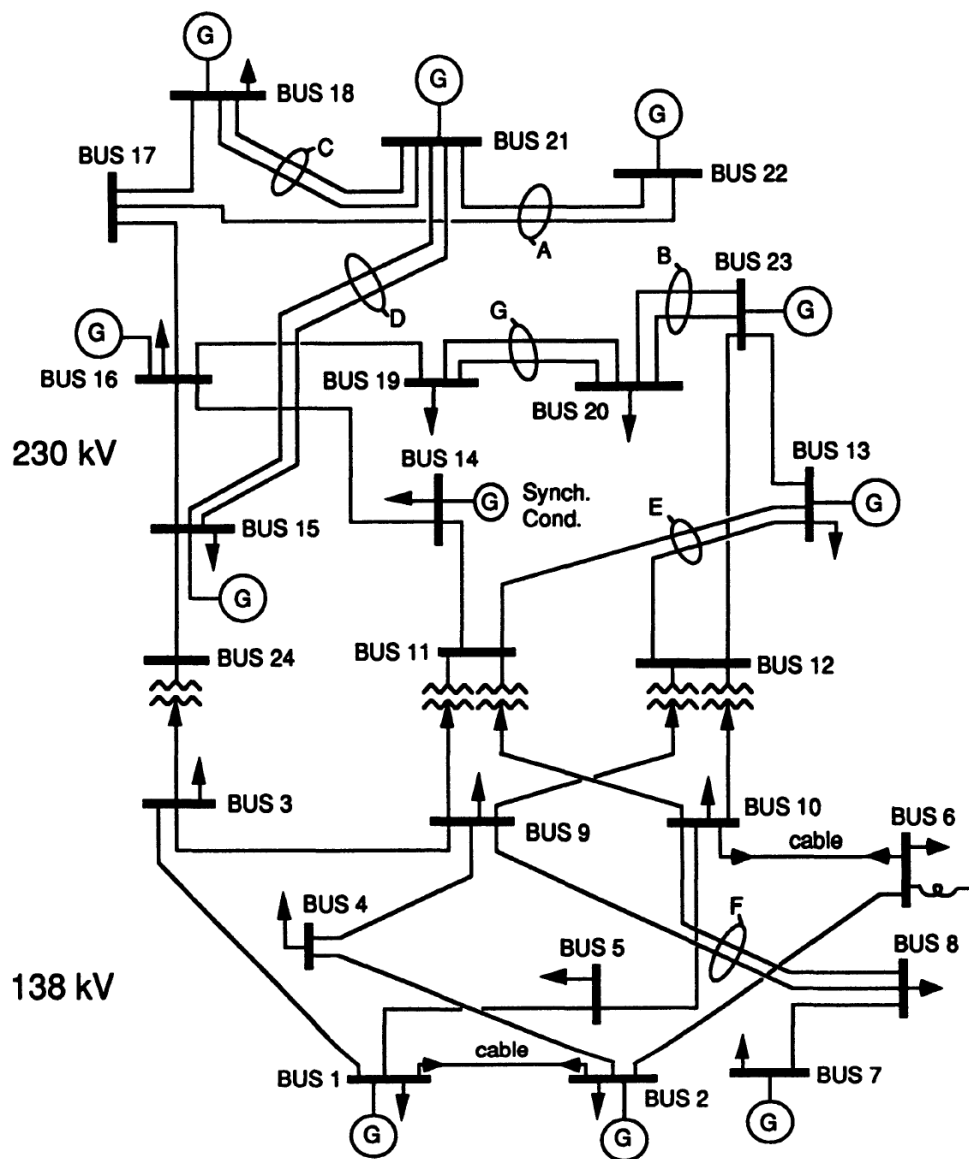


Figure A.3 RTS single line diagram [6]

Table A.3 RTS Unit Generation Reliability Data [163]

Bus number	Type	Voltage [KV]	MW Load	MVAR Load
1	Control	138	108	22
2	Control	138	97	20
3	Load	138	180	37
4	Load	138	74	15
5	Load	138	71	14
6	Load	138	136	28
7	Control	138	125	25
8	Load	138	171	35
9	Load	138	175	36
10	Load	138	195	40
11	Load	230	0	0
12	Load	230	0	0
13	Swing	230	265	54
14	Control	230	194	39
15	Control	230	317	64
16	Control	230	100	20
17	Load	230	0	0
18	Control	230	333	68
19	Load	230	181	37
20	Load	230	128	26
21	Control	230	0	0
22	Control	230	0	0
23	Control	230	0	0
24	Load	230	0	0

Table A.4 RTS Unit Generation Reliability Data [163]

Unit size [MW]	Type	# of units	Forced outage rate	MTTF [hour]	MTTR [hour]
12	Oil/Steam	12	0.02	2940	60
20	Oil	20	0.10	450	50
50	Hydro	50	0.01	1960	20
76	Coal/Steam	76	0.02	1960	40
100	Oil/Steam	100	0.04	1200	50
155	Coal/Steam	155	0.04	960	40
197	Oil/Steam	197	0.05	950	50
350	Coal/Steam	350	0.08	1150	100
400	Nuclear	400	0.12	1100	150

Table A.5 RTS Transmission Lines Reliability Data [163]

From	To	R [p.u.]	X [p.u.]	Failure rate [1/yr]	Repair time [1/yr]
1	2	0.003	0.014	0.24	16
1	3	0.055	0.211	0.51	10
1	5	0.022	0.085	0.33	10
2	4	0.0333	0.127	0.39	10
2	6	0.050	0.192	0.48	10
3	9	0.031	0.119	0.38	10
3	24	0.002	0.084	0.02	768
4	9	0.027	0.104	0.36	10
5	10	0.023	0.088	0.34	10
6	10	0.014	0.061	0.33	35
7	8	0.016	0.061	0.30	10
8	9	0.043	0.165	0.44	10
8	10	0.043	0.165	0.44	10
9	11	0.002	0.084	0.02	768
9	12	0.002	0.084	0.02	768
10	11	0.002	0.084	0.02	768
10	12	0.002	0.084	0.02	768
11	13	0.006	0.048	0.40	11
11	14	0.005	0.042	0.39	11
12	13	0.006	0.048	0.40	11
12	23	0.012	0.097	0.52	11
13	23	0.011	0.087	0.49	11
14	16	0.005	0.059	0.38	11
15	16	0.002	0.017	0.33	11

References

- [1] K. Moslehi and R. Kumar, "A reliability perspective of the smart grid.," *IEEE Trans. Smart Grid*, vol. 1, no. 1, pp. 57–64, 2010.
- [2] Council of European Energy Regulators, "6th Benchmarking report on quality of electricity supply," Brussels, 2016.
- [3] E. & I. S. Department for Business, "Energy Consumption in the UK (ECUK) 1970 to 2018," London.
- [4] T. Ian, "Electricity consumption from all electricity suppliers in the United Kingdom (UK) from 2002 to 2018 (in terawatt-hours)," *Statista*, 2019. .
- [5] Department for Business Energy & Industrial Strategy, "UK ENERGY IN BRIEF 2019," 2019.
- [6] W. Li, *Reliability assessment of electric power systems using Monte Carlo methods*. Springer Science & Business Media, 2013.
- [7] J.-F. Moon, J.-C. Kim, H.-T. Lee, C.-H. Park, S.-Y. Yun, and S.-S. Lee, "Reliability evaluation of distribution system through the analysis of time-varying failure rate," in *Power Engineering Society General Meeting, 2004. IEEE*, 2004, pp. 668–673.
- [8] G. Ji, W. Wu, B. Zhang, and H. Sun, "A renewal-process-based component outage model considering the effects of aging and maintenance," *Int. J. Electr. Power Energy Syst.*, vol. 44, no. 1, pp. 52–59, 2013.
- [9] SmarterBusiness, "UK renewable energy percentage 2018 & 2019," 2018. [Online]. Available: <https://smarterbusiness.co.uk/uk-renewable-energy-percentage-2018/>.
- [10] A. A. Recalde, T. K. Saha, and M. Mosadeghy, "Reliability evaluation with wind turbines and photovoltaic panels," in *Transmission & Distribution Conference and Exposition-Latin America (PES T&D-LA), 2014 IEEE PES*, 2014, pp. 1–5.
- [11] R. Karki, P. Hu, and R. Billinton, "Reliability evaluation considering wind and hydro power coordination," *IEEE Trans. Power Syst.*, vol. 25, no. 2, pp. 685–693, 2009.
- [12] S. S. Martin, A. Chebak, A. El Ouafi, and M. Mabrouki, "Modeling and simulation of hybrid power system integrating wind, solar, biodiesel energies and storage battery," in *Renewable and Sustainable Energy Conference (IRSEC), 2016 International*, 2016, pp. 457–463.
- [13] P. Hu, R. Karki, and R. Billinton, "Reliability evaluation of generating systems containing wind power and energy storage," *IET Gener. Transm. Distrib.*, vol. 3, no. 8, pp. 783–791, 2009.
- [14] W. Qin, P. Wang, X. Han, and X. Du, "Reactive power aspects in reliability assessment of power systems," *IEEE Trans. Power Syst.*, vol. 26, no. 1, pp. 85–92, 2011.
- [15] uniper, "Independent outage support saves cost," 2018.
- [16] M. Shafiee, "Maintenance logistics organization for offshore wind energy: Current progress and future perspectives," *Renew. Energy*, vol. 77, pp. 182–193, 2015.

- [17] A. Abdul-Hannan, “Belief-Based Maintenance Decisions,” University of Manchester, 2008.
- [18] S. Awadallah, “Probabilistic methodology for prioritising replacement of ageing power transformers based on reliability assessment of transmission system.” The University of Manchester (United Kingdom), 2014.
- [19] V. Zille, “Modélisation et évaluation des stratégies de maintenance complexes sur des systèmes multi-composants.” Troyes, 2009.
- [20] F. Besnard, “On optimal maintenance management for wind power systems.” KTH, 2009.
- [21] M. Shafiee and J. D. Sørensen, “Maintenance optimization and inspection planning of wind energy assets: Models, methods and strategies,” *Reliab. Eng. Syst. Saf.*, 2017.
- [22] B. O. Mkandawire, N. Ijumba, and A. Saha, “Transformer risk modelling by stochastic augmentation of reliability-centred maintenance,” *Electr. Power Syst. Res.*, vol. 119, pp. 471–477, 2015.
- [23] T. A. Tveit, R. Kleivi, R. Moen, O.-M. Midtgård, L. S. Gundersen, and A. Nysveen, “System and method to provide maintenance for an electrical power generation, transmission and distribution system.” Google Patents, Feb-2012.
- [24] A. Arab, E. Tekin, A. Khodaei, S. K. Khator, and Z. Han, “Dynamic maintenance scheduling for power systems incorporating hurricane effects,” in *2014 IEEE International Conference on Smart Grid Communications (SmartGridComm)*, 2014, pp. 85–90.
- [25] Z. Ding, T. Wu, and H. Shen, “Based on RFID and temperature tag smart inspection and maintenance technology for distribution power network,” in *Electricity Distribution (CICED), 2016 China International Conference on*, 2016, pp. 1–5.
- [26] M. Maritsch, C. Lesjak, and A. Aldrian, “Enabling smart maintenance services: Broker-based equipment status data acquisition and backend workflows,” in *Industrial Informatics (INDIN), 2016 IEEE 14th International Conference on*, 2016, pp. 699–705.
- [27] J. D. Moseley, W. M. Grady, and S. Santoso, “New approaches for smart device integration and maintenance of power system models utilizing a unified data schema,” in *Innovative Smart Grid Technologies (ISGT), 2013 IEEE PES*, 2013, pp. 1–6.
- [28] M. Kijima, H. Morimura, and Y. Suzuki, “Periodical replacement problem without assuming minimal repair,” *Eur. J. Oper. Res.*, vol. 37, no. 2, pp. 194–203, 1988.
- [29] C. Zapata, “Confiabilidad de sistemas eléctricos de potencia,” *Pereira Univ. Tecnológica Pereira*, p. 85, 2011.
- [30] C. Kahraman, U. Kaymak, and A. Yazici, *Fuzzy logic in its 50th year*. Springer, 2016.
- [31] R. Schmidt, M. Voigt, and R. Mailach, “Latin Hypercube Sampling-Based Monte Carlo Simulation: Extension of the Sample Size and Correlation Control,” in *Uncertainty Management for Robust Industrial Design in Aeronautics*, Springer, 2019, pp. 279–289.
- [32] R. Billinton and R. N. Allan, *Reliability assessment of large electric power systems*. Springer Science & Business Media, 2012.

- [33] R. N. Allan, *Reliability evaluation of power systems*. Springer Science & Business Media, 2013.
- [34] R. Karki, R. Billinton, and A. K. Verma, *Reliability Modeling and Analysis of Smart Power Systems*. Springer Science & Business Media, 2014.
- [35] W. R. Blischke and D. N. P. Murthy, *Reliability: modeling, prediction, and optimization*, vol. 767. John Wiley & Sons, 2011.
- [36] R. Billinton and R. N. Allan, *Reliability evaluation of engineering systems*. Springer, 1992.
- [37] M. Rausand and A. Høyland, *System reliability theory: models, statistical methods, and applications*, vol. 396. John Wiley & Sons, 2004.
- [38] F. Manzano-Agugliaro, A. Alcayde, F. G. Montoya, A. Zapata-Sierra, and C. Gil, “Scientific production of renewable energies worldwide: an overview,” *Renew. Sustain. Energy Rev.*, vol. 18, pp. 134–143, 2013.
- [39] R. Haas, C. Panzer, G. Resch, M. Ragwitz, G. Reece, and A. Held, “A historical review of promotion strategies for electricity from renewable energy sources in EU countries,” *Renew. Sustain. energy Rev.*, vol. 15, no. 2, pp. 1003–1034, 2011.
- [40] S. Ölz and M. Beerepoot, “Deploying renewables in Southeast Asia: Trends and potentials,” OECD Publishing, 2010.
- [41] R. Karki, P. Hu, and R. Billinton, “A simplified wind power generation model for reliability evaluation,” *IEEE Trans. Energy Convers.*, vol. 21, no. 2, pp. 533–540, 2006.
- [42] H. Gunduz and D. Jayaweera, “Reliability assessment of a power system with cyber-physical interactive operation of photovoltaic systems,” *Int. J. Electr. Power Energy Syst.*, vol. 101, pp. 371–384, 2018.
- [43] H. Gunduz, Z. A. Khan, A. Altamimi, and D. Jayaweera, “An Innovative Methodology for Load and Generation Modelling in a Reliability Assessment with PV and Smart Meter Readings,” in *2018 IEEE Power & Energy Society General Meeting (PESGM)*, 2018, pp. 1–5.
- [44] Z. Ren, K. Wang, W. Li, L. Jin, and Y. Dai, “Probabilistic power flow analysis of power systems incorporating tidal current generation,” *IEEE Trans. Sustain. Energy*, vol. 8, no. 3, pp. 1195–1203, 2017.
- [45] I. Felea, C. Panea, and G. Bendea, “Stochastic evaluation of the reliability of the geothermal energy exploitation systems,” *Rev. Roum. des Sci. Tech. Série Électrotechnique Énergétique*, pp. 141–151, 2014.
- [46] E. W. T. Ngai, L. Xiu, and D. C. K. Chau, “Application of data mining techniques in customer relationship management: A literature review and classification,” *Expert Syst. Appl.*, vol. 36, no. 2, pp. 2592–2602, 2009.
- [47] P. D. Diamantoulakis, V. M. Kapinas, and G. K. Karagiannidis, “Big data analytics for dynamic energy management in smart grids,” *Big Data Res.*, vol. 2, no. 3, pp. 94–101, 2015.

- [48] Y. Chen *et al.*, “Short-term electrical load forecasting using the Support Vector Regression (SVR) model to calculate the demand response baseline for office buildings,” *Appl. Energy*, vol. 195, pp. 659–670, 2017.
- [49] Z. A. Khan, D. Jayaweera, and M. S. Alvarez-Alvarado, “A novel approach for load profiling in smart power grids using smart meter data,” *Electr. Power Syst. Res.*, vol. 165, pp. 191–198, 2018.
- [50] S. Ryu, J. Noh, and H. Kim, “Deep neural network based demand side short term load forecasting,” *Energies*, vol. 10, no. 1, p. 3, 2016.
- [51] R. Y. Rubinstein and D. P. Kroese, *Simulation and the Monte Carlo method*, vol. 10. John Wiley & Sons, 2016.
- [52] A. Ridder, “Importance sampling simulations of Markovian reliability systems using cross-entropy,” *Ann. Oper. Res.*, vol. 134, no. 1, pp. 119–136, 2005.
- [53] G. Casella and E. I. George, “Explaining the Gibbs sampler,” *Am. Stat.*, vol. 46, no. 3, pp. 167–174, 1992.
- [54] Z. Shu and P. Jirutitijaroen, “Latin hypercube sampling techniques for power systems reliability analysis with renewable energy sources,” *IEEE Trans. Power Syst.*, vol. 26, no. 4, pp. 2066–2073, 2011.
- [55] A. Smith, *Sequential Monte Carlo methods in practice*. Springer Science & Business Media, 2013.
- [56] A. M. Rei and M. T. Schilling, “Reliability assessment of the Brazilian power system using enumeration and Monte Carlo,” *IEEE Trans. Power Syst.*, vol. 23, no. 3, pp. 1480–1487, 2008.
- [57] J. E. Tate and T. J. Overbye, “Line outage detection using phasor angle measurements,” *IEEE Trans. Power Syst.*, vol. 23, no. 4, pp. 1644–1652, 2008.
- [58] I. Musirin and T. K. A. Rahman, “On-line voltage stability based contingency ranking using fast voltage stability index (FVSI),” in *IEEE/PES Transmission and Distribution Conference and Exhibition*, 2002, vol. 2, pp. 1118–1123.
- [59] C. Rakpenthai, S. Premrudeepreechacharn, S. Uatrongjit, and N. R. Watson, “An optimal PMU placement method against measurement loss and branch outage,” *IEEE Trans. Power Deliv.*, vol. 22, no. 1, pp. 101–107, 2007.
- [60] A. Atputharajah and T. K. Saha, “Power system blackouts-literature review,” in *2009 International Conference on Industrial and Information Systems (ICIIS)*, 2009, pp. 460–465.
- [61] G. M. Huang and N.-K. Nair, “Voltage stability constrained load curtailment procedure to evaluate power system reliability measures,” in *2002 IEEE Power Engineering Society Winter Meeting. Conference Proceedings (Cat. No. 02CH37309)*, 2002, vol. 2, pp. 761–765.
- [62] G. C. Ejebe, W. R. Puntel, and B. F. Wollenberg, “LOAD CURTAILMENT ALGORITHM FOR THE EVALUATION OF POWER TRANSMISSION SYSTEM ADEQUACY.,” in *IEEE Power Eng Soc, Summer Meet, Prepr*, 2017.

- [63] Y. Zhao, Y. Tang, W. Li, and J. Yu, "Composite Power System Reliability Evaluation Based on Enhanced Sequential Cross-Entropy Monte Carlo Simulation," *IEEE Trans. Power Syst.*, 2019.
- [64] C. Singh and J. Mitra, "Reliability Evaluation in Transmission Systems," *Smart Grid Handb.*, pp. 1–17, 2016.
- [65] M. Modarres, M. P. Kaminskiy, and V. Krivtsov, *Reliability engineering and risk analysis: a practical guide*. CRC press, 2016.
- [66] F. Cadini, G. L. Agliardi, and E. Zio, "A modeling and simulation framework for the reliability/availability assessment of a power transmission grid subject to cascading failures under extreme weather conditions," *Appl. Energy*, vol. 185, pp. 267–279, 2017.
- [67] N. Kandalepa, B. W. Tuinema, J. L. Rueda, and M. A. M. M. van der Meijden, "Reliability modeling of transmission networks: an explanatory study on further EHV underground cabling in the netherlands," in *2016 IEEE International Energy Conference (ENERGYCON)*, 2016, pp. 1–6.
- [68] W. Li, "Incorporating aging failures in power system reliability evaluation," *IEEE Trans. Power Syst.*, vol. 17, no. 3, pp. 918–923, 2002.
- [69] E. Zio, "Reliability engineering: Old problems and new challenges," *Reliab. Eng. Syst. Saf.*, vol. 94, no. 2, pp. 125–141, 2009.
- [70] E. Zulu and D. Jayaweera, "Reliability assessment in active distribution networks with detailed effects of PV systems," *J. Mod. Power Syst. Clean Energy*, vol. 2, no. 1, pp. 59–68, 2014.
- [71] A. S. Bouhouras, A. G. Marinopoulos, D. P. Labridis, and P. S. Dokopoulos, "Installation of PV systems in Greece—Reliability improvement in the transmission and distribution system," *Electr. Power Syst. Res.*, vol. 80, no. 5, pp. 547–555, 2010.
- [72] Z. Esau and D. Jayaweera, "Reliability of active distribution networks with PV based strategic micro-grids," in *2013 Australasian Universities Power Engineering Conference (AUPEC)*, 2013, pp. 1–6.
- [73] P. Wang and R. Billinton, "Reliability benefit analysis of adding WTG to a distribution system," *IEEE Trans. Energy Convers.*, vol. 16, no. 2, pp. 134–139, 2001.
- [74] Y. M. Atwa and E. F. El-Saadany, "Reliability evaluation for distribution system with renewable distributed generation during islanded mode of operation," *IEEE Trans. Power Syst.*, vol. 24, no. 2, pp. 572–581, 2009.
- [75] F. Vallee, J. Lobry, and O. Deblecker, "System reliability assessment method for wind power integration," *IEEE Trans. Power Syst.*, vol. 23, no. 3, pp. 1288–1297, 2008.
- [76] M. E. Khodayar, M. Barati, and M. Shahidehpour, "Integration of high reliability distribution system in microgrid operation," *IEEE Trans. Smart Grid*, vol. 3, no. 4, pp. 1997–2006, 2012.
- [77] Y. Xu and C. Singh, "Power system reliability impact of energy storage integration with intelligent operation strategy," *IEEE Trans. Smart Grid*, vol. 5, no. 2, pp. 1129–1137, 2014.

- [78] S. Koochi-Kamali, V. V Tyagi, N. A. Rahim, N. L. Panwar, and H. Mokhlis, "Emergence of energy storage technologies as the solution for reliable operation of smart power systems: A review," *Renew. Sustain. Energy Rev.*, vol. 25, pp. 135–165, 2013.
- [79] P.-Y. Yin, S.-S. Yu, P.-P. Wang, and Y.-T. Wang, "Task allocation for maximizing reliability of a distributed system using hybrid particle swarm optimization," *J. Syst. Softw.*, vol. 80, no. 5, pp. 724–735, 2007.
- [80] R. Maouedj, A. Mammeri, M. D. Draou, and B. Benyoucef, "Performance evaluation of hybrid photovoltaic-wind power systems," *Energy Procedia*, vol. 50, pp. 797–807, 2014.
- [81] X. Liu, S. Islam, A. A. Chowdhury, and D. O. Koval, "Reliability evaluation of a wind-diesel-battery hybrid power system," in *2008 IEEE/IAS Industrial and Commercial Power Systems Technical Conference*, 2008, pp. 1–8.
- [82] A. Kavousi-Fard and T. Niknam, "Optimal distribution feeder reconfiguration for reliability improvement considering uncertainty," *IEEE Trans. Power Deliv.*, vol. 29, no. 3, pp. 1344–1353, 2014.
- [83] A. Kavousi-Fard and M.-R. Akbari-Zadeh, "Reliability enhancement using optimal distribution feeder reconfiguration," *Neurocomputing*, vol. 106, pp. 1–11, 2013.
- [84] R. E. Brown, "Distribution reliability assessment and reconfiguration optimization," in *2001 IEEE/PES Transmission and Distribution Conference and Exposition. Developing New Perspectives (Cat. No. 01CH37294)*, 2001, vol. 2, pp. 994–999.
- [85] S. Osaki, *Stochastic models in reliability and maintenance*. Springer, 2002.
- [86] M. Schläpfer, T. Kessler, and W. Kröger, "Reliability analysis of electric power systems using an object-oriented hybrid modeling approach," *arXiv Prepr. arXiv1201.0552*, 2012.
- [87] G. Celli, E. Ghiani, F. Pilo, and G. G. Soma, "Reliability assessment in smart distribution networks," *Electr. Power Syst. Res.*, vol. 104, pp. 164–175, 2013.
- [88] W. Li, "Evaluating mean life of power system equipment with limited end-of-life failure data," *IEEE Trans. Power Syst.*, vol. 19, no. 1, pp. 236–242, 2004.
- [89] J. F. L. van Casteren, M. H. J. Bollen, and M. E. Schmiege, "Reliability assessment in electrical power systems: the Weibull-Markov stochastic model," *IEEE Trans. Ind. Appl.*, vol. 36, no. 3, pp. 911–915, 2000.
- [90] M. Čepin, *Assessment of power system reliability: methods and applications*. Springer Science & Business Media, 2011.
- [91] B. Retterath, S. S. Venkata, and A. A. Chowdhury, "Impact of time-varying failure rates on distribution reliability," in *2004 International Conference on Probabilistic Methods Applied to Power Systems*, 2004, pp. 953–958.
- [92] K. Mihic, T. Simunic, and G. De Micheli, "Reliability and power management of integrated systems," in *Euromicro Symposium on Digital System Design, 2004. DSD 2004.*, 2004, pp. 5–11.

- [93] A. Chowdhury and D. Koval, *Power distribution system reliability: practical methods and applications*, vol. 48. John Wiley & Sons, 2011.
- [94] G.-A. Klutke, P. C. Kiessler, and M. A. Wortman, "A critical look at the bathtub curve," *IEEE Trans. Reliab.*, vol. 52, no. 1, pp. 125–129, 2003.
- [95] W. Li, *Risk assessment of power systems: models, methods, and applications*. John Wiley & Sons, 2014.
- [96] M. Modarres, *What every engineer should know about reliability and risk analysis*. CRC Press, 2018.
- [97] Y. Y. Haimes, *Risk modeling, assessment, and management*. John Wiley & Sons, 2015.
- [98] F. Yi, C. Jia, W. Zhang, X. Yang, and P. Zhang, "Simulation of HVDC transmission system failure rate bathtub curve based on Weibull distribution," in *Future Energy Electronics Conference (IFEEEC), 2015 IEEE 2nd International*, 2015, pp. 1–5.
- [99] H. Li, J. Ding, J. Huang, Y. Dong, and X. Li, "Reliability evaluation of PV power systems with consideration of time-varying factors," *J. Eng.*, vol. 2017, no. 13, pp. 1783–1787, 2017.
- [100] H. Li, H. Zuo, Y. Su, J. Xu, and Y. Yin, "Study on segmented distribution for reliability evaluation," *Chinese J. Aeronaut.*, vol. 30, no. 1, pp. 310–329, 2017.
- [101] L. S. Czarnecki and P. M. Haley, "Unbalanced power in four-wire systems and its reactive compensation," *IEEE Trans. Power Deliv.*, vol. 30, no. 1, pp. 53–63, 2015.
- [102] A. Askarzadeh, "Capacitor placement in distribution systems for power loss reduction and voltage improvement: a new methodology," *IET Gener. Transm. Distrib.*, vol. 10, no. 14, pp. 3631–3638, 2016.
- [103] A. H. Al-Mubarak, M. H. Khan, and M. Z. Al-Kadhem, "Dynamic reactive power compensation for voltage support using static var compensator (SVC) in Saudi Arabia," in *2015 IEEE Electrical Power and Energy Conference (EPEC)*, 2015, pp. 484–490.
- [104] P. Soumya and K. S. Swarup, "Optimal capacitor placement in a smart grid using demand side management as a resource," in *2017 IEEE Power and Energy Conference at Illinois (PECI)*, 2017, pp. 1–6.
- [105] A. H. Etemadi and M. Fotuhi-Firuzabad, "Distribution system reliability enhancement using optimal capacitor placement," *IET Gener. Transm. Distrib.*, vol. 2, no. 5, pp. 621–631, 2008.
- [106] B. Canizes, J. Soares, Z. Vale, and C. Lobo, "Optimal approach for reliability assessment in radial distribution networks," *IEEE Syst. J.*, vol. 11, no. 3, pp. 1846–1856, 2017.
- [107] R. M. A. Velásquez and J. V. M. Lara, "Reliability, availability and maintainability study for failure analysis in series capacitor bank," *Eng. Fail. Anal.*, vol. 86, pp. 158–167, 2018.
- [108] H. Myneni, G. S. Kumar, and D. Sreenivasarao, "Dynamic DC voltage regulation of split-capacitor DSTATCOM for power quality improvement," *IET Gener. Transm. Distrib.*, vol. 11, no. 17, pp. 4373–4383, 2017.

- [109] T. Gonen, *Electric power distribution engineering*. CRC press, 2016.
- [110] M. S. Alvarez-Alvarado, C. D. Rodríguez-Gallegos, and D. Jayaweera, “Optimal planning and operation of static VAR compensators in a distribution system with non-linear loads,” *IET Gener. Transm. Distrib.*, vol. 12, no. 15, pp. 3726–3735, 2018.
- [111] R. Billinton, M. Fotuhi-Firuzabad, and S. O. Faried, “Power system reliability enhancement using a thyristor controlled series capacitor,” *IEEE Trans. Power Syst.*, vol. 14, no. 1, pp. 369–374, 1999.
- [112] M. Fotuhi-Firuzabad, R. Billinton, and S. O. Faried, “Subtransmission system reliability enhancement using a thyristor controlled series capacitor,” *IEEE Trans. Power Deliv.*, vol. 15, no. 1, pp. 443–449, 2000.
- [113] R. Billinton, M. Fotuhi-Firuzabad, S. O. Faried, and S. Aboreshaid, “Impact of unified power flow controllers on power system reliability,” *IEEE Trans. Power Syst.*, vol. 15, no. 1, pp. 410–415, 2000.
- [114] R. Billinton, M. Fotuhi-Firuzabad, S. O. Faried, and S. Aboreshaid, “Composite system reliability evaluation incorporating an HVDC link and a static synchronous series compensator,” in *IEEE CCECE2002. Canadian Conference on Electrical and Computer Engineering. Conference Proceedings (Cat. No. 02CH37373)*, 2002, vol. 1, pp. 42–47.
- [115] A. Boström, R. Grunbaum, M. Dahlblom, and H. V Oheim, “SVC for reliability improvement in the NSTAR 115 kV cape cod transmission system,” in *2013 IEEE Power & Energy Society General Meeting*, 2013, pp. 1–5.
- [116] A. P. Jayam, N. K. Ardesna, and B. H. Chowdhury, “Application of STATCOM for improved reliability of power grid containing a wind turbine,” in *2008 IEEE Power and Energy Society General Meeting-Conversion and Delivery of Electrical Energy in the 21st Century*, 2008, pp. 1–7.
- [117] S. K. Saha, “Reliability Contingency Analysis by Static Synchronous Series Compensator in Optimal Power Flow,” *Int. J. Comput. Electr. Eng.*, vol. 2, no. 5, p. 908, 2010.
- [118] K. Ma and J. Mutale, “Risk and reliability worth assessment of power systems under corrective control,” in *41st North American Power Symposium*, 2009, pp. 1–6.
- [119] A. K. Verma, A. Srividya, and B. C. Deka, “Impact of a FACTS controller on reliability of composite power generation and transmission system,” *Electr. Power Syst. Res.*, vol. 72, no. 2, pp. 125–130, 2004.
- [120] S.-M. Moghadasi, A. Kazemi, M. Fotuhi-Firuzabad, and A.-A. Edris, “Composite system reliability assessment incorporating an interline power-flow controller,” *IEEE Trans. Power Deliv.*, vol. 23, no. 2, pp. 1191–1199, 2008.
- [121] A. Tiwari and V. Ajjarapu, “Optimal allocation of dynamic VAR support using mixed integer dynamic optimization,” *IEEE Trans. Power Syst.*, vol. 26, no. 1, pp. 305–314, 2011.
- [122] R. K. Mittapalli, A. Kumar, Y. Pal, and S. Chanana, “Optimal load curtailment in hybrid electricity market and impact of FACTS,” in *2012 2nd International Conference on Power, Control and Embedded Systems*, 2012, pp. 1–7.

- [123] K. P. Nguyen, G. Fujita, and V. N. Dieu, “Cuckoo search algorithm for optimal placement and sizing of static var compensator in large-scale power systems,” *J. Artif. Intell. Soft Comput. Res.*, vol. 6, no. 2, pp. 59–68, 2016.
- [124] I. Lazakis, O. Turan, and S. Aksu, “Increasing ship operational reliability through the implementation of a holistic maintenance management strategy,” *Ships Offshore Struct.*, vol. 5, no. 4, pp. 337–357, 2010.
- [125] British Standards, “Glossary of terms used in terotechnology.” BS 3811, London, 1993.
- [126] IACS, “A guide to managing maintenance.” IACS Rec. 74, London, 2001.
- [127] P. R. Barnes, J. W. Van Dyke, B. W. McConnell, S. M. Cohn, and S. L. Purucker, “The feasibility of replacing or upgrading utility distribution transformers during routine maintenance,” Oak Ridge National Lab., TN (United States), 1995.
- [128] “IEEE Guide for Maintenance, Operation, and Safety of Industrial and Commercial Power Systems (Yellow Book),” *IEEE Std 902-1998*. pp. 1–160, 1998.
- [129] G. Niu, B.-S. Yang, and M. Pecht, “Development of an optimized condition-based maintenance system by data fusion and reliability-centered maintenance,” *Reliab. Eng. Syst. Saf.*, vol. 95, no. 7, pp. 786–796, 2010.
- [130] J. Woodhouse, “Putting the total jigsaw puzzle together: PAS 55 standard for the integrated, optimized management of assets,” in *International Maintenance Conference*, 2006.
- [131] J. Moubray, *Reliability-centered maintenance*. Industrial Press Inc., 2001.
- [132] R.-B. Inspection, “API Recommended Practice 580,” *Am. Pet. Inst.*, 2009.
- [133] N. S. Arunraj and J. Maiti, “Risk-based maintenance—Techniques and applications,” *J. Hazard. Mater.*, vol. 142, no. 3, pp. 653–661, 2007.
- [134] N. Zhang *et al.*, “A convex model of risk-based unit commitment for day-ahead market clearing considering wind power uncertainty,” *IEEE Trans. Power Syst.*, vol. 30, no. 3, pp. 1582–1592, 2015.
- [135] M. Jadidbonab, H. Mousavi-Sarabi, and B. Mohammadi-Ivatloo, “Risk-constrained scheduling of solar-based three state compressed air energy storage with waste thermal recovery unit in the thermal energy market environment,” *IET Renew. Power Gener.*, 2018.
- [136] Y. Wang, C. Chen, J. Wang, and R. Baldick, “Research on resilience of power systems under natural disasters—A review,” *IEEE Trans. Power Syst.*, vol. 31, no. 2, pp. 1604–1613, 2015.
- [137] A. Khosrojerdi, S. H. Zegordi, J. K. Allen, and F. Mistree, “A method for designing power supply chain networks accounting for failure scenarios and preventive maintenance,” *Eng. Optim.*, vol. 48, no. 1, pp. 154–172, 2016.
- [138] A. Koksai and A. Ozdemir, “Improved transformer maintenance plan for reliability centred asset management of power transmission system,” *IET Gener. Transm. Distrib.*, vol. 10, no. 8, pp. 1976–1983, 2016.

- [139] R. Abbassi, J. Bhandari, F. Khan, V. Garaniya, and S. Chai, “Developing a quantitative risk-based methodology for maintenance scheduling using Bayesian network,” *Chem. Eng. Trans.*, vol. 48, pp. 235–240, 2016.
- [140] General Electric, “External report on maintenance schedule checklist for GEPC - RM commissioning & services hydro generators,” USA, 2017.
- [141] D. Liu Jr, “Application of risk based inspection (RBI), reliability centered maintenance (RCM) and risk based maintenance (RBM).” University of Stavanger, Norway, 2013.
- [142] A. Volkanovski, B. Mavko, T. Boševski, A. Čauševski, and M. Čepin, “Genetic algorithm optimisation of the maintenance scheduling of generating units in a power system,” *Reliab. Eng. Syst. Saf.*, vol. 93, no. 6, pp. 779–789, 2008.
- [143] K. P. Dahal and N. Chakpitak, “Generator maintenance scheduling in power systems using metaheuristic-based hybrid approaches,” *Electr. Power Syst. Res.*, vol. 77, no. 7, pp. 771–779, 2007.
- [144] E. Umamaheswari, S. Ganesan, M. Abirami, and S. Subramanian, “Reliability/risk centered cost effective preventive maintenance planning of generating units,” *Int. J. Qual. Reliab. Manag.*, 2018.
- [145] M. Fattahi, M. Mahootchi, H. Mosadegh, and F. Fallahi, “A new approach for maintenance scheduling of generating units in electrical power systems based on their operational hours,” *Comput. Oper. Res.*, vol. 50, pp. 61–79, 2014.
- [146] M. Yildirim, X. A. Sun, and N. Z. Gebraeel, “Sensor-driven condition-based generator maintenance scheduling—part II: Incorporating operations,” *IEEE Trans. Power Syst.*, vol. 31, no. 6, pp. 4263–4271, 2016.
- [147] L. C. Wolstenholme, *Reliability modelling: a statistical approach*. Routledge, 2017.
- [148] M. S. Alvarez-Alvarado and D. Jayaweera, “Reliability model for a static var compensator,” in *2017 IEEE Second Ecuador Technical Chapters Meeting (ETCM)*, 2017, pp. 1–6.
- [149] M. J. Crowder, *Statistical analysis of reliability data*. Routledge, 2017.
- [150] E. Tómasson and L. Söder, “Improved importance sampling for reliability evaluation of composite power systems,” *IEEE Trans. Power Syst.*, vol. 32, no. 3, pp. 2426–2434, 2017.
- [151] M. Benidris, J. Mitra, and C. Singh, “Integrated evaluation of reliability and stability of power systems,” *IEEE Trans. Power Syst.*, vol. 32, no. 5, pp. 4131–4139, 2017.
- [152] A. Ahadi, N. Ghadimi, and D. Mirabbasi, “An analytical methodology for assessment of smart monitoring impact on future electric power distribution system reliability,” *Complexity*, vol. 21, no. 1, pp. 99–113, 2015.
- [153] G. Muñoz-Delgado, J. Contreras, and J. M. Arroyo, “Reliability assessment for distribution optimization models: a non-simulation-based linear programming approach,” *IEEE Trans. Smart Grid*, vol. 9, no. 4, pp. 3048–3059, 2018.
- [154] R. Agapito, “Cálculo exacto de la matriz exponencial,” *Pro Math.*, vol. 28, no. 55, pp. 57–84, 2014.

- [155] Y. Yang, H. Wang, A. Sangwongwanich, and F. Blaabjerg, "Design for reliability of power electronic systems," in *Power Electronics Handbook*, Elsevier, 2018, pp. 1423–1440.
- [156] C. P. Jawahar and P. A. Michael, "A review on turbines for micro hydro power plant," *Renew. Sustain. Energy Rev.*, vol. 72, pp. 882–887, 2017.
- [157] F. Pugliese, F. De Paola, N. Fontana, M. Giugni, and G. Marini, "Experimental characterization of two pumps as turbines for hydropower generation," *Renew. energy*, vol. 99, pp. 180–187, 2016.
- [158] X. Liu, Y. Luo, and Z. Wang, "A review on fatigue damage mechanism in hydro turbines," *Renew. Sustain. Energy Rev.*, vol. 54, pp. 1–14, 2016.
- [159] Office of Energy Efficiency & RENEWABLE, "Types of Hydropower Plants," <https://www.energy.gov/eere/water/types-hydropower-plants>, 2010. .
- [160] M. K. Padhy and R. P. Saini, "Study of silt erosion on performance of a Pelton turbine," *Energy*, vol. 36, no. 1, pp. 141–147, 2011.
- [161] M. Zhang, D. Valentín, C. Valero, M. Egusquiza, and E. Egusquiza, "Failure investigation of a Kaplan turbine blade," *Eng. Fail. Anal.*, 2019.
- [162] H. A. Menarin, H. A. Costa, G. L. M. Fredo, R. P. Gosmann, E. C. Finardi, and L. A. Weiss, "Dynamic modelling of Kaplan turbines including flow rate and efficiency static characteristics," *IEEE Trans. Power Syst.*, 2019.
- [163] C. Grigg *et al.*, "The IEEE reliability test system-1996. A report prepared by the reliability test system task force of the application of probability methods subcommittee," *IEEE Trans. power Syst.*, vol. 14, no. 3, pp. 1010–1020, 1999.
- [164] D. Agudelo, "Report: Common Failures in Generators," Newark-USA, 2018.
- [165] R. Kehlhofer, F. Hannemann, B. Rukes, and F. Stirnimann, *Combined-cycle gas & steam turbine power plants*. Pennwell Books, 2009.
- [166] M. P. Boyce, *Gas turbine engineering handbook*. Elsevier, 2011.
- [167] T. E. Ekstrom, "Reliability/availability guarantees of gas turbine and combined cycle generating units," *IEEE Trans. Ind. Appl.*, vol. 31, no. 4, pp. 691–707, 1995.
- [168] F. J. G. Carazas, C. H. Salazar, and Gfm. Souza, "Availability analysis of heat recovery steam generators used in thermal power plants," *Energy*, vol. 36, no. 6, pp. 3855–3870, 2011.
- [169] H. L. Bernstein and J. M. Allen, "Analysis of cracked gas turbine blades," in *ASME 1991 International Gas Turbine and Aeroengine Congress and Exposition*, 1991, p. V005T12A003-V005T12A003.
- [170] A. Benato, A. Stoppato, and S. Bracco, "Combined cycle power plants: A comparison between two different dynamic models to evaluate transient behaviour and residual life," *Energy Convers. Manag.*, vol. 87, pp. 1269–1280, 2014.
- [171] J. S. Yoon, S. Y. Kim, B. H. Chang, and D. H. Baek, "Application of FACTS technology for power system control," in *2005 International Conference on Electrical Machines and Systems*, 2005, vol. 3, pp. 2498–2501.

- [172] S. A. Rahman, R. K. Varma, and W. H. Litzemberger, “Bibliography of FACTS applications for grid integration of wind and PV solar power systems: 1995–2010 IEEE working group report,” in *2011 IEEE Power and Energy Society General Meeting*, 2011, pp. 1–17.
- [173] J. Chivite-Zabalza, M. A. R. Vidal, P. Izurza-Moreno, G. Calvo, and D. Madariaga, “A large power, low-switching-frequency voltage source converter for FACTS applications with low effects on the transmission line,” *IEEE Trans. power Electron.*, vol. 27, no. 12, pp. 4868–4879, 2012.
- [174] F. H. Gandoman *et al.*, “Review of FACTS technologies and applications for power quality in smart grids with renewable energy systems,” *Renew. Sustain. energy Rev.*, vol. 82, pp. 502–514, 2018.
- [175] A. Gelen and T. Yalcinoz, “The behaviour of TSR-based SVC and TCR-based SVC installed in an infinite bus system,” in *2008 IEEE 25th Convention of Electrical and Electronics Engineers in Israel*, 2008, pp. 120–124.
- [176] J. Urquizo, P. Singh, N. Kondrath, R. Hidalgo-León, and G. Soriano, “Using D-FACTS in microgrids for power quality improvement: A review,” in *2017 IEEE Second Ecuador Technical Chapters Meeting (ETCM)*, 2017, pp. 1–6.
- [177] J. Faiz and G. Shahgholian, “Modeling and damping controller design for static var compensator,” in *Power Engineering, Energy and Electrical Drives (POWERENG), 2015 IEEE 5th International Conference on*, 2015, pp. 405–409.
- [178] S. Cheng, N. Zhang, X. Cui, and Z. Fu, “Research on Reactive Compensation Technology Based on SVC-APF,” in *2018 IEEE 3rd Advanced Information Technology, Electronic and Automation Control Conference (IAEAC)*, 2018, pp. 1547–1551.
- [179] T. R. Khramshin, I. R. Abdulvelev, and G. P. Kornilov, “Mathematical model of the power circuit of STATCOM of large capacity,” *Russ. Internet J. Electr. Eng.*, vol. 2, no. 1, pp. 38–46, 2016.
- [180] Y. Ma, A. Huang, and X. Zhou, “A review of STATCOM on the electric power system,” in *2015 IEEE International Conference on Mechatronics and Automation (ICMA)*, 2015, pp. 162–167.
- [181] L. K. Haw, M. S. A. Dahidah, and H. A. F. Almurib, “A new reactive current reference algorithm for the STATCOM system based on cascaded multilevel inverters,” *IEEE Trans. Power Electron.*, vol. 30, no. 7, pp. 3577–3588, 2015.
- [182] P. E. Melin *et al.*, “Study of Reactive Power Compensation Capabilities and LC Filter Design for a Three-Phase Current-Source STATCOM,” in *2018 IEEE International Conference on Automation/XXIII Congress of the Chilean Association of Automatic Control (ICA-ACCA)*, 2018, pp. 1–5.
- [183] M. Fotuhi-Firuzabad, R. Billinton, and S. O. Faried, “Transmission system reliability evaluation incorporating HVDC links and FACTS devices,” in *2001 Power Engineering Society Summer Meeting. Conference Proceedings (Cat. No. 01CH37262)*, 2001, vol. 1, pp. 321–326.

- [184] G. M. Huang and Y. Li, "Composite power system reliability evaluation for systems with SVC and TCPAR," in *2003 IEEE Power Engineering Society General Meeting (IEEE Cat. No. 03CH37491)*, 2003, vol. 2, pp. 771–776.
- [185] A. Janke *et al.*, "SVC operation & reliability experiences," in *Power and Energy Society General Meeting, 2010 IEEE*, 2010, pp. 1–8.
- [186] D. Agudelo, "Report: FACTS failure and repair," Newark-USA, 2018.
- [187] M. S. Alvarez-Alvarado and D. Jayaweera, "A New Approach for Reliability Assessment of a Static V ar Compensator Integrated Smart Grid," in *2018 IEEE International Conference on Probabilistic Methods Applied to Power Systems (PMAPS)*, 2018, pp. 1–7.
- [188] Z. Lu and W. Liu, "Reliability Evaluation of STATCOM Based on the k-out-of-n: G Model," in *2006 International Conference on Power System Technology*, 2006, pp. 1–6.
- [189] N. G. Hingorani, L. Gyugyi, and M. El-Hawary, *Understanding FACTS: concepts and technology of flexible AC transmission systems*, vol. 1. IEEE press New York, 2000.
- [190] W. Wu and H. Liu, "Research status and development of static synchronous compensator," *J. East China Jiaotong Univ.*, vol. 22, no. 2, pp. 89–94, 2005.
- [191] M. Fotuhi-Firuzabad, R. Billinton, S. O. Faried, and S. Aboreshaid, "Power system reliability enhancement using unified power flow controllers," in *PowerCon 2000. 2000 International Conference on Power System Technology. Proceedings (Cat. No. 00EX409)*, 2000, vol. 2, pp. 745–750.
- [192] B. Hu, K. Xie, and R. Karki, "Reliability evaluation of bulk power systems incorporating UPFC," in *2010 IEEE 11th International Conference on Probabilistic Methods Applied to Power Systems*, 2010, pp. 259–264.
- [193] A. Noruzi, T. Banki, O. Abedinia, and N. Ghadimi, "A new method for probabilistic assessments in power systems, combining monte carlo and stochastic-algebraic methods," *Complexity*, vol. 21, no. 2, pp. 100–110, 2015.
- [194] M. Aien, A. Hajebrahimi, and M. Fotuhi-Firuzabad, "A comprehensive review on uncertainty modeling techniques in power system studies," *Renew. Sustain. Energy Rev.*, vol. 57, pp. 1077–1089, 2016.
- [195] E. Zio, M. Delfanti, L. Giorgi, V. Olivieri, and G. Sansavini, "Monte Carlo simulation-based probabilistic assessment of DG penetration in medium voltage distribution networks," *Int. J. Electr. Power Energy Syst.*, vol. 64, pp. 852–860, 2015.
- [196] P. Henneaux, F.-X. Bouchez, and L. Rese, "Confidence intervals for adequacy assessment using Monte Carlo sequential simulation," in *2016 IEEE International Energy Conference (ENERGYCON)*, 2016, pp. 1–6.
- [197] R. Billinton and W. Zhang, "Cost related reliability evaluation of bulk power systems," *Int. J. Electr. power energy Syst.*, vol. 23, no. 2, pp. 99–112, 2001.
- [198] R. Billinton and X. Tang, "Selected considerations in utilizing Monte Carlo simulation in quantitative reliability evaluation of composite power systems," *Electr. power Syst. Res.*, vol. 69, no. 2–3, pp. 205–211, 2004.

- [199] P. Wang, Y. Ding, and L. Goel, “Reliability assessment of restructured power systems using optimal load shedding technique,” *IET Gener. Transm. Distrib.*, vol. 3, no. 7, pp. 628–640, 2009.
- [200] Y. Wang, N. Zhang, Q. Chen, J. Yang, C. Kang, and J. Huang, “Dependent discrete convolution based probabilistic load flow for the active distribution system,” *IEEE Trans. Sustain. Energy*, vol. 8, no. 3, pp. 1000–1009, 2017.
- [201] M. S. Alvarez-Alvarado and D. Jayaweera, “Aging Reliability Model for Generation Adequacy,” in *2018 IEEE International Conference on Probabilistic Methods Applied to Power Systems (PMAPS)*, 2018, pp. 1–6.
- [202] M. S. Alvarez-Alvarado and D. Jayaweera, “Bathtub curve as a Markovian process to describe the reliability of repairable components,” *IET Gener. Transm. Distrib.*, vol. 12, no. 21, pp. 5683–5689, 2018.
- [203] Y. Xiang, Z. Ding, Y. Zhang, and L. Wang, “Power system reliability evaluation considering load redistribution attacks,” *IEEE Trans. Smart Grid*, vol. 8, no. 2, pp. 889–901, 2017.
- [204] W. Sheng, X. Meng, T. Fan, and S. Du, “Reliability evaluation of distribution system considering sequential characteristics of distributed generation,” in *MATEC Web of Conferences*, 2016, vol. 55, p. 3008.
- [205] R. Billinton and P. Wang, “Teaching distribution system reliability evaluation using Monte Carlo simulation,” *IEEE Trans. Power Syst.*, vol. 14, no. 2, pp. 397–403, 1999.
- [206] Y. Zhang, L. Wang, Y. Xiang, and C.-W. Ten, “Power system reliability evaluation with SCADA cybersecurity considerations,” *IEEE Trans. Smart Grid*, vol. 6, no. 4, pp. 1707–1721, 2015.
- [207] H. Metzler and C. A. Sierra, “Linear autonomous compartmental models as continuous-time Markov chains: Transit-time and age distributions,” *Math. Geosci.*, vol. 50, no. 1, pp. 1–34, 2018.
- [208] M. S. Alvarez-Alvarado and D. Jayaweera, “A Multi-Stage Accelerated Quantum Particle Swarm Optimization for Planning and Operation of Static Var Compensators,” in *2018 IEEE Third Ecuador Technical Chapters Meeting (ETCM)*, 2018, pp. 1–6.
- [209] C. D. R. -Gallegos *et al.*, “Placement and sizing optimization for PV-battery-diesel hybrid systems,” in *2016 IEEE International Conference on Sustainable Energy Technologies (ICSET)*, 2016, pp. 83–89.
- [210] C. D. Rodríguez-Gallegos *et al.*, “A Siting and Sizing Optimization Approach for PV–Battery–Diesel Hybrid Systems,” *IEEE Trans. Ind. Appl.*, vol. 54, no. 3, pp. 2637–2645, 2018.
- [211] M. Clerc and J. Kennedy, “The particle swarm-explosion, stability, and convergence in a multidimensional complex space,” *IEEE Trans. Evol. Comput.*, vol. 6, no. 1, pp. 58–73, 2002.
- [212] K. Zielinski and R. Laur, “Stopping criteria for a constrained single-objective particle swarm optimization algorithm,” *Informatica*, vol. 31, no. 1, 2007.

- [213] M.-H. Tayarani-N and M. R. Akbarzadeh-T, “Magnetic optimization algorithms a new synthesis,” in *2008 IEEE Congress on Evolutionary Computation (IEEE World Congress on Computational Intelligence)*, 2008, pp. 2659–2664.
- [214] J. Sun, W. Xu, and B. Feng, “A global search strategy of quantum-behaved particle swarm optimization,” in *IEEE Conference on Cybernetics and Intelligent Systems, 2004.*, 2004, vol. 1, pp. 111–116.
- [215] Z.-L. Yang, A. Wu, and H.-Q. Min, “An improved quantum-behaved particle swarm optimization algorithm with elitist breeding for unconstrained optimization,” *Comput. Intell. Neurosci.*, vol. 2015, p. 41, 2015.
- [216] C. Monroe, D. M. Meekhof, B. E. King, and D. J. Wineland, “A “Schrödinger Cat” Superposition State of an Atom,” *NIST Tech. note*, vol. 1523, 2002.
- [217] J. Sun, B. Feng, and W. Xu, “Particle swarm optimization with particles having quantum behavior,” in *Evolutionary Computation, 2004. CEC2004. Congress on*, 2004, vol. 1, pp. 325–331.
- [218] M. Shicong, G. Jianbo, H. Qing, Z. Jian, D. Mian, and Y. Zhao, “Guide for voltage regulation and reactive power compensation at 1000kV AC and above with IEEE P1860 standard,” in *Power System Technology (POWERCON), 2014 International Conference on*, 2014, pp. 2092–2097.
- [219] J. A. Wheeler and W. H. Zurek, *Quantum theory and measurement*, vol. 49. Princeton University Press, 2014.
- [220] I. S. O. (International O. for Standardization), “ISO 55000: Asset management—overview, principles and terminology,” 2014.
- [221] N. F. P. Association, *NFPA 70B: Recommended Practice for Electrical Equipment Maintenance 2016*. 2015.
- [222] M. S. Alvarez-Alvarado and D. Jayaweera, “Smart Maintenance Model for Operational Planning of Static Synchronous Compensators,” in *13th IEEE PES PowerTech Conference*, 2019.
- [223] M. S. Alvarez-Alvarado and D. Jayaweera, “Reliability Based Smart Maintenance of Generators in Smart Power Systems,” *IEEE Trans. Smart Grid*, 2019.
- [224] M. S. Alvarez-Alvarado and D. Jayaweera, “Operational risk assessment with smart maintenance of power generators,” *Int. J. Electr. Power Energy Syst.*, vol. 117, p. 105671, 2020.
- [225] A. Nasr, S. Gasmi, and M. Sayadi, “Estimation of the parameters for a complex repairable system with preventive and corrective maintenance,” in *Electrical Engineering and Software Applications (ICEESA), 2013 International Conference on*, 2013, pp. 1–6.
- [226] M. S. Alvarez-Alvarado and D. Jayaweera, “Reliability model for a Static Var Compensator,” in *2017 IEEE Second Ecuador Technical Chapters Meeting (ETCM)*, 2017, pp. 1–6.

- [227] R. F. Stapelberg, *Handbook of reliability, availability, maintainability and safety in engineering design*. Springer Science & Business Media, 2009.
- [228] D. Agudelo, “Report: Degree of Maintenance and Operational Risk,” Public Service Enterprise Group (PSEG), Newark-New Jersey-USA, 2018.
- [229] M. Alvarez-Valverde, “Report: Fuzzy Logic and Operational Risk,” National Corporation of Electricity of Ecuador (CNEL), Guayaquil-Ecuador, 2018.
- [230] India Power Corp Ltd, “Generators membership function,” India, 2018.
- [231] National Grid, “Availability and risk of thermal and hydro generation,” London,UK, 2017.
- [232] S. Zitao, “Maintenance of power generators procedia,” Beijing, China, 2018.